All-polymer biosensor for label-free point of care diagnostics

Dapra, Johannes

Publication date:
2013

Document Version
Early version, also known as pre-print

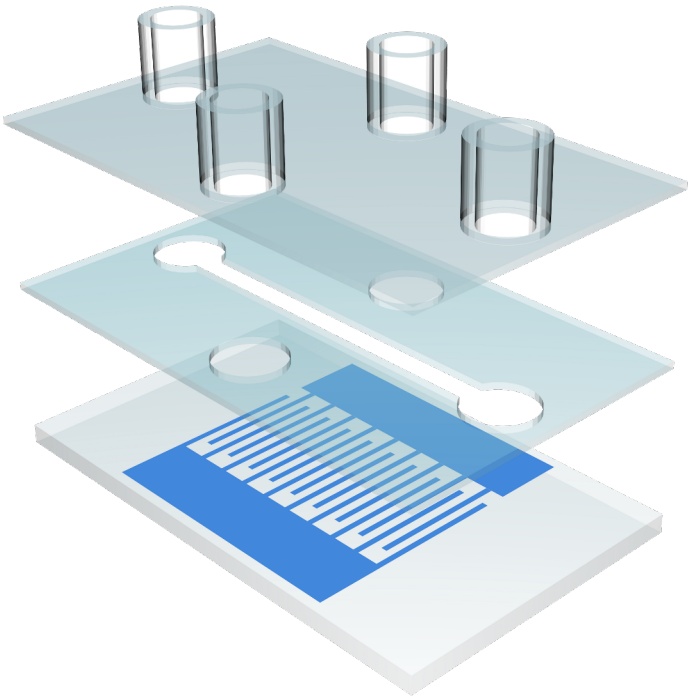

All-polymer biosensor for label-free point of care diagnostics

Johannes Daprà

PhD Thesis

DTU Nanotech
Department of Micro- and Nanotechnology

PhD Thesis

All-polymer biosensor for label-free point of care diagnostics

johannes.dapra@gmail.com

Supervisor:

Noemi Rozlosnik

Submission:

February 14, 2013

Abstract

Personalised medicine and diagnostics is a rapidly growing field of research and general interest. Important tools for individual patient care are so called point-of-care devices. These typically simple and inexpensive instruments allow the untrained user to perform simple diagnostic analyses without the need for a specialised laboratory. Other fields of application are for example health care projects in developing countries where access to modern high-throughput facilities is often impossible or sectors not related to the medical field, like environmental monitoring or food safety.

The aim of this PhD project was to develop a modular platform based on electrochemical impedimetric sensing. This device can easily be modified by changing the biological receptors and therefore offers a broad range of possible applications. To keep the costs and the environmental footprint low the entire biosensor was designed in plastic; featuring a microfluidic channel and an electrode system fabricated from conductive polymers. Aptamers were used as recognition elements providing a more stable alternative to antibodies for easier handling and a longer shelf life. Moreover, aptamers have a much wider range of possible target molecules than antibodies.

The biosensor platform was successfully adapted to different tasks and tested against three very different analytes: DNA, antibiotics and virus particles. Throughout the experiments the sensors showed high sensitivity and were able to detect very low analyte concentrations in both buffered solutions, milk and saliva samples.

Dansk Resumé

Begrebet skræddersyet medicin og diagnostik er forbundet med stor interesse og det er et forskningsområde i kraftig vækst. Netop udviklingen af diagnostiske tests er et centralt element for at kunne tilpasse individuelle behandlingsforløb. Denne type diagnostiske redskaber er typisk simple og billige og kan anvendes af den utrænede bruger til at udføre simple diagnostiske analyser uden behov for et specialiseret laboratorium. Andre anvendelsesområder er for eksempel i sundhedsprojekter i udviklingslande hvor moderne højteknologiske faciliteter ikke er tilgængelige, eller i sektorer der ikke er relaterede til medicin såsom miljøovervågning og fødevaresikkerhed.

Formålet med dette ph.d. projekt var at udvikle en modulær platform baseret på elektrokemisk impedimetrisk registrering. Dette instrument kan let modificeres ved at ændre de biologiske receptorer og har derfor en bred vifte af mulige applikationer. Biosensoren er designet udelukkende i plastik med tanke på miljøet og for at holde prisen lav – den består af en mikrofluid kanal og et elektrodesystem i ledende polymerer. Aptamerer blev brugt som genkendelseselementer. De er et stabilt alternativ til antistoffer, er langt lettere at arbejde med og har en længere levetid. Desuden har aptamerer en langt bredere skare af mulige målmolekyler end antistoffer.

Denne biosensor platform var med succes tilpasset forskellige opgaver og er testet med tre vidt forskellige analytter: DNA, antibiotika og virus. Sensoren udviste høj sensitivitet ved alle eksperimenter, og kunne detektere meget lave koncentrationer af analytten – både i bufferopløsninger, mælk og spytprøver.

Acknowledgements

I would like to express my gratitude to all those people who accompanied me on the long way to the completion of this thesis.
My excellent supervisor Noemi Rozlosnik, who never failed to motivate me for new exciting projects and advised me in countless situations.
My co-supervisor Kristoffer Almdal, who always had an open door and an open ear for my questions.
All of the current and former members of the PolyMeDiag group, who were always good for discussions, cake and bike races.
The students I had the joy to supervise, especially Alex, Selva and Solène.
All the rest of the Nanotech staff and in particular Dorota, Johan, Niels, Ina, Ole, Lotte, Paolo, Maciej, Jirka, Luigi and Karsten for the good collaborations and advice, for all the help I got and all the fun we had both in the labs and on tropical beaches.
Finally I would like to thank my family, my girlfriend Katharina (who is proof-reading all this) and her family, who all supported me in all sorts of circumstances and gave me the motivation to carry on and get as far as I am now.

Contents

List of figures

List of tables

Abbreviations and nomenclature

The abbreviations used in this thesis are explained in the following. New abbreviations have only been adopted where they contribute to readability or clarity; otherwise terms commonly found in the literature have been used.

LOD	Limit of detection
MRL	Maximum residue limit
pfu	Plaque forming units
RT-PCR	Reverse transcription PCR
T_g	Glass transition temperature

1. General introduction

1.1. Motivation

> *"How great would it be if you could go down to the pharmacy, pick up a cheap and easy-to-use device to check your blood for early stages of cancer, and then toss it in the recycling bin when you're done? It would allow people to be aware of their health issues way before they reach a dangerous level . . . in the end, more lives would be saved.*[1]*"*

Not only the steady presence of cancer, but also epidemics or food scandals from the recent past show that there is a growing demand for rapid and inexpensive diagnostic or analytical devices. Today's diagnostic analyses are most often carried out with the help of table-top high throughput machinery operated by a specialised technician and located in centralised laboratories. This means that all collected samples have to be shipped there; prolonging the processing time enormously. Many of the techniques are also very expensive in both operation as well as materials cost and therefore less samples can be analysed within a budget.

In the future analyses will be done de-centralised and right after the sample was collected. This requires so called point-of-care (POC) devices capable of rapid detection of certain pathogens or analytes. Biosensors, analytical devices based on biological recognition elements, allow the development of POC tools by integrating them into closed microfluidic environments. A final product should be designed in a way that allows the operation by untrained personnel and give a non-ambiguous readout. Only then, and if they can be produced at reasonable

[1] Luigi Sasso, *"Fish eye insight to illness"*, The Press, `press.co.nz` 1 Feb. 2013

costs, POC sensors can compete with today's established systems and help in the fight against cancer, spreading pandemics or foodborne illnesses.

In this thesis the development of an electrochemical biosensor platform based on a conductive polymer and aptamers as recognition elements is described. The technology was tested for several different applications and protected by an international patent.

Structure of the thesis

Chapter 2 will give a theoretical introduction into the main topics of the thesis: different types of biosensors and electrochemical impedance spectroscopy.

Chapter 3 will then describe the attempted synthesis of one monomer for later use in the conductive polymer electrodes.

Chapter 4 explains how the polymer microelectrodes were fabricated and describes the characterisation of the conductive polymer layer with different methods.

Chapter 5 provides an overview over the selection of aptamers and our different approaches to that matter.

Chapter 6 will provide a brief discussion about different immobilisation methods. Two of these will be described in more detail and experimental results as well as a chemical characterisation are shown.

Chapter 7 shows the use of this novel technology in three different biosensor applications. Experimental results from the measurements of DNA hybridisation as well as the determination of very low concentrations of antibiotics and influenza A viruses will be provided in this chapter.

2. Theoretical background

This chapter will provide a general insight into the main topics of this thesis: biosensors and electrochemical impedance spectroscopy. More background information specific to the following chapters will be provided in their respective introductory sections.

2.1. Biosensors

Over millions of years of constant evolution nature has developed molecules with greatly specialised properties. One of these properties is the capability to establish strong and highly specific non-covalent bonds with other molecules to trigger a biochemical action or mechanism. Examples for such molecules are enzymes, antibodies or riboswitches.

In the field of biosensors, researchers try to employ these biomolecules for analytical purposes in a range of novel devices. A common definition for a biosensor is:

> A biosensor is a chemical sensing device in which a biologically derived recognition entity is coupled to a transducer, to allow the quantitative development of some complex biochemical parameter [**Mohanty2006**].

Mostly enzymes or antibodies are used for such devices, but recently aptamers, i. e. short oligonucleotide sequences with specific binding capability, have gained increasing attention. Popular transducers are semiconductors, metals or piezoelectric elements. A schematic representation of a biosensor is shown in figure 2.1.

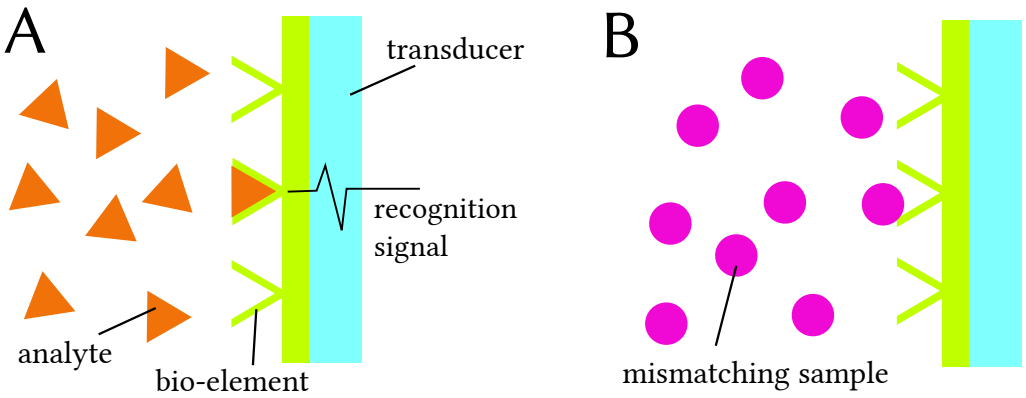

Figure 2.1.: Schematic representation of a biosensor. In example A on the left side the analyte binds to the specific bioreceptors and the resulting interaction with the transducer lead to a readable signal. In example B (right) no binding event takes place; no signal is registred.

In the last few decades a plethora of different combinations of bioprobes and transducing elements or technologies have been developed [**Chemla2000**, **Clark1962**, **Haes2002**, **Muhammad-Tahir2003**, **Ramanathan2001**, **Rasmussen2003**, **Rodriguez2005**, **Schoening2003**, **Svendsen2012**, **Xia005**, **Xia02005confo**, **Zhylyak1995**, 7, 9]:

Optical detection is often used for biosensors employing fluorescent markers or coloured additives. Related methods are surface plasmon resonance (SPR) and surface enhanced Raman spectroscopy (SERS). Applications for these techniques range from simple laminar flow assays as found in pregnancy tests to high-tech solutions like DNA-microarrays.

Resonant biosensors rely on the measurement of changing oscillation modes of a substrate caused by a changing surface coverage. Two examples for this technique are quartz crystal microbalances (QCM) or cantilevers coated with biomolecules.

Ion sensitive field effect transistors (ISFET) are usually semiconductor nanowires with immobilised bioprobes. Binding of a target molecule changes the electrical charges near the surface of the wire and thereby causes a shift in its conductivity.

Thermometric biosensors measure temperature differences in a liquid medium caused by enzyme catalysed endo- or exothermic reactions with high accuracy.

Magnetic biosensors use magnetic microbeads equipped with biomolecules for detection of analytes in a solution.

Cell based biosensors use, as the name suggests, live cells as recognition entities. Such sensors can, for instance, be used to study the influence of drugs on a cell culture or to quantify pathogens in an unknown sample.

Electrochemical biosensors are a very large group of biosensors which transform a chemical reaction or process into an electric signal. The biosensors described in this thesis belong into this class and so a more detailed description of the category is given in the following.

2.2. Electrochemical biosensors

Compared to the other classes of biosensors mentioned shortly above, electrochemical sensors have probably received the most attention recently; especially amperometric systems have become quite popular [**Mohanty2006**]. Aside from amperometric devices there exist also conductometric, potentiometric and impedimetric sensor systems.

Amperometric sensors measure a current as a product of electrochemical reactions on the surface of the electrode. The biomolecule (usually an enzyme) itself is not necessarily the electroactive species, but in presence of the analyte it will produce or consume electroactive molecules which, in turn, can be detected. The best example, perhaps, for this type of biosensor is the amperometric glucose sensor, which was the first documented biosensor and, at the same time, the commercially most important biosensor on the market [**Mohanty2006**]. In the glucose sensor the enzyme glucose oxidase (GOD) is immobilised onto a platinum electrode. The enzyme catalyses the reaction of glucose to gluconic acid consuming oxygen in the process. The oxygen concentration can be mea-

sured with the platinum electrode, allowing the determination of the glucose concentration in the sample [**Clark1962**].

In a conductometric biosensor the resistance of a solution is measured, allowing inferences about the ion concentration therein. One example for such a device was presented by **Zhylyak1995** and it had the capability of measuring heavy-metal ion concentrations in water. The measuring principle was rather simple: after placing a membrane made of cross-linked bovine serum albumin and the enzyme urease onto an array of interdigitated gold electrodes the conductivity across the membrane was measured. The conductivity is proportional to the ion concentration which depends on the activity of the enzyme. Different heavy-metal ions inhibit the function of the enzyme and cause a reduction of the conductivity. The sensitivity of such sensors is not very high and due to the wide range of different ions all inhibiting the enzyme, the device is also not very specific [**Zhylyak1995**].

The parameter measured with potentiometric biosensors is the oxidation or reduction potential of a molecule on the surface of an electrode. This molecule can be the analyte; this is usually the case when, for example, the dopamine production of neurons fixed to an electrode is measured. Another possibility is to equip a bioprobe with a redox marker, which is released or brought close to the electrode in the presence of the analyte. This principle was employed, for example, to construct a biosensor to measure the concentration of the protein thrombin in a liquid sample. An aptamer (the bioprobe, which will be described in chapter 5, page 46 et seq.) specific to thrombin was immobilised together with a partly complementary DNA strand tagged with methylene blue (MB) onto a gold electrode. As is illustrated in figure 2.2, complex formation between thrombin and the aptamer caused both DNA strands to separate. As a result of the conformation change the MB tag was brought closer to the electrode surface allowing the transfer of electrons [**Xiao05**, **Xiao2005confo**]. Typical characterisation methods for potentiometric sensors are alternating-current voltammetry and cyclic voltammetry.

Impedance spectroscopy is a powerful method to analyse the complex electrical resistance of a system and it is sensitive to changes on the electrode

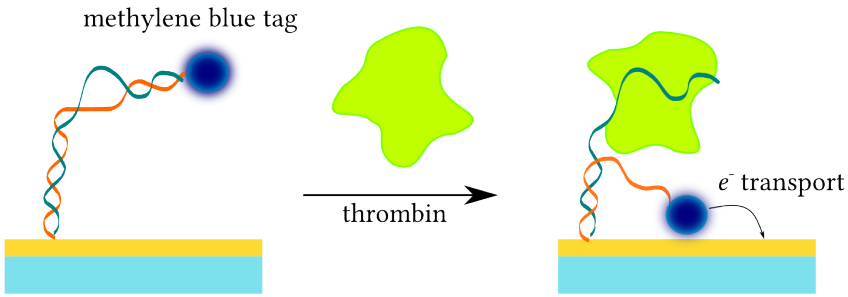

Figure 2.2.: Schematic representation of an electrochemical aptasensor using methylene blue (MB) as electroactive marker. Adapted from **Xia02005confo**

surface and changes of the bulk properties. Electrochemical detection using electrochemical impedance spectroscopy (EIS) is advantageous because of its label-free and reagentless character and high sensitivity, as recently reviewed by **Paenke08** Thus, impedance detection is particularly suited to follow binding events in the field of biosensors. Examples for the application of this method range from antibody-functionalised microbeads, whose sizes change when binding to analytes [**Svendsen2012**] over monitoring of cells situated on interdigitated electrodes [7] to sandwich assays on conducting surfaces [**Rodriguez2005**]. As this is the technology used for the biosensors developed during this PhD project, a more detailed explanation of the measuring principle is provided in section 2.4.

Most of the published work about electrochemical biosensors involves electrodes fabricated from noble metals like gold or platinum [5]. While providing excellent properties such as high conductivity and good environmental stability, the purchase price of these materials is extremely high and still rising; additionally they require expensive clean room fabrication in many cases and are difficult to recycle.

Conductive polymers, on the other hand, offer very suitable properties to master the specialised task of transducing a binding event between an analyte and a biological probe. They have been used as an alternative to traditional

electrode materials because of the additional advantageous properties of inexpensive electrode fabrication and easy electrode functionalisation [6, 7].

Because of their excellent compatibility with biological samples polypyrrole (PPy) and poly (3,4-ethylenedioxythiophene) (PEDOT) have repeatedly been used for sensors in biological environments [7–13]. Even though pyrrole is the less expensive monomer compared to 3,4-ethylenedioxythiophene (EDOT), and PPy shows equally good air-stability, PEDOT was used exclusively in this study because of its superior stability in phosphate buffers and its higher conductivity [15–17].

Biosensors cannot only be classified by their transducer type or detection method, but also by the type of bioprobe. The main goal of this thesis was to develop a biosensor using aptamers (a so called aptasensor) as diagnostic platform for a broad range of applications. This type of biosensor will be illuminated in the following section.

2.3. Aptasensors

By far the most commonly used recognition elements in biosensors are proteins such as antibodies or enzymes. The reason for choosing these proteins over other molecules can easily be found in their highly developed specificity towards their designated target molecules. However, proteins do have their limitations: most of these molecules are highly sensitive regarding their chemical environment, so that an improper pH, for instance, can render them functionless. Proteins can also easily be irreversibly denatured by elevated temperatures or be degenerated by proteases [**Binz2005**, **Hoogenboom2005**]. Moreover, the production of antibodies is generally difficult and expensive.

As an alternative to antibodies, aptamers have recently attracted increasing attention due to their capability to bind a wide range of targets: nucleic acids, proteins, metal ions and other molecules with high affinity and sensitivity [**Song2012Sensors**, **Hong2012**].

Aptamers are peptides or oligonucleotides (RNA or single stranded DNA) that bind to a specific target molecule. The aptamers typically fold into a

three-dimensional structure, whose conformation is changing upon ligand binding. Aptamer-like structures can also be found in nature: riboswitches in bacteria and eukaryotes control translation depending on ligand binding [**Winkler:2002gd**]. A more thorough description of aptamers and how they are selected follows in chapter 5, page 46.

Together with the growing interest in aptamers, biosensors using those molecules as recognition elements – so called aptasensors – are gaining more and more popularity. One example for an aptasensor for potentiometric detection of thrombin was already mentioned in section 2.2 on page 5. Another application was shown by Xie, Luo, and Yu [9] where conductive polymer nanowires were functionalised with thrombin-binding aptamers. Binding of the target molecule resulted in a change of the negative charge density above the nanowire, altering its conductivity. This behaviour equals the change of source-drain current in a common field effect transistor (FET) when changing the gate potential.

Impedimetric aptasensors are not a novelty either [**Lingerfelt2007**, **Paenkeo8**, **Kloesgen11**], but so far there were no reports of such sensors fabricated entirely from polymers, i. e. without any metals or other inorganic conducting materials, and also without the addition of any redox marker such as methylene blue or ferro-/ferricyanide. The benefits of such a device are clear: the use of inexpensive polymers instead of noble metals makes it suitable for the use in disposable chips for rapid diagnostic tests. The avoidance of redox markers both in the solution as well as coupled to the bioprobes makes sample handling easier and less prone to human error, and saves costs on the production of the probes, respectively.

2.4. Electrochemical impedance spectroscopy

Electrochemical impedance spectroscopy (EIS) is a very sophisticated method of label free analysis of interface bound chemical processes.

The impedance Z is a complex electrical property consisting of a real part, the resistance R, and an imaginary part, the reactance X [**Lingerfelt2007**]

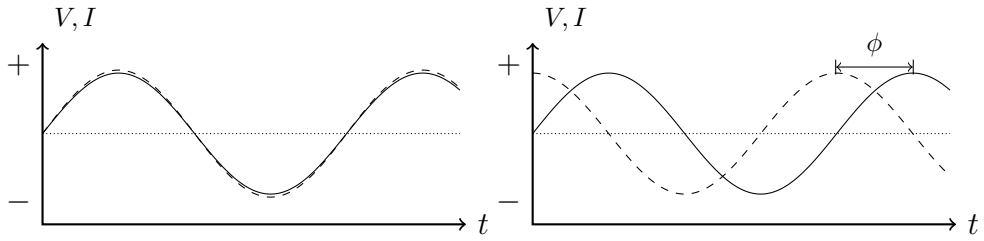

(a) The current I through a resistor is directly proportional to the applied potential V.

(b) A capacitor causes a 90° phase shift (ϕ) of current I and potential V.

Figure 2.3.: Different current response to an alternating potential applied to a resistor (a) and a capacitor (b).

Applying a sinusoidal alternating current signal to a simple electrical system consisting of one resistor (R) and one capacitor (C) connected in a parallel network will give such a complex current response. The current I through the resistor will follow the potential V proportionally, while the capacitor-current will undergo a 90° phase shift ϕ in respect to the voltage (see figure 2.3). In general, impedance can be described as function of time t with:

$$Z = \frac{V(t)}{I(t)} = \frac{V_0 \cdot \sin(2\pi f t)}{I_0 \cdot \sin(2\pi f t + \phi)} \tag{2.1}$$

For EIS the impedance is measured for a range of different frequencies f. The impedance of a system can then be illustrated by plotting the absolute value $|Z|$ and the phase shift ϕ as a function of log f (Bode plot) or as Nyquist plot, where the imaginary component Z_{I} is plotted against the real component Z_{R} [**Paenkeo8**]. Examples of typical Bode and Nyquist plots for a simple R-C circuit are shown in figure 2.4.

Such plots can then be used to build a model of the investigated system as an equivalent circuit using building blocks such as resistors, capacitors, inductors, constant phase elements or Warburg resistances. This model system should reflect – in a sensible way – the observed behaviour of the real system. Some of these circuit elements are constant (resistance is a material property), some are frequency dependent (capacitors let high frequencies pass, while inductors

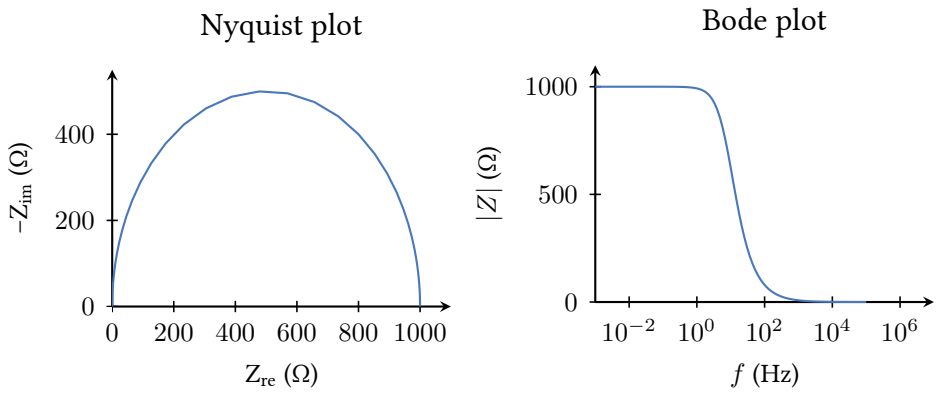

Figure 2.4.: Examples of Bode and Nyquist plots for a parallel R-C circuit. The diameter of the semicircle in the Nyquist plot corresponds to the resistance of the system; the position of the inflexion point in the Bode diagram is depend on the capacitance.

block them) and some have a more complex behaviour, which can depend on other parameters such as surface area of the electrode or mobility of certain ions in the electrolyte or electrode (in the case of a porous electrode). All of these circuit elements have an influence on the shape of the impedance spectrum and by adjusting their intrinsic parameters a spectrum can be simulated, which then helps to understand the processes in the real system. The theory behind these processes is very complex and would exceed the limits of this introduction. For a more thorough insight into this topic the book **Orazem2008** by **Orazem2008** can be recommended.

Since EIS is most qualified for investigations of interfaces, the largest number of applications utilise this method for corrosion studies of multi-layer materials such as painted metals. However, also in the newer and very different field of biosensors, some interesting applications for impedance spectroscopy were found. In most cases a bioprobe was immobilised onto an electrode and exposed to a sample solution containing the analyte (often small organic molecules) and the redox-active ion pair ferro-/ferricyanide ($[Fe(CN)_6]^{3-/4-}$). Depending on the analyte concentration, a different amount of the redox-active ions approached the electrode surface due to electrostatic interactions [**Ruan2002**, **Rodriguez2005**]. Other sensors monitored the status of live cells by investigating their membranes using impedance spectroscopy [**Kloesgen11**, 7].

During this PhD project sensors with bioprobes tethered to the electrodes were developed, but contrary to other works, polymer electrodes were used exclusively and no redox-active ions were added. Highly charged single stranded DNA probes were employed instead whose binding-related conformational changes caused a difference in the measured impedance. In this thesis the development of an all-polymer impedimetric sensor is detailed from the fabrication of the microelectrodes to the use in three related but different applications: the same device was used to measure hybridisation of DNA oligomers and for the detection of minute concentrations of two different antibiotics using specific aptamers as probes. The usability of the sensor was also tested with a spiked milk sample, showing that the device was capable of detecting concentrations far lower than the official maximum residue limits in the European Union. To test the performance as a diagnostic tool, the device was also used to detect low concentrations of influenza A virus in a saliva sample using specific aptamers.

3. Monomer synthesis

3.1. Introduction

One of the most fundamental aims of this work was the development of a disposable electrochemical biosensor system. To keep costs and environmental impact low, traditional electrode materials, i. e. usually noble metals such as gold or platinum, were not an option. It was, therefore, decided to use the conductive polymer poly(3,4-ethylenedioxythiophene) (PEDOT) instead.This material possesses reasonable properties for the intended application and it was already studied extensively at the department.

Electric conductivity in polymers can be established by different mechanisms describing charge transport via electrons or associated ions. Real intrinsic conductivity can be observed in polymers containing a backbone with a conjugated system of π-bonds.

In contrast to polymers which owe their conductivity to the presence of loosely bound ions (often protons) or electrons "hopping" from one redox site to another, intrinsically conducting polymers (ICP) conduct electricity over their own backbone, or more accurately a conjugated system of π-bonds. These π-bonds are found in chemical double or triple bonds, e. g. between carbon atoms and are a form of orbital interaction. In an alkene the $2s$ orbital and two $2p$ orbitals hybridise to form a planar sp^2 orbital with bonding angles of 120°. The remaining p_z orbital stands perpendicular to the sp^2 hybrid as illustrated in figure 3.1. The overlapping sp^2 orbitals form so-called σ-bonds, while neighbouring p_z orbitals establish π-bonds. In a conjugated system of alternating single and double bonds the electrons in the p_z orbitals have a high mobility and form a delocalised π-system. In such a system a discrimination between single and double bonds is not possible any more [**Vollhardt2003**].

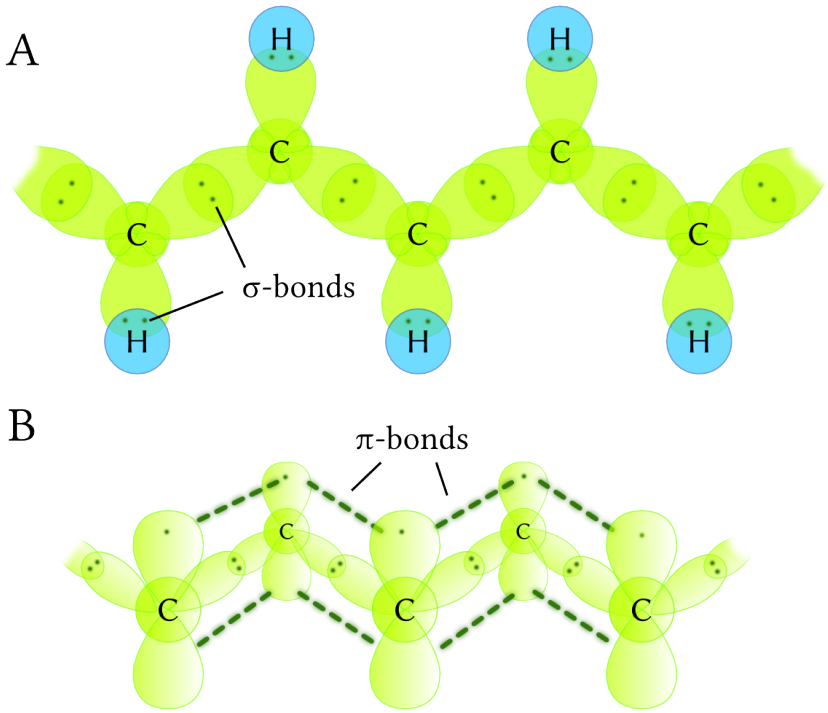

Figure 3.1.: Hybridised sp^2 orbitals overlap with each other and s orbitals from hydrogen atoms to form σ-bonds (A). Neighbouring p_z orbitals form π-bonds, allowing high electron mobility (B).

Neutral, i. e. uncharged, conjugated polymers are not conductive because their valence band is filled and their band gap is too wide for thermal excitation of electrons into the unoccupied energetic states of the conducting band [**Inzelt2012**]. For PEDOT, the band gap, which is the quantum mechanically forbidden zone of energetic states between the valence and conducting bands in a semiconductor, is about 1.6 – 1.7 eV [**Groenendaal2003**]. As was discovered in the late 1970's by future Nobel laureates Alan Heeger, Alan MacDiarmid and Hideki Shirakawa conjugated polymers need to be doped with ions to become conductive. Analogue to a p-doped semiconductor an oxidised conjugated polymer contains delocalised electron defects (holes) which allow a net transport of charges along the π-system. Those so-called polarons are stabilised by anions and their amount and distribution is responsible for the conductivity of the polymer. On the example of *p*-toluenesulfonate (tosylate)

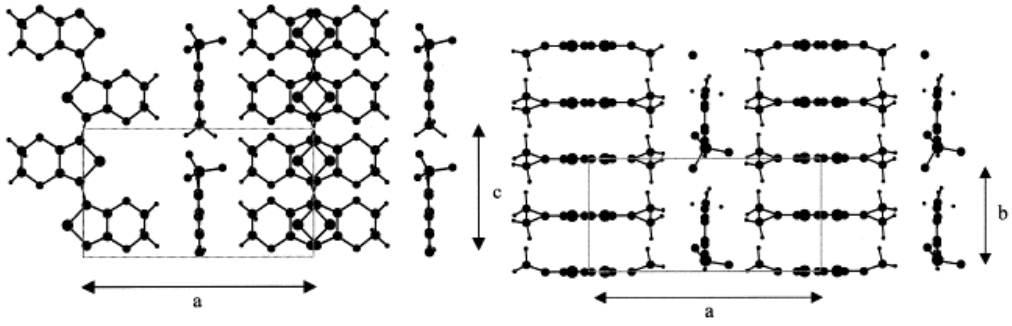

Figure 3.2.: Crystallographic structure of tosylate doped PEDOT as suggested by **Aasmundtveit2000** The left illustration shows a projection along the *b* axis; the right projection is shown along the *c* axis.

doped PEDOT it was shown by Aasmundtveit et al. in X-ray diffraction studies that the negatively charged tosylate ions have fixed places in the crystal lattice of the polymer and thus do not contribute directly to the charge transport [**Aasmundtveit2000**, 22]. The crystal structure of a unit cell is shown in figure 3.2.

Mathematical models predicting the band gap, while being quite accurate for short oligomers, used to fail for long polymer chains, underestimating the real values found in photospectrometric experiments. **Zade2006** suggested a new model where the band gap narrows linearly with the chain length up to a certain number of monomer units, from where on the value starts stabilising until reaching a constant energy. Obtaining experimental proof for these findings is difficult because of the low solubility of long conjugated oligomers, but the calculated band gaps for infinite chain lengths are in remarkably well agreement with experimental values found for conductive polymer thin films [**Zade2006**].

On the chemical side, however, PEDOT does not have any functional groups which allow grafting of other molecules to the polymer without destroying the electric conductivity established by the conjugated π-system of the backbone. In order to develop an all-polymer biosensor with covalently attached sensing probes one of the first steps was the synthesis of a modified monomer to introduce further functionality into the polymer. Even though several modifications to the monomer unit 3,4-ethylenedioxythiophene (EDOT) were described in the

literature, none were commercially available at the time. Thus the synthesis from scratch was necessary.

Starting from polythiophene as base material, a lot of effort has been made to improve its properties in terms of solubility and processability. Different 3,4-disubstituted thiophene monomers were synthesised to prevent formation of α–β linkages during polymerisation and to stabilise the polymer in its oxidised state [**Groenendaal2003**, **McCullough1993**, **Waltman1986**]. However, the alkyl-substituents led to distortion of the conjugated π-system due to steric interaction and thus decreased conductivity [**Roncali1987**, **Tourillon1984**]. The steric hindrance was lessened by connecting the 3 and 4 substituents to form cycles [**Roncali1987Steric**]. This structure was later improved further by introduction of heteroatoms such as oxygen or sulphur [**Wang1995**][**Blanchard2002**], leading finally to the synthesis of the probably most prominent of this family: 3,4-ethylenedioxythiophene or EDOT [**Jonas1991**]. Since this monomer has been commercially available for a long time now, it was not necessary to synthesise it for the experiments described herein. Its hydroxymethyl derivative EDOT-OH, however, had to be made. The synthesis has been described in the past by different authors [**Akoudad2000PE**, 20] and their protocols were followed in this work to a large extent. This chapter describes the attempted synthesis of 3,4-ethylenedioxythiophene derivatives with functional groups accessible for grafting reactions. The synthesis of (2,3-dihydrothieno[3,4-*b*][1,4]dioxin-2-yl)methanol was performed in six steps starting with the formation of the thiophene ring. The details of each reaction step will be described in the following section.

3.2. Experimental part

In this section the synthesis of 2,3-dihydrothieno[3,4-*b*]-1,4-dioxin-2yl-methanol is described in detail. All chemicals were purchased from Sigma-Aldrich (Schnelldorf, Germany). The synthesis was tried once, but failed, probably due to undesired polymerisation of an intermediate product. During the experimental work of a second batch, the desired product became commercially available at a convenient price, therefore, it would have been unreasonable to continue with the synthesis.

3.2.1. Synthesis step 1

The first synthesis step is the preparation of diethyl thioglycolate by acid catalysed esterification of thiodiglycolic acid **1**. A two-necked round flask equipped with reflux condenser and $CaCl_2$ guard was filled with a solution of 25 g (167 mmol) thiodiglycolic acid in 125 mL absolute ethanol. Over a period of approximately 5 minutes and under continued stirring 10 mL concentrated sulfuric acid were slowly added. The solution was then heated to reflux for another 24 h. After cooling it was poured into 150 mL water and extracted five times with dichloromethane (DCM). The organic layer was washed three times with a saturated aqueous Na_2CO_3 solution, dried over $MgSO_4$ and concentrated with a rotary evaporator to give 11.28 g (yield: 28 %) of a light yellow oily liquid, **2**.

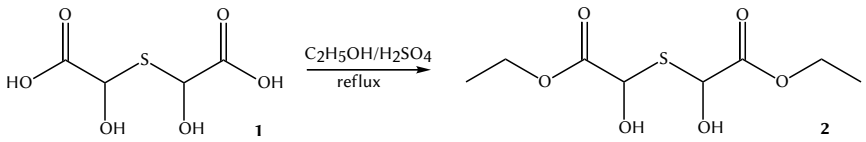

Figure 3.3.: Step 1: Acid catalysed esterification of thiodiglycolic acid **1**.

3.2.2. Synthesis step 2

In the second step the thiophene ring is formed. Under N_2 atmosphere all of the product from the first step (11.28 g, 47 mmol) and 20.11 mL (158 mmol) diethyl oxalate were added dropwise over approx. 20 minutes to a cooled (0 °C) solution

of 16.9 g (248 mmol) sodium ethoxide in 125 mL absolute ethanol. The reaction mixture turned to a very deep orange and a precipitate formed. After complete addition, the solution was heated to reflux for 1 h. The yellow precipitate was filtered, washed with ethanol and dried under vacuum over night. It is evident from the yield of 17 g (107 %) that the product diethyl 3,4-dihydroxythiophene-2,5-dicarboxylate disodium salt (**3**) was either not completely dry or contained impurities.

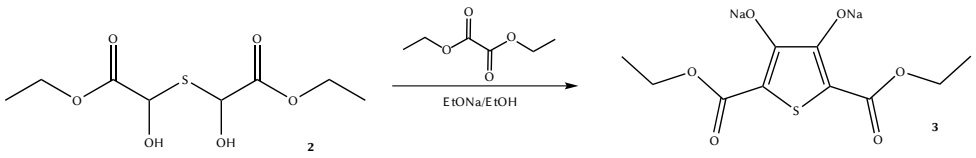

Figure 3.4.: Step 2: Formation of the thiophene ring.

3.2.3. Synthesis step 3

The entire product from the second step was dissolved in 600 mL milli-Q water under slight heating (approx. 50 °C). Insoluble particles were removed by filtration. The dark orange filtrate was acidified with 5 mL concentrated HCl. The newly formed precipitate was filtrated; further acidification of the filtrate led to no precipitation. Drying the filter residue in vacuum at 100 °C for three hours yielded 6.9 g (52 % based on step 2 input) diethyl 3,4-dihydroxythiophene-2,5-dicarboxylate (**4**) as a light brown solid.

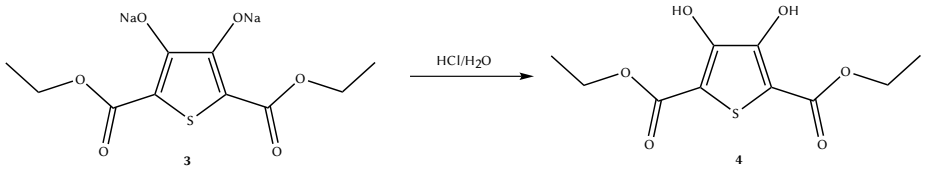

Figure 3.5.: Step 3: Precipitation of the intermediate product by acidification.

3.2.4. Synthesis step 4

All of the product from step 3 was dissolved in 180 mL boiling ethanol, then 0.8 g (6 mmol) K_2CO_3 and 7.9 g (58 mmol) 2,3-dibrompropan-1-ol in 40 mL of

water were added. After boiling to reflux for 1 h another 13.8 g (101 mmol) 2,3-dibrompropan-1-ol and 0.43 g (3 mmol) K_2CO_3 in 10 mL water were added and the solution was heated to reflux for 72 h. In the course of this procedure the colour of the solution turned from a dark yellow to emerald green. After cooling down, the reaction mixture was poured into 150 mL 5 % HCl which resulted in the formation of a white precipitate and a brown liquid phase. This suspension was extracted twice with 100 mL chloroform; the organic phase was first washed with 5 % KCl and then dried over $MgSO_4$. After removing the solvent by rotary evaporation a dark crystalline solid remained. Lima et al. [20] recrystallised this product from diethyl ether, but access to this solvent was unfortunately prohibited for safety reasons. Different similar solvents were tested, but a clean separation was not possible by recrystallisation. The reaction product was therefore extracted using a Soxhlet apparatus and *n*-hexane as extractant. The extraction yielded a light brown crystalline product, which was recrystallised once more from *n*-hexane to give approx. 10 g almost white crystalline diethyl 2-(hydroxymethyl)-2,3-dihydrothieno[3,4-*b*]-1,4-dioxine-5,7-dicarboxylate (**5**).

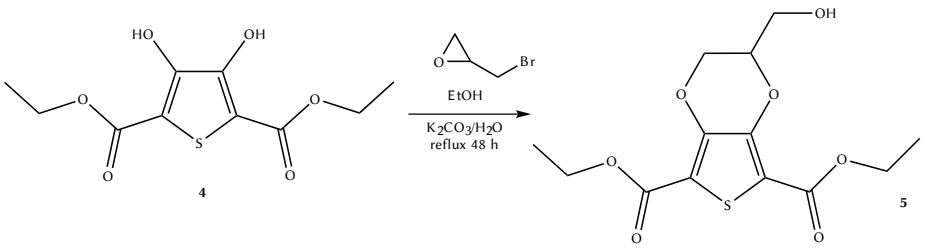

Figure 3.6.: Step 4: Esterification of the 3 and 4 hydroxy-groups.

3.2.5. Synthesis step 5

The fifth step of this synthesis is the saponification of the ethylesters on the 2 and 5 position of the thiophene ring. Compund **5** was solubilised in 250 mL water together with 12 g KOH. and heated to reflux for 2 h. The liquid volume was reduced to approximately one third of its original amount by rotary evaporation. The remaining solution was cooled in an ice bath and concen-

trated HCl was added slowly under constant stirring. Conversely to the description of a white precipitate in the literature [20] a black foam formed. The resulting dark and muddy solution was filtrated and the black precipitate was extracted with ethanol. In this step the product diethyl 2-(hydroxymethyl)-2,3-dihydrothieno[3,4-*b*]-1,4-dioxine-5,7-dicarboxylic acid (**6**) might have been lost due to polymerisation. The formed polymer was insoluble, so a thorough analysis was not possible.

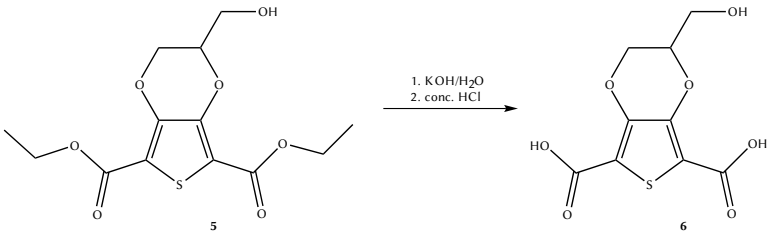

Figure 3.7.: Step 5: Saponification of the ethylesters on the 2 and 5 positions of the thiophene ring.

3.2.6. Synthesis step 6

The last step describes the copper chromite catalysed decarboxylation of **6** to yield the final product 2,3-dihydrothieno[3,4-*b*]-1,4-dioxin-2yl-methanol (**7**). A mixture of 900 mg step 5 product and 100 mg copper chromite catalyst in 10 mL freshly distilled quinoline was refluxed under nitrogen for 2 h. After cooling, the mixture was diluted with DCM and filtrated. The filtrate was first washed with 100 mL 5 % HCl (four extractions), then with 50 mL 5 % KCl (three extractions) and then dried over $MgSO_4$. After removing the solvent by rotary evaporation, 1.5 g of a brown oily liquid were obtained. NMR analysis of this liquid confirmed that no product was obtained.

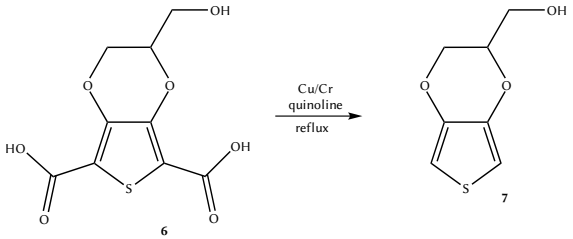

Figure 3.8.: Step 6: Catalytic decarboxylation of the 2 and 5 positions of the thiophene ring.

3.3. Summary

The production of a monomer unit for a conductive polymer with an accessible hydroxymethyl group ((2,3-dihydrothieno[3,4-*b*][1,4]dioxin-2-yl)methanol) was attempted through a six-step synthesis. Polymerisation of this molecule would result in a derivative of the widely used electrically conductive polymer poly(3,4-ethylenedioxythiophene) (PEDOT) but with the added capability for functionalisation through the hydroxyl group. This property makes the material interesting for the use as signal transducer in electrochemical all-polymer biosensors, and it was already employed for that purpose in several systems [**Luo09**, 9]. In connection with these research projects one main synthesis route was established and also modified to yield related PEDOT-derivatives [20].

The synthesis failed in one of the last steps of the first try, where, presumably, most of the product polymerised, forming an insoluble black mass, which was impossible to analyse. Halfway through a second, improved attempt the product became commercially available and the time consuming synthesis was discontinued.

Future developments and findings might require additional modification of this monomer unit. A likely derivative could for instance be equipped with a polyethylene glycol (PEG) chain to prevent bio-fouling of implantable devices or other sensors which are exposed to the sample for a very long time. This and similar modifications could then be made rather easily using the monomer described in this chapter as precursor.

4. Microelectrode fabrication

4.1. Introduction

In early stages of development rapid and low cost prototyping procedures are welcome tools to allow flexibility and a high throughput of prototypes. For the polymerisation of the conductive polymer poly(3,4-ethylenedioxythiophene) (PEDOT) several methods are known. Probably the most popular way to prepare the polymer is electropolymerisation [9, 15, 18–21]. Alternatives are chemical oxidation polymerisation in liquid [22–26] as well as in vapour phase [27–29]. The oxidative chemical pathway is advantageous because – unlike electrochemical techniques – it does not require a conductive substrate.

We chose a liquid phase method with Fe^{III} as oxidant, which starts a radical polymerisation. To achieve uniform, thin films of the polymer, spin coating is a widely used technique. A flat substrate is usually fixated on a rotor and a solution containing either the dissolved polymer or a reactive mixture of the necessary precursors is applied to the centre of the substrate disc. By spinning the rotor, centrifugal force drives the liquid over the substrate, leaving a thin and uniform layer on the surface. The properties of this film are essentially governed by the viscosity of the solution, the spin rate of the substrate and the surface energy. As a rule, high spin rates and low viscosity lead to thin films; a high surface energy can cause disruptions in the film because of insufficient wetting.

For the desired biosensor application it is necessary to pattern the film to obtain sensing electrodes and connection patches. Micropatterning of conductive polymers is regularly done using cleanroom based photolithographic techniques. However, although such processes are versatile, they are not well-suited for fabricating inexpensive biosensor platforms due to their costs. To

address this issue an alternative micropatterning procedure was developed recently at our institute. This simple rapid prototyping method is based on contacting PEDOT thin films with a micro-structured agarose stamp soaked in a solution of aqueous hypochlorite and a non-ionic detergent [25, 30]. Where contacted, PEDOT is removed and the underlying substrate exposed. By employing a cyclic olefin copolymer (COC) substrate we were able to fabricate nucleotide-functionalised PEDOT microelectrodes on a COC background with a low degree of unspecific binding of DNA, in a simple and inexpensive manner.

In the experimental section of this chapter the preparation of polymer microelectrodes will be described in detail. The results section will concentrate on presenting data obtained from the characterisation of the physical and chemical properties of the microelectrodes.

Throughout this thesis the conducting polymers PEDOT and PEDOT-OH will be used exclusively with the dopant *p*-toluenesulfonate, widely known as tosylate, and commonly abbreviated TsO. For the sake of clarity the author will refrain from the use of the notations PEDOT:TsO or PEDOT-OH:TsO, respectively. In situations where there is a possibility of confusion between different materials, the extended notation will be used.

4.2. Experimental part

4.2.1. Conducting polymer film deposition

The conductive polymer PEDOT and its derivative PEDOT-OH used during the work presented in this thesis are not soluble in any of the common solvents. In order to spin coat these materials, a reactive solution containing the monomer and other chemicals necessary for the polymerisation need to be pre-mixed, applied onto the substrate and then the polymerisation can be started. For the experiments in this work conductive thin films of tosylate doped PEDOT were made by spin coating the reaction solution containing the monomer and thermal activation according to the following procedure:

For each chip 260 µL of 40 wt% $Fe^{(III)}$tosylate in *n*-butanol (commercially available as Baytron® C from Heraeus, Germany) was mixed thoroughly with 80 µL *n*-butanol, 6 µL pyridine and 4.4 µL of the monomer 3,4-ethyldioxythiophene (EDOT, marketed as Baytron® M). The base pyridine acts as inhibitor and is removed at a later stage to start the polymerisation reaction.

The reactive mixture was then filled into a syringe equipped with a filter (pore size 400 nm). Cleaned Topas® 5013 discs ($\varnothing = 50.8$ mm) were mounted on the rotor of the spin-coater and ca. 300 µL of the reactive mixture was applied at the centre of the disc. Spinning with 1000 rpm for 60 s with an acceleration rate of 500 rpm/s yielded a uniform yellow coating. Coated polymer discs were then heated to 70 °C for ca. 5 minutes. During this process pyridine evaporates and the progress of polymerisation can be observed by a colour change from yellow towards a dark greenish blue. Pictures of the colour change are shown in figure 4.1. Excess reactants and by-products were rinsed off with deionised water. After drying the discs obtained the characteristic blue colour

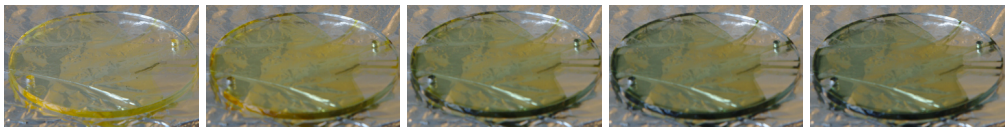

Figure 4.1.: The spin coated reaction mixture polymerises on a hot plate forming the conductive polymer PEDOT. The pictures were taken at approximately one minute intervals.

of PEDOT (see figure 4.2). Layers of PEDOT-OH:TsO were cast using 70.5 mg of the monomer 2,3-dihydrothieno[3,4-*b*]-1,4-dioxin-2yl-methanol also known as hydroxymethyl-EDOT or EDOT-OH instead of EDOT. It is advisable to dissolve this waxy component in *n*-butanol prior to mixing it with Baytron® C and pyridine. This conductive polymer provides a possible grafting site for later functionalisation.

As shown in the results section of this chapter (section 4.3.2, page 29), PEDOT has a higher conductivity than PEDOT-OH. To increase the sensitivity of the sensors in most experiments described here, bilayers consisting of PEDOT covered with PEDOT-OH were employed.

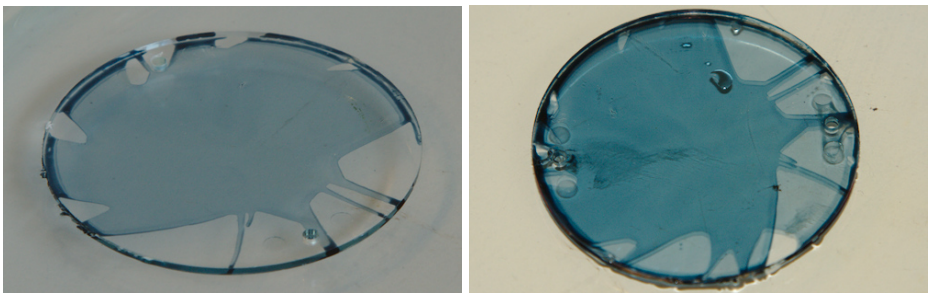

Figure 4.2.: The polymer layers obtain their characteristic blue colour after rinsing excess reactants off the coated Topas® discs. The right image shows a discs with a bilayer.

4.2.2. Microelectrode preparation

Interdigitated microelectrodes were fabricated by agarose stamping, as described in detail by Hansen et al. [25] and more recently by Lind et al. [30]. At first, the desired pattern is etched as a relief into a silicone wafer by standard clean room procedures. It was found that structures with high aspect ratio (i. e. around 1:4) performed best. Then a 10 wt% agarose gel was prepared by suspending 4 g agarose in 40 mL de-ionised water and melting it in a microwave oven. The agarose was ready to use when it had turned into a clear, viscous liquid. The freshly plasma treated Si master was placed on a hot plate at approximately 70 °C and equipped with a round cast around the pattern. Liquid agarose gel was filled into the cast and covered to avoid dehydration. It

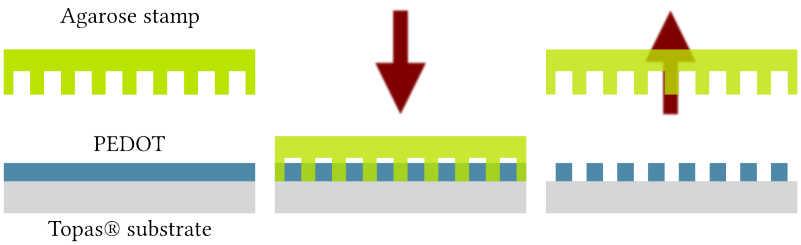

Figure 4.3.: An agarose stamp soaked with a solution containing 1 – 1.5 % sodium hypochlorite and 0.1 % Triton™ x-100 was used to oxidise exposed parts of a PEDOT layer.

was kept on the hot plate for 10 minutes to allow air bubbles to surface. After making sure that no bubbles stuck to the silicon (causing flaws in the stamp), master and gel were cooled in the refrigerator for 10 minutes to solidify the gel. The agarose gel slab was peeled from the master and cut to the right size with a scalpel. It was then soaked in a 1 – 1.5 % solution of sodium hypochlorite in water containing 0.1 % of the surfactant Triton™ x-100. After 5 to 10 minutes the stamp was removed from the solution and its surface was dried with pressurised nitrogen. Care has to be taken to not dry out the gel entirely to avoid deformation and other damage, however any liquid droplets must be removed from the patterned face of the stamp. After manual alignment of the pattern, the gel slab was pressed firmly by hand onto a PEDOT covered Topas® wafer. After 45 s the stamp was removed and immediately immersed into the sodium hypochlorite solution. Treated in this way, the stamp could be re-used for about 15 applications before severe degradation was visible. An illustration of the process is shown in figure 4.3, the necessary tools are shown in figure 4.4.

The freshly patterned disc was rinsed with ethanol and de-ionised water to wash off any residual over-oxidised PEDOT. The remaining pattern of conductive polymer now had a dark purple hue, characteristic for PEDOT in a reduced state. To re-dope the polymer, the disc was immersed shortly in a 10 % Baytron® C solution and rinsed with de-ionised water. During this process the colour of the polymer changed from dark to light blue indicating the conversion from a reduced state to a more conductive oxidised state with higher degree of doping. The stamp design comprised interdigitated electrodes with a width of

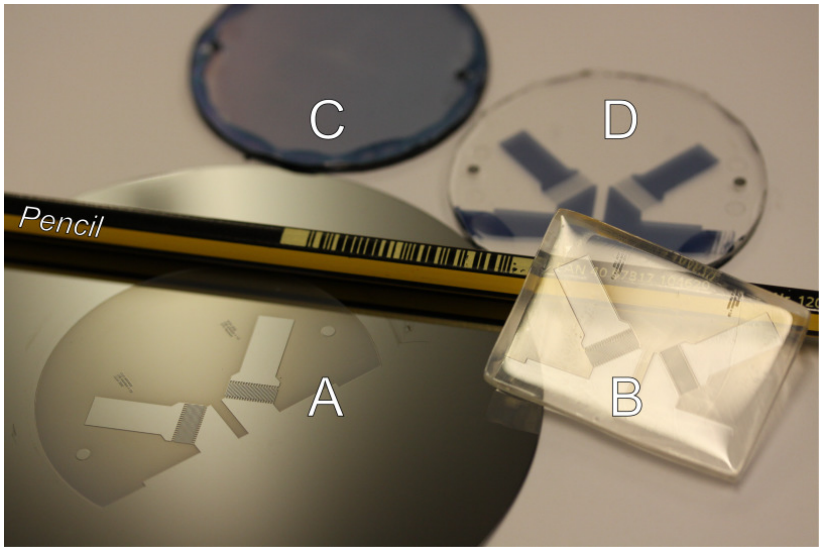

Figure 4.4.: A: Silicon wafer with deep etched template for casting the gel stamp. B: Solid agarose gel with microelectrode pattern. C: Topas® disc with multiple PEDOT layers. D: Patterned PEDOT microelectrodes. The pencil is included as scale (Picture courtesy of Johan U. Lind [30]).

20 µm. The spacing between the single wires was the same as their width. An alternative pattern with wires of 100 µm width and spacing was tested, but not employed for the final sensor applications due to a prospected lower sensitivity.

4.3. Results and discussion

The conductive polymer films prepared as described above were characterised with atomic force microscopy (AFM), profilometry and the four point probe technique for the determination of the sheet resistance. The agarose stamping procedure was then analysed with the help of a simplified wire pattern and different characterisation methods. Lastly the stamped interdigitated electrode patterns were investigated.

Some of the following experiments were carried out by Alexander Bakos Leirvåg, who was a master student under the supervision of the author. A more detailed summary of his work can be found in his thesis [**Leirvaag2012**].

4.3.1. Film thickness

The thickness of spin coated PEDOT layers depending on the spin rate was investigated and correlated to the substrate (silicone dioxide or Topas®). Measurements were done using a profilometer (Dektak 8) on the Topas® discs and an AFM (XE150, Park Systems, South Korea) for silicon wafers. It was expected to see differences between the two substrates due to their individual surface energy. The increased centrifugal force caused by higher spin rates was expected to result in thinner PEDOT layers.

Our observations are shown in figure 4.5. As can be seen from the graphs, there is a linear correlation of the spin rate and the film thickness on both substrates. The obtained films were in general thinner on SiO_2 than on Topas®, which can be related to the more hydrophilic properties of SiO_2 compared to the polymer Topas®, causing a lower contact angle of the relatively polar reactive mixture. The lower standard deviations of the values measured on silicon wafers can be attributed to both the different instrumentation and the more even surface of the highly polished substrate. The surface roughness of the polymer films was determined on a silicon wafer. The average roughness was found to be 0.23 ± 0.06 nm. The morphology of oxidised and reduced films did not differ at a level measurable with our instrumentation.

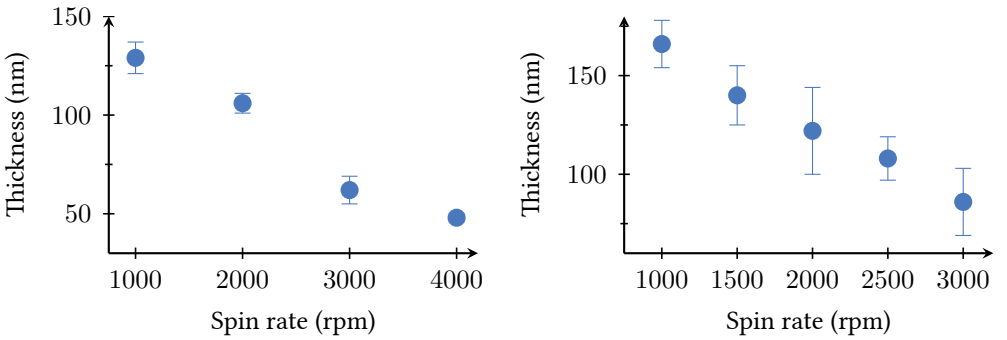

Figure 4.5.: The effect of the spin rate on the thickness of resulting polymer layers is shown on two substrates. A higher spin rate led to thinner layers. Films on silicon (left) were in general thinner than on Topas® (right).

4.3.2. Film conductivity

The four point probe method allows the measurement of the sheet resistance of a material by driving a current through the outer pins of a four electrode array and measuring the potential drop between the inner two electrodes [**Smits1958**]. Data recorded by the four point probe typically contains some strong outliers in the lower current range as seen in the sparkline . This is due to contact resistance and would influence the mean when centring the data. For this reason it was decided to use the median instead for all further calculations.

The measured sheet resistance $\rho_\square$ and the layer thickness d were used to calculate the resistivity ρ of the PEDOT films according to

$$\rho = \rho_\square \cdot d \tag{4.1}$$

As can be seen in figure 4.6, the sheet resistance decreased linearly with thinner PEDOT layers, however, the resistivity remained mostly unchanged for polymer layers thinner than 120 nm and decreased only for sheets thicker than that.

A list containing measured values for layer thickness and resistivity is given in table 4.1. The slightly lower resistivity of PEDOT on SiO_2 compared to Topas® could be explained by the smoother polymer films obtained on the Si wafer. The reactive mixture which was used to coat the SiO_2 substrate was filtered while the mixture for the Topas® was not. This could mean that small impurities

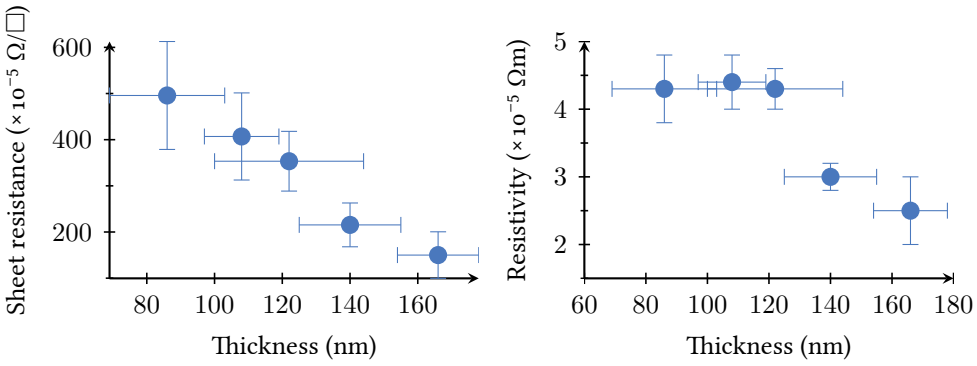

Figure 4.6.: The sheet resistance decreases linear with the layer thickness (left). Layers thinner than 120 nm have the same resistivity, while thicker layers become more conductive (right).

(PEDOT lumps or iron tosylate crystals) were incorporated into the films. An investigation with AFM using a conductive tip in contact mode revealed that there are in fact micro particles in the film and their conductivity was less than that of the surrounding polymer (figures 4.7 a and b).

To reduce measurement artefacts and noise in the AFM images a mean filtering was applied to the raw data. Mean filtering is an algorithm which averages an area of n neighbouring pixels in a dataset. The resulting images make the correlation of the protrusions in the topographic image (figure 4.7 c) with the dark, less conducting areas in the conductivity image (figure 4.7 d) more apparent.

The resistance values reported above are all for single layers of PEDOT. For the biosensor application we were interested in the performance of the derivative PEDOT-OH, because of its reported lower conductivity [**Hsiao10**], or in the conductivity of a PEDOT:PEDOT-OH bilayer. The conductivity σ of the PEDOT films was calculated from the sheet resistance $\rho_{\square}$ measured with a four point probe and the layer thickness d according to

$$\sigma = \frac{1}{\rho_{\square} \cdot d} \tag{4.2}$$

Our findings for PEDOT were 424 ± 57.2 S/cm and for PEDOT-OH 81 ± 10.7 S/cm. The bilayer material showed a conductance of 275 ± 61.2 S/cm. These values

Table 4.1.: Influence of the spin rate on thickness and resistivity of PEDOT thin films produced with spin coating.

Thickness (nm)	SD (nm)	Resistivity (Ωm)	SD (Ωm)	Spin rate (rpm)	Substrate
48	2	$2.2 \cdot 10^{-5}$	$5 \cdot 10^{-6}$	4000	SiO_2
62	7	$2.5 \cdot 10^{-5}$	$4 \cdot 10^{-6}$	3000	SiO_2
86	17	$4.3 \cdot 10^{-5}$	$5 \cdot 10^{-6}$	3000	Topas
106	5	$3.1 \cdot 10^{-5}$	$8 \cdot 10^{-6}$	2000	SiO_2
108	11	$4.4 \cdot 10^{-5}$	$4 \cdot 10^{-6}$	2500	Topas
122	22	$4.3 \cdot 10^{-5}$	$3 \cdot 10^{-6}$	2000	Topas
129	8	$1.8 \cdot 10^{-5}$	$1 \cdot 10^{-5}$	1000	SiO_2
140	15	$3.0 \cdot 10^{-5}$	$2 \cdot 10^{-6}$	1500	Topas
166	12	$2.5 \cdot 10^{-5}$	$5 \cdot 10^{-6}$	1000	Topas

are within the expected range as they compare very well with previous results published by Winther-Jensen and West [23], Hansen et al. [25] and **Hsia010**

It was reported previously that thermal annealing processes of spin coated thin films of poly(styrenesulfonate) doped PEDOT (PEDOT:PSS) increased their conductivity substantially. This effect is related to structural changes in the polymer where non-conductive domains of PSS interrupt the PEDOT sheet [**Farah2012**]. Our own experiments could not proof such an effect for tosylate doped PEDOT (PEDOT:TSO). This suggests that PEDOT:TSO is, unlike PEDOT:PSS, already quite homogeneous and a rearrangement of polymer chains leads to no benefits regarding conductivity.

Dry heating up to 120 ℃ did not have any effect on the polymer, so some samples were heated in a liquid medium to study possible changes. A set of parameters consisting of three solutions, three temperatures and three heating periods was created. To reduce the total number of experiments and since the parameters are independent of each other, several parameters could be tested in parallel according to the Taguchi-matrix displayed in table 4.2.

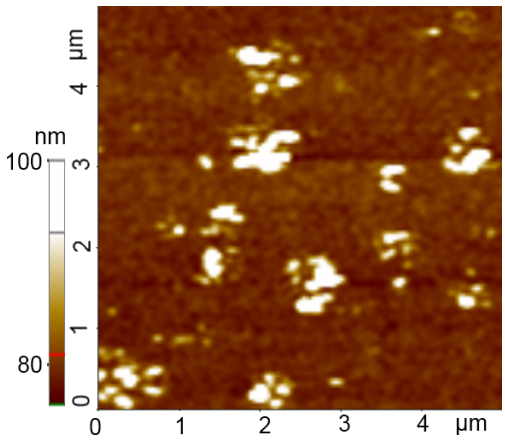

(a) Impurities seen on a topographic AFM image.

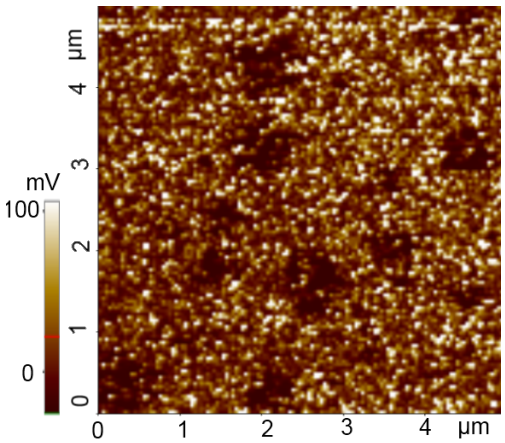

(b) Conductive AFM shows that the contaminations are not conductive.

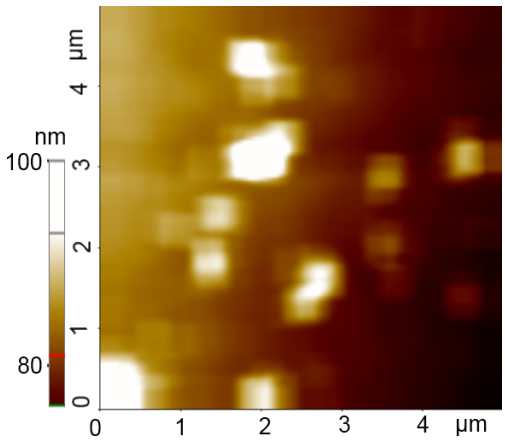

(c) Figure 4.7a enhanced by mean filtering.

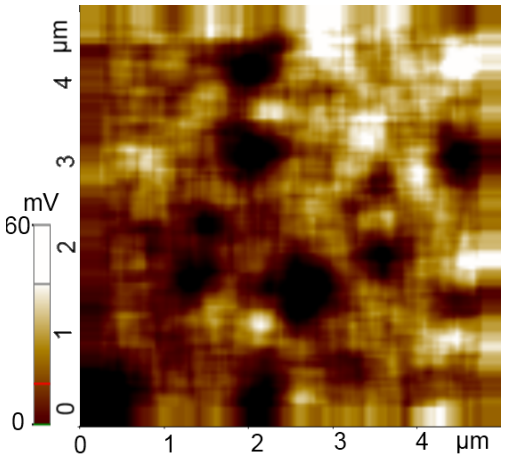

(d) Figure 4.7b enhanced by mean filtering.

Figure 4.7.: AFM images from spin coated PEDOT layers showing impurities which are not conductive and could therefore increase the resistivity of the bulk material.

Table 4.2.: A Taguchi matrix was used to test a complex set of parameters with a reduced number of experiments.

Experiment	Temperature (°C)	Time (min)	Solution
1	25 (A)	5 (A)	milli-Q (A)
2	25 (B)	10 (B)	SSC[a] (B)
3	25 (C)	15 (C)	DPBS[b] (C)
4	50	5	SSC
5	50	10	DPBS
6	50	15	milli-Q
7	75	5	DPBS
8	75	10	milli-Q
9	75	15	SSC

[a] Saline sodium citrate
[b] Dulbecco's phosphate buffered saline

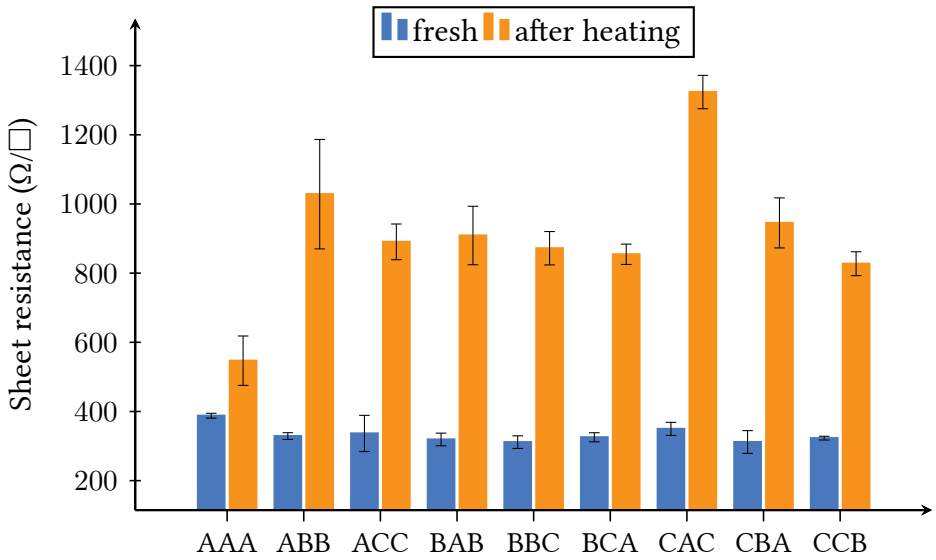

Figure 4.8.: Comparison of the sheet resistance of the samples in their fresh state (blue) and after the different heat treatments (orange). The letters on the x-axis correspond to the settings listed in table 4.2; as an example, AAA means 25 ℃, 5 minutes and milli-Q.

This method allows the testing of several parameters in parallel instead of testing them individually. Every experiment was done in triplicates and the sheet resistance was measured before and after each step of the experiment. All experimental results are shown in figure 4.8. It is clear that every treatment caused an increase of the sheet resistance and thus a decrease of conductivity.

To find the parameter which influences the electrode most (largest relative change), the "signal-to-noise ratio" (SN_i) of every trial and experiment was calculated with

$$SN_i = -10 \log \left(\frac{1}{N_i} \sum_{u=1}^{N_i} \frac{1}{y_u^2} \right) \tag{4.3}$$

where

i	experiment number
N_i	number of trials per experiment
u	trial number
y	relative change in sheet resistance

A new matrix was constructed which contains one SN-value for every parameter and setting. Comparing the values for the single settings (Δ) shows how much the outcome of the experiment was influenced by every particular parameter (large number means more influence) [**Rao2008**].

Table 4.3.: The influence of each individual parameter can be evaluated by comparing the variation of the signal to noise ratio. A large difference means that the parameter has a strong influence on the outcome.

Setting	Temperature	Time	Solution
A	−32.47	−33.14	−33.98
B	−34.81	−35.14	−33.49
C	−36.05	−35.05	−35.85
Δ	**3.58**	**2.00**	**2.36**

We learn from table 4.3 that temperature was the governing parameter, followed by the type of solvent. This is no surprise, since the higher temperature would accelerate any reaction going on. The ion content of the different solutions might also contribute to potential changes; PBS, which corresponds to setting **C** seems to have the strongest effect.

After one day of waiting, the sheet resistance was measured again and after that all samples were dipped for 10 s into a 4 % aqueous solution of iron tosylate. Figure 4.9 shows histograms of the sheet resistance distribution among the samples in their pristine state as well as after every experiment. The different heat treatments cause a wider spread in the distribution of sheet resistance values. After one day the resistance increased, but the range and the distribution did not change much. After dipping the samples into the iron tosylate solution, conductivity increased again and the spread was reduced. The sheet resistance of freshly prepared samples (333 ± 34 Ω/□) differed from those treated with iron tosylate (268 ± 42 Ω/□) by about 24 %.

It can be concluded, that the heating procedure does influence the conductivity of PEDOT, but the change is reversible by re-doping the polymer with tosylate. The assumption is that heating the sample in the presence of a solvent causes the dopant tosylate to diffuse out of the PEDOT matrix. The lower doping grade of the polymer leads to a reversible decrease in conductivity.

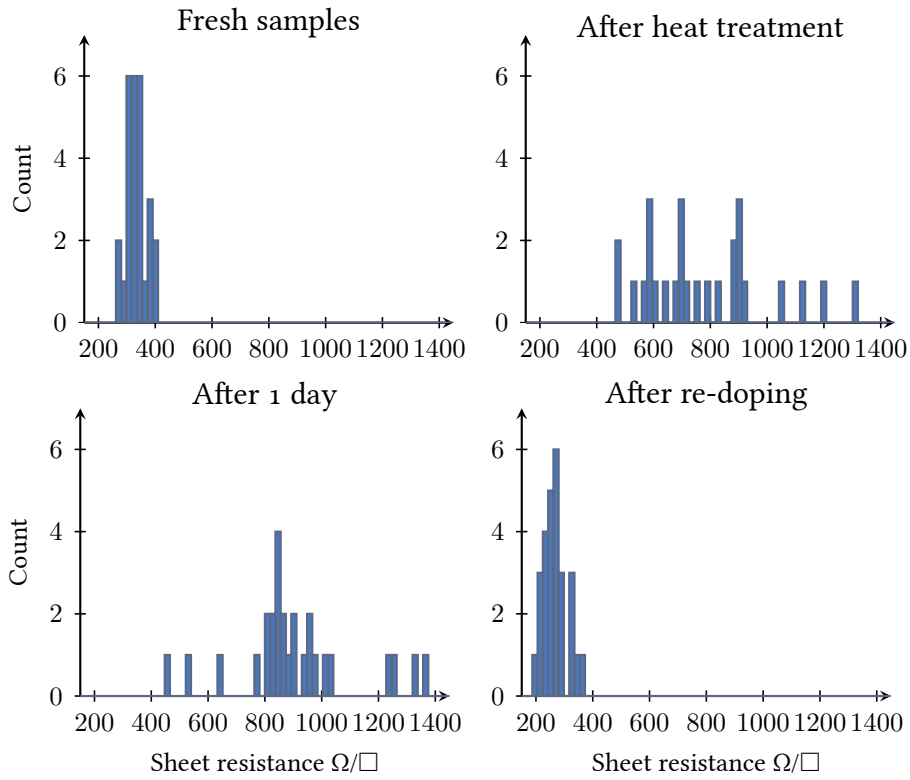

Figure 4.9.: Histograms showing the range and distribution of sheet resistance values for the investigated samples after different treatments.

4.3.3. Agarose stamping

The microfabrication procedure using agarose stamping for a chemical wet etch as described previously in section 4.2.2, page 25 was studied and optimised with a simplified pattern. This pattern comprises a series of microwires connected to individual contact patches (see figure 4.10 for micrographs of the mask and the silicon master). The smallest wire (2 µm) could unfortunately not be reproduced, so all measurements were done using the remaining four wires.

Our interests were especially in studying the influence of the stamping time on the resulting wire width and conductance. Another field of interest was the re-usability of the stamp, i. e. the number of times one and the same stamp can be used to reproduce a comparable pattern.

A series of patterns was stamped on PEDOT thin films using stamping times

from 30–120 s and a hypochlorite concentration of 1 %. The actual wire width was then measured with optical microscopy and a lens providing 50 times magnification. The measurement uncertainty was estimated to be 50 pixels, corresponding to 1 µm. The resistance of the wires was measured with an uncertainty of 0.01 %. In figure 4.11 the wire resistance was plotted against wire width for different stamping times. It is apparent that the resistance of the wires increased strongly with longer stamping times, while the observed width of the wires had a smaller effect.

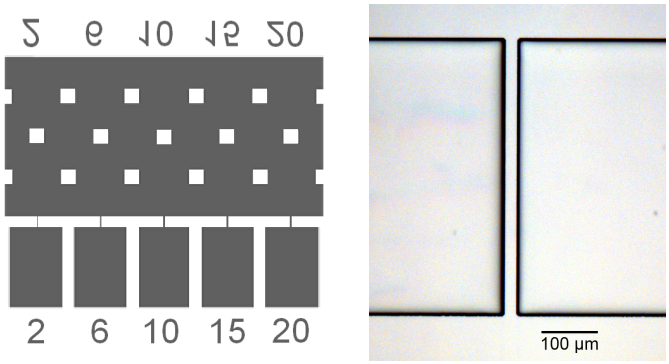

Figure 4.10.: The mask with five different wires (left) and the silicon master fabricated with deep reactive ion etching (right).

Assuming an ideally stamped wire of the width w, thickness h and length l with rectangular cross section and the specific resistivity ρ, the resistance R is

$$R = \frac{\rho \cdot l}{w \cdot t} \tag{4.4}$$

For the wires in the pattern length, thickness and resistivity were assumed to be the same for all samples, leaving the width w as variable. Using a power fit with the function $R = aw^b$ on the values shown in figure 4.11 allowed to compare the data.

The exponent b has the value −1 for inversely proportional factors as seen here. However, it was found that b decreased with longer stamping times from −1 for 30 s to −3.5 for 120 s stamping time (see table 4.4). This suggests that the conductive cross sectional area does not correspond to the measured values for wire with and height.

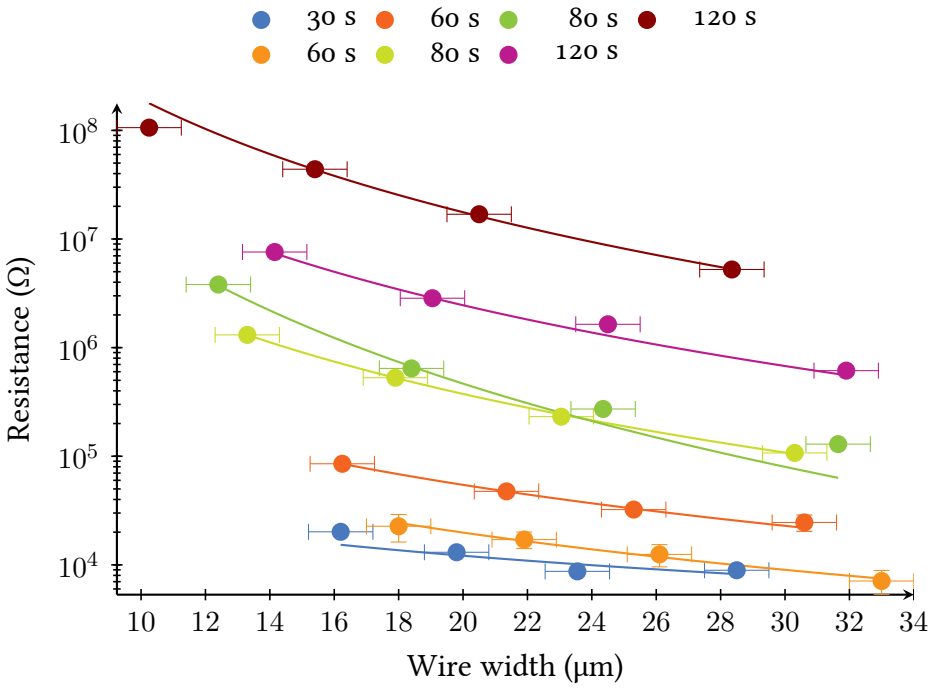

Figure 4.11.: The stamping time affected both the wire width and their resistance. Stamping longer than 60 s caused a great loss in conductivity.

This irregularity was investigated further with conductive AFM. A 105 nm thick PEDOT layer on a silicon wafer was stamped for 60 s. A comparison of the topographic AFM data with the conductive image is given in figure 4.12. As can clearly be seen, the conductivity of the wire was much lower than that of the

Table 4.4.: Fitting parameters for wire width/resistance data shown in figure 4.11.

t (s)	R^2	a	SD	b	SD
30	0.544	$8 \cdot 10^{-2}$	$4 \cdot 10^{-1}$	-1	0.50
60	0.977	$1.40 \cdot 10^{-5}$	$3 \cdot 10^{-5}$	-1.9	0.2
60	0.996	$5 \cdot 10^{-6}$	$4 \cdot 10^{-6}$	-2.14	0.08
80	0.999	$1.4 \cdot 10^{-9}$	$5 \cdot 10^{-10}$	-3.07	0.03
80	0.978	$2 \cdot 10^{-15}$	$5 \cdot 10^{-15}$	-4.4	0.3
120	0.993	$3 \cdot 10^{-9}$	$6 \cdot 10^{-9}$	-3.2	0.2
120	0.981	$1 \cdot 10^{-9}$	$2 \cdot 10^{-9}$	-3.5	0.2

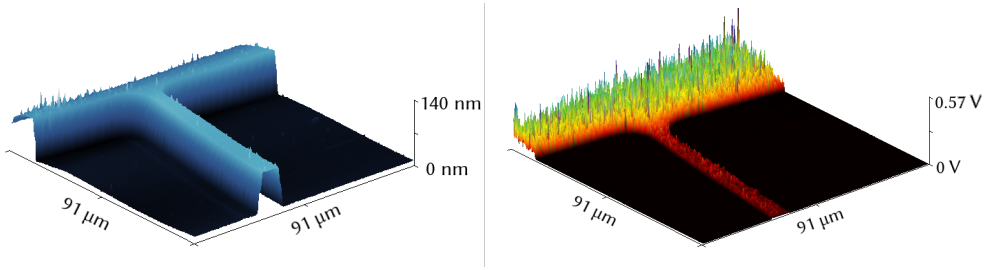

Figure 4.12.: A topographic image of a stamped PEDOT microwire (left) and a map of its conductivity (right) measured with AFM using a conductive tip in contact mode.

contact patch (area in the background), even though the height of the polymer layer was the same.

In figure 4.13 two-dimensional trace overlays are displayed; they show the topographic width of four wires together with the measured current signal. These measurements prove that a substantial portion (in average 5.5 ± 1.6 µm) of the wires was not conductive any more. The observed effect is most probably due to diffusion of hypochlorite or gaseous chlorine from the stamp into the PEDOT wire, over oxidising the conductive polymer partly in the process. This effect was also reported by Hansen et al. [25]. Since diffusion is time dependent this hypothesis explains the increasing conductivity loss for longer stamping times (see figure 4.14).

For future experiments it was decided to use 60 s stamping time, because it ensured that the PEDOT was etched all the way through to the substrate, while showing only minor deactivation due to diffusion. Another indication confirming the diffusion hypothesis is the comparison of the conductance of wires with different widths which were all stamped for the same time (60 s). Figure 4.15 shows the linear correlation of width and conductance as it would be expected in such a case.

While stamping using the same stamp repeatedly on a batch of PEDOT coated Topas® discs with the same stamping parameters it was observed that the resulting wires became larger and larger. A time series experiment was designed and its results are shown in figure 4.16. It was found that for all four wire sizes the actual width increased with the age of the stamp. From micrographs show-

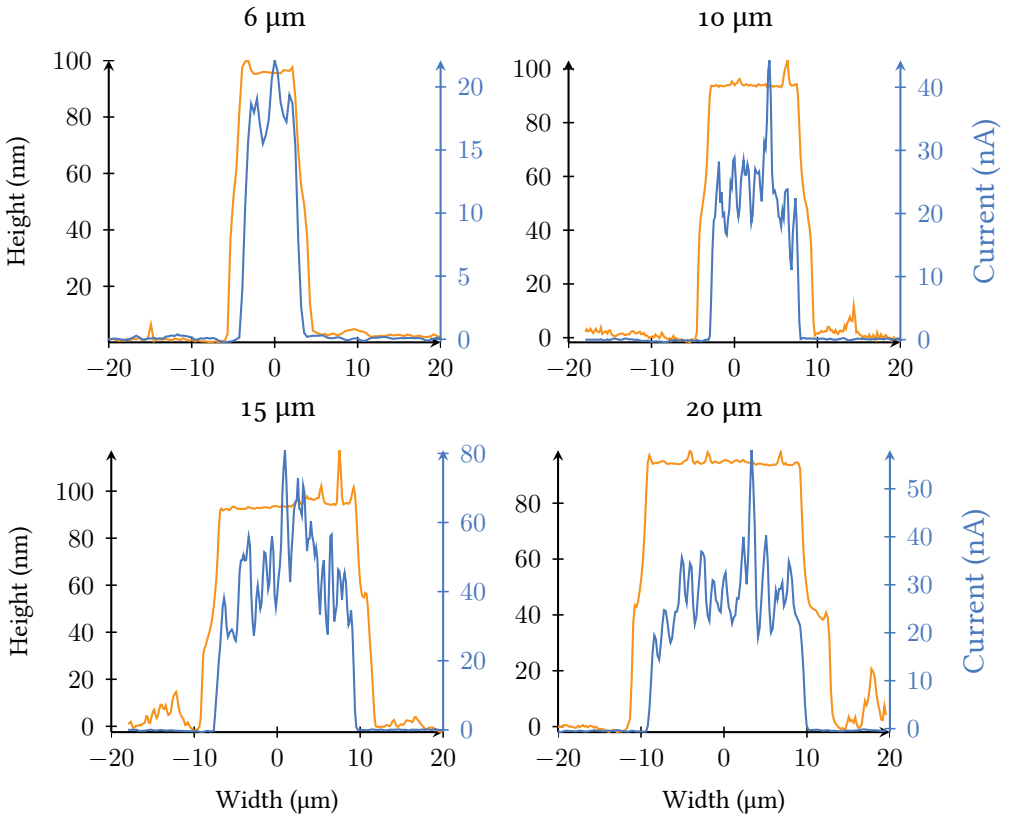

Figure 4.13.: Line profiles of topographic and conductive AFM measurements. The topographic profile (orange) suggests a wider wire, while the conductive measurements (blue) revealed the true dimensions of the wire. It should be noted, that no information about the effective height of the wires can be deducted from these images. The graph titles show the designed wire width.

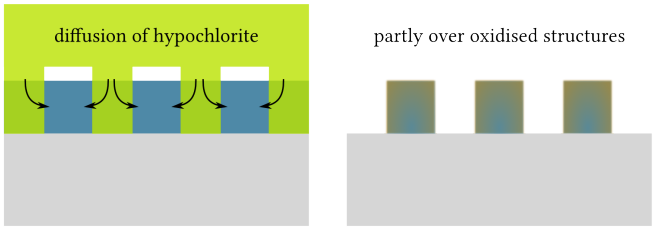

Figure 4.14.: Diffusing oxidation agents from the agarose stamp can attack polymer which is originally not exposed to the stamp. Long exposure time enhances the effect.

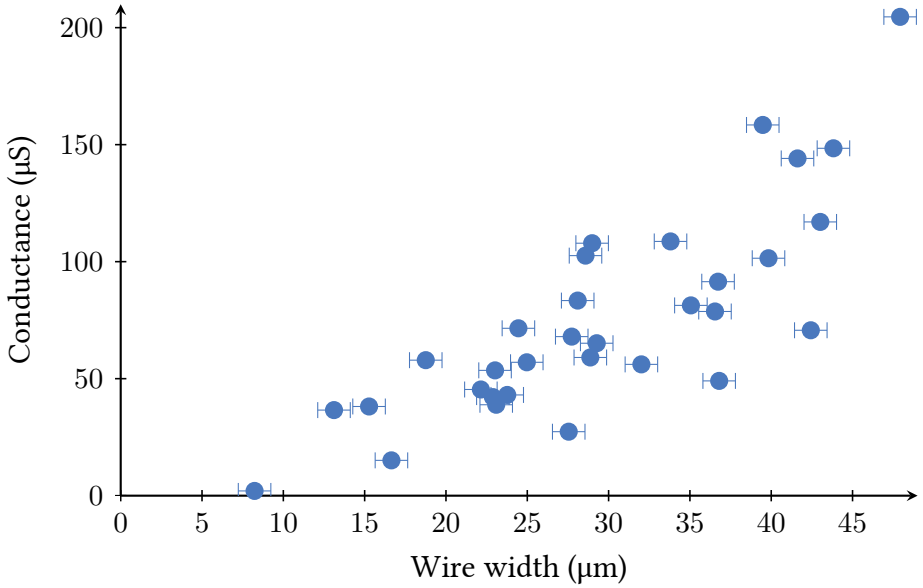

Figure 4.15.: The conductance of the wires correlated with their width if the stamping time was the same. All wires here were stamped for 60 s.

ing a fresh stamp and the same stamp after 1 h of repeated use (figure 4.17) it is clear that the trench defining the wire pattern was widened over time, causing the growing deviations from the originally designed size. This degradation was faster during the first few applications of the stamp and stabilised later.

4.3.4. Microelectrode fabrication

Using the parameters found in the previous study of the stamping process, interdigitated microelectrodes were fabricated in the same way. The silicon template was designed with a wire width and spacing of 20 µm. The size of the patterns allowed to use optical microscopy to measure wire widths of the electrodes and assess the overall quality of the pattern. In figure 4.18 optical micrographs of the Si master (a) and stamped patterns (b and c) are shown. It is obvious from these pictures that the pattern has not been reproduced very well in terms of wire width. The regularity of the pattern, however, was quite good. That means that the electrodes could be used for experiments, but it was necessary to measure the average wire size on each chip and take it into account

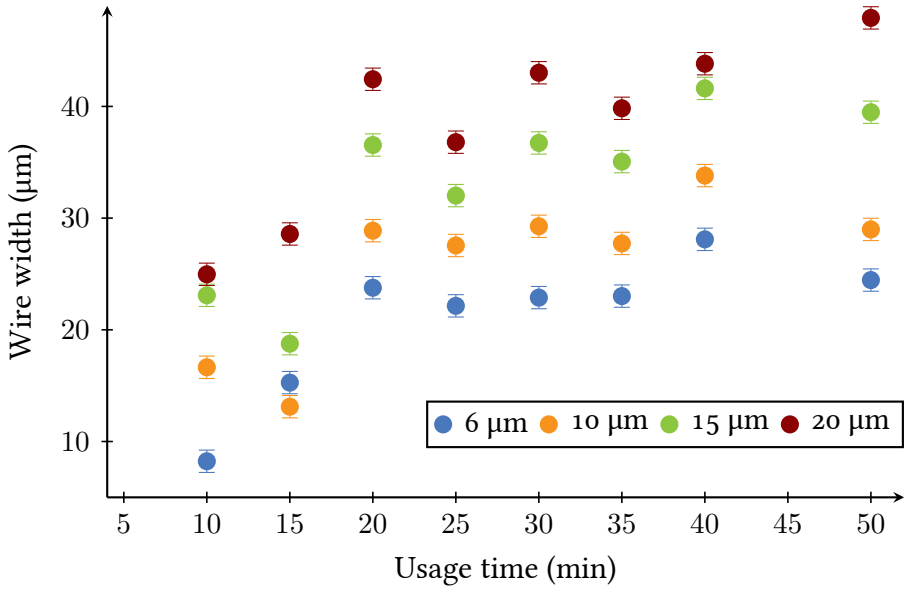

Figure 4.16.: The older the stamp becomes, the wider the wires turn out. The plot shows data from wires stamped with the same stamp over a period of time.

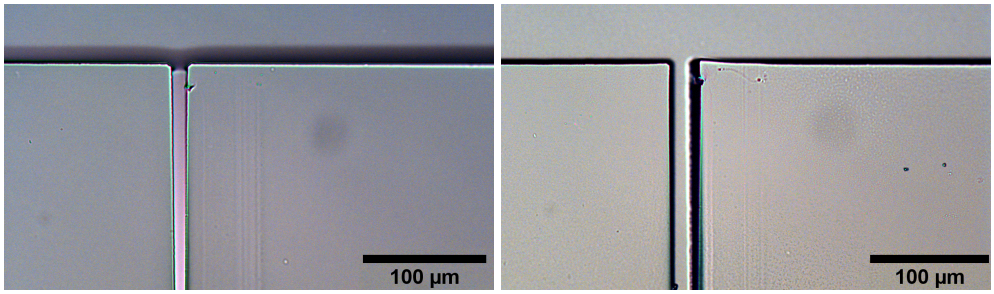

Figure 4.17.: An agarose stamp before (left) and after (right) use.

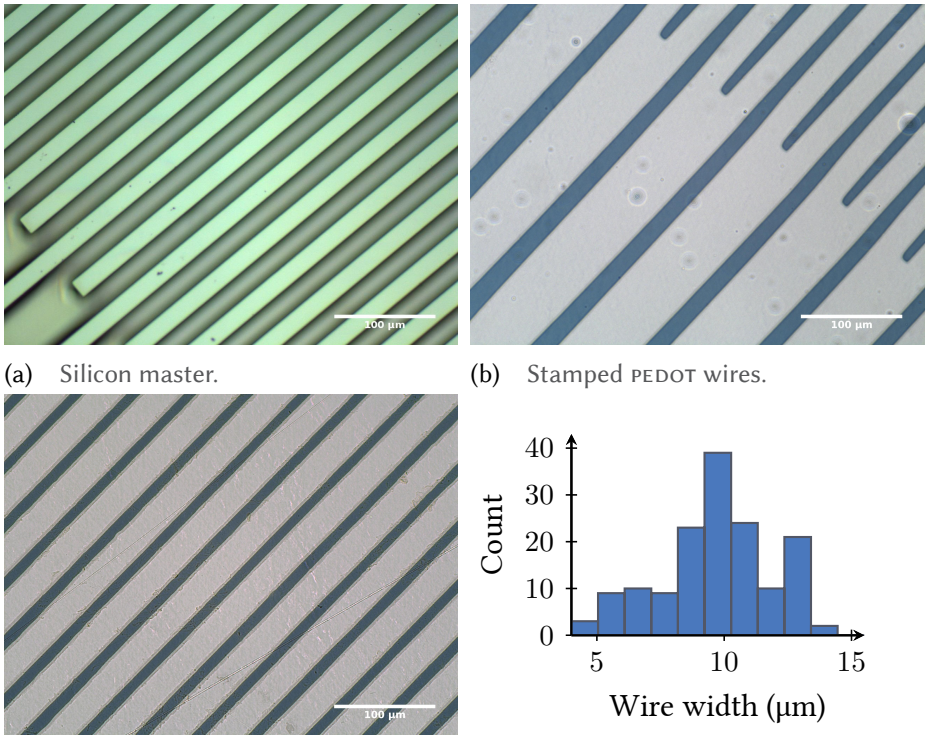

(a) Silicon master.

(b) Stamped PEDOT wires.

(c) Stamped PEDOT wires.

(d) Width distribution among the same batch.

Figure 4.18.: Micrographs of the silicon master (a) and stamped PEDOT wires (b, c). In image (b) the tips of the wires were slightly overexposed. All scale bars are 100 µm long. The histogram (d) shows the distribution of the wire width obtained from the same stamp.

when comparing results from different electrodes. The distribution of wires sizes within a single batch of stamped electrodes, i. e. they were all prepared with the same gel at the same day, is displayed as a histogram in figure 4.18 d.

Although being designed for 20 µm, a mean width of 9.7 ± 2.2 µm was found. As described above in section 4.3.3, page 35 the large deviation from the original wire size can be explained by diffusion processes occurring during stamping. Shortening the exposure time would certainly reduce the effect, however, the etching of the desired areas would not be complete then, resulting in residual conductivity between the wires. The degradation of the stamp by both time and repeated use as observed with the other pattern could also add to the uncertainty. It is possible that, due to the different geometry, not the trenches

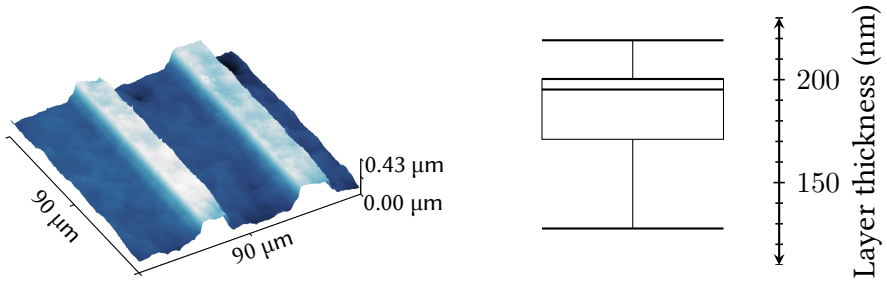

(a) A three-dimensional representation of an AFM image of stamped wires.

(b) Box plot showing statistical data of AFM height measurements.

Figure 4.19.: The three-dimensional AFM image shows two PEDOT wires from a stamped pattern (a). Line traces over such wires were used to determine the film thickness, summarised in the box plot (b).

in the stamp widened, but the agarose dividers were squashed, thus resulting in narrower trenches. A third factor adding to the poor reproducibility may also be owed to the manual application of the stamp without the possibility of uniform pressure control.

AFM measurements were used to investigate the patterns further. Figure 4.19 a shows a three-dimensional representation of two stamped electrode wires. Evaluation of line profiles over scans from seven different chips showed that the average film thickness was 186.6 ± 29.5 nm. The box plot in figure 4.19 b displays further statistical data. This value is less than what would be expected considering the data presented in section 4.3.1, but it can well be that there was a remainder of over oxidised PEDOT left on the surface.

4.4. Conclusion

The coating of Topas® and silicon wafers with thin films of the conductive polymer PEDOT and the patterning of these films has been studied. The films were prepared by spin coating a reactive mixture containing the monomer 3,4-ethylenedioxythiophene onto the two substrates. The thickness of these layers was controlled within a narrow margin by adjusting the spin rate. As expected, higher spin rates led to thinner layers.

By measuring the sheet resistance of the layers it was found that the conductivity of PEDOT was independent of the layer thickness within one order of magnitude; applying thicker layers or bilayers, however, increased the conductivity. Unlike previously reported for PEDOT:PSS [**Farah2012**], the conductivity of tosylate doped PEDOT, as it was used here exclusively, was not permanently increased by heating in dry condition. However, immersing the polymer in an aqueous medium and heating it there caused a significant but reversible increase of the sheet resistance.

The patterning of PEDOT was studied using a simple template with wire structures of different sizes. It was found that the stamping time can affect the conductivity of the patterned wires, even though their visible dimensions stayed in a similar range. Conductive AFM measurements revealed that the physical wire width was considerably larger than the "conductive wire width". This suggests that hypochlorite or chlorine diffused from the stamp into the pattern, over oxidising the conductive polymer in the process. Interdigitated electrodes for later applications as biosensors were also produced in this way. A compromise allowing complete oxidation of the exposed portions of the pattern, while keeping the diffusion induced conductivity losses in the wires at a minimum was found with a stamping time of about 60 s. Wires fabricated with this setting showed a fairly linear correlation of conductance and wire width; this confirms that the ratio of physical and conductive wire width did not vary significantly.

The mean wire width achieved using this technique turned out to be approximately 50 % of the designed value and some electrodes were too thin for good measurements. Additional optimisation of the stamping procedure is therefore

required, but also a template with larger structures might improve the yield of good patterns. It was further observed that repeated use of one and the same stamp caused a steady change in the reproduced patterns due to wear and tear. In conclusion this means that agarose stamping has been proved to be a useful way for rapid prototyping. For applications at a larger scale, however, it would be advisable to rely on faster and more reproducible methods, like for example roll-to-roll processing as it is used already for the production of polymer photovoltaic cells [**Krebs2009**].

5. Aptamer selection process

5.1. Introduction

As alternatives to antibodies, aptamers have recently attracted increasing attention due to their capability to bind a wide range of targets: nucleic acids, proteins, metal ions and other molecules with high affinity and sensitivity [**Song2012Sensors**, **Hong2012**].

Aptamers are peptides or oligonucleotides (RNA or single stranded DNA; ssDNA) that bind to a specific target molecule. The aptamers typically fold into a three-dimensional structure, whose conformation is changing upon ligand binding.Their biological analogues are riboswitches – parts of the messenger RNA capable of regulating the translation by specific ligand binding [**Winkler:2002gd**]. Uses for aptamers have therefore been proposed in the sector of macromolecular drugs as artificial riboswitches for the treatment of cancer or other diseases. For analytical purposes aptamers compete with the well established and characterised antibodies, but they have a few advantages. While showing similar affinity and specificity towards their target molecules as antibodies, aptamers are more stable against environmental influences like heat or harsh chemical conditions, because they do not necessarily denature irreversibly. Kept under sterile conditions, their shelf life is virtually indefinite. Their target range is also not limited to immunogenic compounds, but comprises a vast quantity of small and large molecules, viruses, bacteria, whole cells, and even single ions. The in vitro selection and production of aptamers poses major advantages over the in vivo processing of antibodies, since it excludes batch-to-batch variations and reduces costs, while being faster at the same time [**Lee08**]. For some analytical methods the size difference of aptamers and antibodies is also an important factor. Impedimetric sensors or field effect

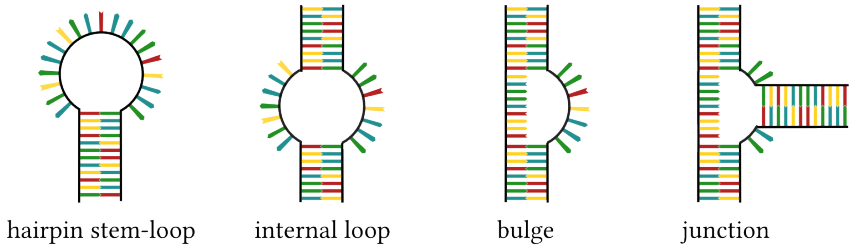

Figure 5.1.: A few examples of common RNA secondary structures.

transistors are most sensitive when the binding event happens within the so called Debye screening range. This distance is determined by the ion concentration in the electrolyte surrounding the electrode; for biologically relevant solutions it is in the range of 5–10 nm. Aptamers typically fall into this size range, while proteins are much larger than that. The oligonucleotide aptamers can also easily be modified with signal moieties and can be produced at low cost. Up to now, a variety of assays have been successfully developed for aptamer-based detection of biomolecules [**Guo2008**, **Centi2007**, **Wu2011**, **Yan2010**].

The affinity of an aptamer towards a ligand is mainly owed to the stabilisation of secondary structural motifs in the presence of the right ligand. Typical motifs are hairpins, duplexes, loops, G-quadruplexes, bulges, junctions and internal loops [**Batey1999**]. Graphical representations of a few motifs are shown in figure 5.1.

The target molecules are integrated into those structures and can form pseudo-basepairs with single nucleotides over hydrogen bonds or electrostatic interactions. Planar molecules such as theophylline or flavin mononucleotide can also stack on top of coplanar structural motifs of the aptamer [**Patel1997**, **Famulok1999**, **Hermann2000**].

To force certain structures or to protect aptamers from degradation through nucleases, artificial bases were inserted into oligonucleotides to form so called xeno-nucleic acids (XNA) or locked nucleic acids (LNA) which establish oxymethylene bridges to retain certain motifs [**Veedu2010**, **Pinheiro2012**].

These modifications can also be made after the selection procedure described in the following [54].

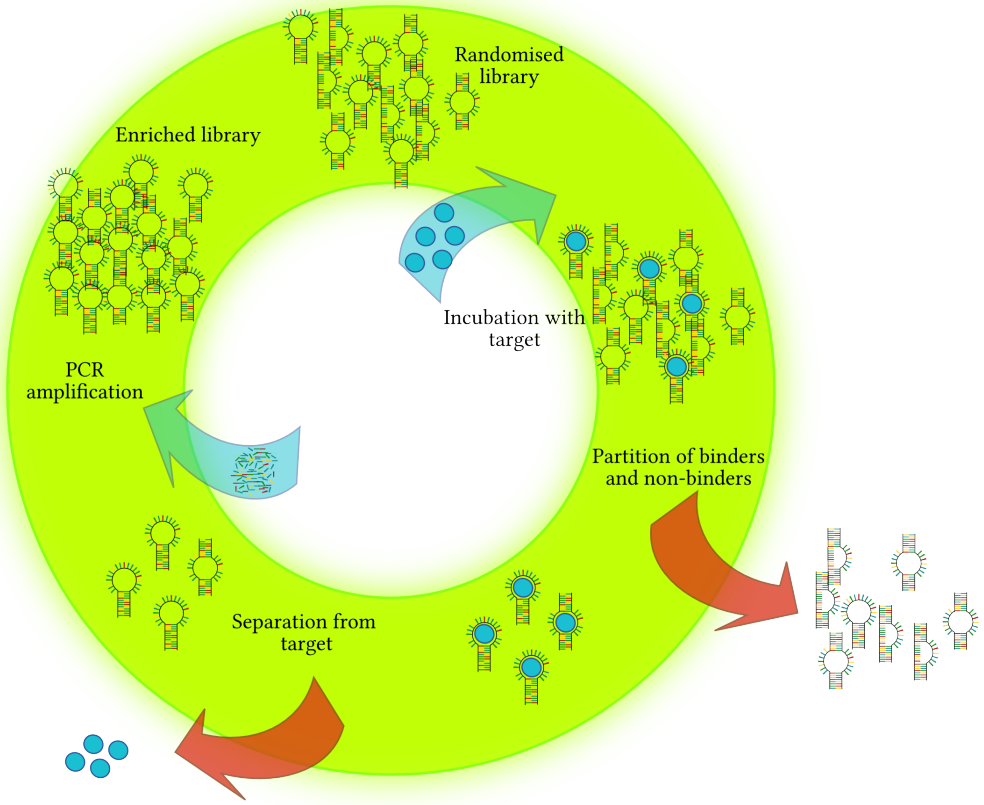

Figure 5.2.: Illustration of the SELEX process. A random DNA pool (library) is incubated with a target molecule. Some of the strands bind to the target, the others are discarded. Binding strands are then amplified via PCR and used for another selection round.

Novel aptamers can be developed using a process called **s**ystematic **e**volution of **l**igands by **ex**ponential enrichment (SELEX) [**Ellington1990**, **Tuerk1990**]. SELEX describes the iterative selection of high affinity aptamers from a large pool of randomised oligonucleotides. Figure 5.2 shows a graphical representation of the process. The cycle is started with a random pool consisting of oligonucleotides. This so called library comprises oligonucleotides which are typically between 30 and 80 bases long and have defined regions for primer annealing on both ends and random sequences in the middle. The library is then incu-

bated with purified target molecules in a buffered solution, the selection buffer. In the next step, target/DNA (or RNA) complexes are separated from the non-binders in the pool. After stripping the complexes of the targets, the DNA can be amplified via polymerase chain reaction (PCR) . The resulting double stranded product must be denatured and separated. If an RNA pool was used for selection, transcription steps are necessary. The enriched pool resulting from this first round of selection is incubated again with the target and the whole procedure is repeated. Depending upon the quality of the separation of binders and non-binders, up to 20 rounds of selection are necessary before aptamers with reasonable affinity can be obtained. To increase the selectivity of the resulting aptamers, it is often necessary to include counter-selection steps where a pool is incubated with a substance similar to the real target and only the remaining oligonucleotides are used for further selection. Other measures to increase the quality of the selected aptamers include increasing the stringency of the selection process by varying temperature or salt concentration of the selection buffer.

After a sufficient number of cycles the enriched library is cloned and sequenced. Comparing the sequences can give hints of the region responsible for the affinity to the target. To find out which of the aptamers is the best, affinity assays are usually carried out using different methods [**Tuerk1990**, **Ellington1990**, **Lee08**].

Probably the most challenging part of the SELEX process is the separation of binders and non-binders. In this crucial step it is very important to remove as many of the weakly or unspecifically binding DNA sequences as possible in order not to amplify them in the PCR step [**Gopinath2007**, **Stoltenburg2007**]. Not only will a good separation method help reduce the number of necessary selection rounds, it will also increase PCR performance because the chance for unspecific annealing is reduced in a less random pool. To address this issue, many possible solutions were developed in the recent past. **Gopinath2007** compiled an extensive list of different partitioning techniques together with their individual benefits and shortcomings [**Gopinath2007**]. Likely the most important of these methods are the immobilisation of the target onto an affinity

matrix such as sepharose or agarose [**Liu2005**, **Tombelli2005**] or onto magnetic beads [**Kikuchi2003**, **Lupold2002**, **Stoltenburg2005**]. Both of these methods require very little instrumentation but could cause undesired chemical modifications of the target during immobilisation. If ultracentrifugation over nitrocellulose [**Bianchini2001**, **Schneider1993**, **Tuerk1990**] or capillary electrophoresis [**Mendonsa2004**, **Mosing2005**, **Tang2006**] are used to separate target/aptamer complexes from non-binders the ligand can be used free in solution; also lower amounts of target are required using these techniques.

Less used methods comprise flow cytometry [**Davis1996**], surface plasmon resonance [**Misono2005**], centrifugation [**Rhie2003**], UV-crosslinking (photoSELEX) [**Jensen1995**] and electrophoresis [**Smith1995**]. There have also been attempts to automate the whole process [**Cox1998**, **Cox2001**, **Eulberg2005**], but so far none of these techniques is used at a larger scale.

In our attempts to select aptamers against the inositol triphosphate receptor (IP3) or the metalloprotease-like enzyme karilysin we mainly used three of these methods. The selection of IP3 was tried on magnetic beads with immobilised target. For the selection of karilysin aptamers the protein was in a first attempt immobilised onto a standard polystyrene microtiterplate. After problems had arisen using this protocol the separation method was changed and capillary electrophoresis (CE) was used instead.

Unfortunately it turned out that too many problems came up after several rounds of selection and that the ultimate goal, finding an aptamer against a virus, could not be achieved within a reasonable time frame that allowed further development of the sensor system. For this reason we fell back on the use of aptamer sequences from the recent literature for proof of concept experiments with our biosensor.

This chapter describes the different SELEX protocols used for the selection of aptamers against IP3 and karilysin. A discussion about the problems encountered and suggestions for solving them as well as a possible way to use capillary electrophoresis in classified labs with limited space are presented.

5.2. Experimental part

This section will detail the experimental conditions for the aptamer selection procedures tried in the course of the PhD project. Although three different methods were tested, they differ mainly in the separation step, while the rest of the procedure remains the same or is very similar. As described at length on page 49 the SELEX cycle starts with the incubation of the random library with the target molecule. DNA molecules with little or no affinity to the target are washed away, while binding oligonucleotides are transferred to the next step. There, they are released from the target and amplified using polymerase chain reaction (PCR). After removing one strand from the double stranded reaction product, the enriched library is incubated again with fresh target and the procedure is repeated.

In the following the selection of aptamers against the receptor IP3 is described.

5.2.1. Preparation of the initial library

A randomised DNA pool was purchased from Eurofins (Germany) and had to be amplified. A PCR master mix was prepared from concentrated solutions according to table 5.1. For a small scale test-PCR 100 µL master mix were blended with 0.5 µL Taq polymerase (DreamTaq®, 5 u/µL) and split up into two PCR tubes; one as control without template, one with 1 µL template, yielding a DNA concentration of 200 pM. The reaction was run with the parameters listed in table 5.2 a.

To evaluate the PCR product a 4 % agarose gel was cast from ultra pure agarose (Invitrogen) and 1×trisborate EDTA (TBE) buffer. Before casting 5 µL ethidium bromide were added to the gel. Agarose gels were usually prepared in large scale and stored at 4 ℃ in a sealed bag. The gel was run for 15 minutes with 2.5 µL sample and 2.5 µL gel loading solution (Invitrogen) in each but one well and a ladder (GeneRuler™ Ultra Low Range Ladder, Invitrogen) as length marker. The applied potential was 120 V. After verifying that there was only a single band in the sample well the PCR was repeated at a larger scale (2×100 µL)

Table 5.1.: PCR mastermix prepared as stock solution for later reactions.

Amount	Substance
100 µL	10× DreamTaq® buffer containing 20 nM $MgCl_2$
20 µL	10 nM dNTP (d-nucleotide mixture)
60 µL	50 nM $MgCl_2$ (end concentration: 5 nM)
20 µL	10 nM NSLRbt (reverse primer with biotin tag)
20 µL	10 nM NSLF (forward primer without biotin tag)
820 µL	Milli-Q water; 40 µL more were added to compensate for pipetting errors

Table 5.2.: Thermocycler protocols for PCR and denaturation of a single stranded DNA library.

(a) Time and temperature protocol for PCR.

Time (s)	Temperature (°C)	
120	95	
30	95	7 cycles
30	55	
30	72	
300	72	
∞	4	

(b) Time and temperature protocol for denaturation and folding.

Time (s)	Temperature (°C)	
120	95	3 cycles
60	25	
300	95	
∞	25	

with the same settings. Gel electrophoresis confirmed the success of the reaction.

5.2.2. Strand separation

The PCR product was double stranded DNA (dsDNA), so one strand had to be removed for the aptamer selection. For this step 10 µL streptavidin coated magnetic beads (⌀= 1 µm, SiMag) were washed twice in 150 µL phosphate buffered saline (PBS) using a magnetic separator. The beads were then incubated with 150 µL PCR product for 30 minutes After removing the supernatant, the beads were washed with PBS and incubated with 100 µL 100 nM NaOH for exactly 10 minutes The supernatant was transferred to a fresh vial and mixed with 2 µL

glycogen (1 mg/mL), 10 µL sodium acetate (3 M, pH 5.5) and 300 µL cold ethanol to precipitate single stranded DNA (ssDNA). The mixture was cooled for 30 minutes at −20 °C, centrifuged for 15 minutes at 20 000 g, washed with cold 70 % ethanol, centrifuged again with the same settings and dried after removal of the supernatant.

5.2.3. First selection round

For the first round of selection 10 µL magnetic beads (⌀= 1 µm, hydroxyl groups on surface, hexyl linkers) functionalised with IP3 were washed twice with 100 µL of the binding buffer 100 nM K_2PO_4 + 5 nM $MgCl_2$ (pH 7). The precipitated and dried ssDNA library was dissolved in 50 µL binding buffer and heated in a thermal cycler according to the procedure listed in table 5.2 b to denature and fold the strands. The solution was then transferred to the magnetic beads where it was incubated for 1 h at room temperature during which the suspension was shaken every 15 minutes. The beads were then washed five times with binding buffer before binding DNA strands were eluted using 100 nM NaOH. Dissolved ssDNA was then precipitated from the eluent as described in section 5.2.2.

5.2.4. PCR amplification

The precipitated ssDNA pellet from the first selection round was dissolved in 10 µL milli-Q water. A small scale pre-amplification was run using 35 µL of the master mix (table 5.1), 0.25 µL Taq polymerase and 1 µL template DNA. PCR parameters were the same as in table 5.2 a but with 21 cycles instead of seven. The remainder of the DNA was stored at −20 °C as backup and for later reference. After confirming the success of the PCR with gel electrophoresis, 4 µL of the product were amplified in two 100 µL batches using the protocol from table 5.2 a. As preparation for the next round, the strands were separated as described before (section 5.2.2).

5.2.5. Negative selection and second cycle

To exclude DNA which binds to the beads instead of the target, a pre-selection was made with denatured DNA from the first cycle against hydroxyl-modified magnetic beads. After 1 h incubation time at room temperature the supernatant was transferred directly onto washed IP3 functionalised beads and the selection round was continued like the first cycle.

5.2.6. Further selection rounds

A third SELEX round was started after moving to our new laboratories but unfortunately the results obtained before at SDU in Odense were not reproducible in our facilities. After several unsuccessful trials the project was discontinued in favour of new SELEX protocols for two other target molecules, karilysin and amyloid β42, to support one of our collaboration partners and a fellow PhD student, respectively.

5.2.7. SELEX with surface bound target

The following experiments were done in close collaboration with Lasse Holm Lauridsen who was a research assistant in our group at the time and worked on the selection of an anti-karilysin aptamer. As mentioned before, most steps do not differ substantially from those described in connection with the selection of IP3 aptamers and therefore only the partition techniques will be detailed here. While in the procedure shown above magnetic beads were used to separate binding DNA from non-binding strands, the peptide amyloid β42 (Aβ42) was immobilised directly into a reaction vessel of a 96-well plate. A 1 µg/mL solution of Aβ42 in sterile filtered PBS was prepared and 100 µL were transferred into one well of a standard polystyrene microtiterplate (96-well, Nunc). Another well was filled with 100 µL sterile filtered PBS for the negative selection. The well plate was incubated over night at 4 °C. After removing the liquid, the surface of the wells was blocked by adding 100 µL of a 4 % bovine serum albumin (BSA) solution and incubation on a shaker (300 rpm) for 2 h at room temperature.

Both wells were then washed five times with washing buffer (0.1 % Tween® 20 in PBS).

The library was prepared by heating it to 95 °C for 5 minutes and then cooling it on ice. 100 µL of a 1:1 mixture of library and 4 % BSA solution in PBS were added to the well for negative selection (no peptide). After 20 minutes this solution was transferred to the well containing Aβ42 and incubated there for another 30 minutes The well was washed ten times with washing buffer, then binding strands were eluted with 100 µL 6 M guanidinium-HCl for 25 minutes Afterwards the dissolved DNA was precipitated as described in section 5.2.2, page 52 and amplified with PCR running the protocol in table 5.2 a with ten cycles.

5.3. Results and summary

Although a great deal of time was spent on the development of aptamers against the receptor IP3, the peptide Aβ42 or the protein karilysin, unfortunately no results can be presented here. However, the problems should be discussed and possible solutions or improvements should be suggested.

The main problem observed during both the selection with magnetic beads, as well as when the target molecules were immobilised on a solid support (polystyrene) was the same: after several rounds of selection (typically between four to six) only little DNA was left in the eluent and therefore the template concentrations were low, requiring a large number of PCR cycles. With an increasing number of cycles, however, the band of the PCR product became more and more widened in the gel electrophoresis. This suggests that DNA strands might have hybridised randomly in the mixed pool and that those unspecific products were amplified together with the desired sequences. Another problem which arises in later SELEX rounds is that impurities are often dragged along with the DNA and accumulate over time. An additional problem with Aβ42 was, that the peptide seems to inhibit the polymerase.

To overcome these problems a method with better separation performance was tried: capillary electrophoresis (CE) was reported to allow aptamer selections in only a few rounds and a protocol called non-SELEX was suggested. During the non-SELEX procedure several selection rounds are made without amplification steps. That means, that binding strands are separated from the non-binders with non-equilibrium capillary electrophoresis and incubated with ever lower target concentrations [**Berezovski2005**, **Berezovski2006Art**]. This technique required advanced instrumentation, but could be automated to a certain extent. After an initial success with good separation it turned out, that the glycogen used as co-precipitant in the strand separation procedure accumulated in the working solutions and associated with the DNA. The glycogen impurity migrated also at a similar rate to the target/aptamer complex in the capillary, thus making a further isolation impossible.

It can be summarised that CE has the biggest potential of all tried solutions

because it offers a better separation performance and can be semi-automated. In order to use it, though, other modifications to the SELEX protocol have to be made. The strand separation could for instance be improved by using a specific nuclease which would digest a properly tagged strand. This method would also avoid the use of glycogen in the post-processing of this step. Further efforts could also include the development of a lab-on-chip solution for CE-SELEX. This would reduce sample volume and could be fully automated. The small size of the device would it make especially interesting for selection of anti-virus aptamers, because of the limited bench space required in a classified laboratory and the possibility of making it disposable.

We decided that the optimisation of one of the tested SELEX protocols would require much more time than scheduled for the aptamer selection and so retard the development of the biosensor (which was the primary goal of the thesis). So the aptamer work was discontinued for this project and we used known sequences from literature for the proof of concept experiments.

6. Functionalisation of the microelectrodes

6.1. Introduction

As already described in section 2.1, page 3, electrochemical biosensors comprise a sensing layer usually consisting of biological building blocks such as oligonucleotides or proteins (e. g. antibodies, enzymes, streptavidin). Although there are many different configurations of biosensors, most of them require the irreversible immobilisation of the biological entity to a substrate or transducing element.

It was therefore of continuous interest in the past to find suitable methods for tethering biomolecules to surfaces, so it is no wonder that there are a number of viable solutions to this problem. Since this thesis is entirely about polymeric devices, the numerous immobilisation methods for silicon or gold-based substrates are intentionally left out. However, some of the procedures described herein might also be transferable to non-polymeric compounds.

The conducting polymer layer required for the electrochemical sensing is often polymerised in situ because of the poor solubility of most conductive polymers. To combine the synthesis with the immobilisation, one approach is to synthesise the polymer in the presence of the biological component and rely on random entrapment of the biological macromolecule. While being a very simple technique which does not require any modification of the biomolecule, it certainly has its drawbacks. There is little or no possibility to control the final conformation of the molecules and many will be inaccessible to the analyte or have reduced functionality because of spacial constraints [4].

Not as stable as most covalent bonds, but still frequently used, is the strong interaction between the protein streptavidin and biotin. The protein is usually applied to a surface and immobilised by physisorption. The target molecule,

i. e. the capture probe which is to be immobilised, carries a biotin extension which then docks to the streptavidin layer. This method does not require the use of other chemicals and is rather fail-safe. However, harsh environmental conditions (e. g. high/low pH, elevated temperature) can easily cleave the bond or even denature the protein, rendering it permanently ineffective [**Hoogenboom2005**, **Binz2005**].

There exist a very large number of procedures to link biomolecules to a polymer substrate via strong covalent bonds. An exhaustive review summarising and comparing many covalent linkers and cleaving strategies for solid phase organic synthesis was published by **Guillier2000** Many of these reactions are also suitable for immobilisation purposes. Among those, carbodiimide coupling methods have been used to form amide bonds between different substrates and biomolecules. One prominent advantage of this approach is that the reaction can be accomplished by utilising functional groups which are naturally available in proteins: amines or carboxylic acids. Oligonucleotides need to be modified to obtain either of these moieties. A disadvantage of this kind of reaction is the lack of selectivity: once a substrate-bound carboxylic acid group is activated with the carbodiimide, any amine will bind to it. A more specific possibility is Huisgen-type click chemistry as has recently been used on a biosensor by Lind et al. [30]. In this copper catalysed reaction an alkyne forms a stable bond with an azide. Reaction conditions are mild, but suitable chemical modification of both substrate and biological component are required.

As opposed to these wet-chemical techniques, recently the dry immobilisation of unmodified oligonucleotides on different polymers based on UV-induced crosslinking was reported [**Dufva2006**, **Kimura2006**, **Sabourin2010**]. The method is very suitable for DNA fixation and less expensive than comparable procedures using non-nucleic acid terminal modifications as linkers [**Sun2012**]. An example for these techniques was published by **Koch2000** and works with anthraquinone as photo-active agent.

For the work in this thesis, three premises were made regarding the functionalisation of the electrodes: firstly, it is important to keep the binding probe close to the surface. This necessity is owed to the working principle of impedance

spectroscopy (detailed in section 2.4, page 9). The sensitivity is attenuated with growing distance from the surface, therefore a short linker is preferable. To allow room for probe-target interaction, however, the linker must not be too short. The second premise is the versatility of the method, i. e. it should allow us to use the sensor as a platform where different probes can be grafted on in the same fashion according to the particular needs of the respective application. Thirdly, we were limited in the assortment of viable PEDOT derivatives with functional groups ready for further grafting steps.

The monomer with the best availability besides plain EDOT was the hydroxymethyl derivative EDOT-OH (see section 3.1, page 13 for further details). Hydroxyl moieties are not very reactive compared to other functional groups, but they have received much attention in the field of glycoside synthesis [**Guillier2000**]. Two methods were found to be promising to fulfil the requirements mentioned above: phosphoramidite coupling and carbodiimide based reactions.

Phosphoramidites are phosphite derivatives with an amino substituent. They are most popular in the automated in vitro synthesis of DNA-oligonucleotides on solid supports [**Nurminen2000**]; but this kind of reactions has also been used for phosphorylation of sugars via their hydroxyl groups [**Cooke1987**, **Hamblin1987**].

As shown in figure 6.1, a phosphate linker is formed between the hydroxyl moiety of the polymer and the molecule to be immobilised during the reaction. The first stage is the substitution of the chloride with the alcohol in presence of an organic base. *N*,*N*-diisopropylethylamine (DIPEA, Hünig's base) is suitable for this task and commonly employed. Coupling of the target molecule (illustrated as R_1–OH) over its hydroxyl group is done in presence of the acidic catalyst 1*H*-tetrazole. Since hydrolysis of the phosphoramidite is a competitive reaction, all reactions have to be carried out in water-free conditions and at ambient temperature. Suitable solvents are tetrahydrofuran (THF), dichloromethane (DCM) or acetonitrile. Both THF and DCM dissolve the substrate Topas®, so acetonitrile is the best choice.

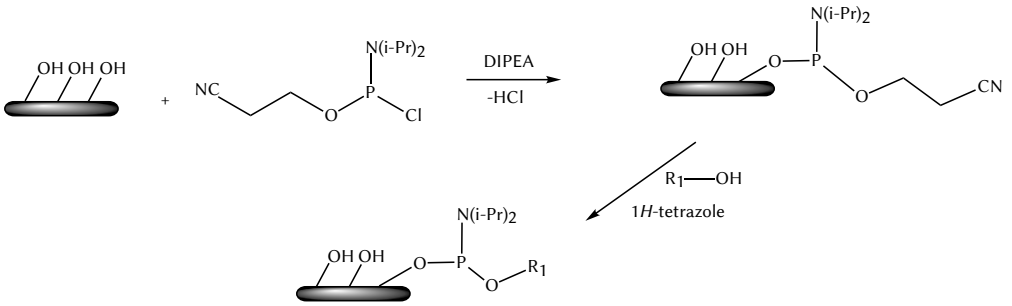

Figure 6.1.: Reaction mechanism of the phosphoramidite mediated immobilisation of a target molecule R_1 to a solid support (grey).

Carbodiimide mediated coupling reactions on the other hand are very common in glycoside chemistry [**Guillier2000**], but have also been used for immobilisation purposes on solid support [**Janolino1982**]. These reactions facilitate formation of an amide bond between a carboxylic acid and a primary amine group. Since the conductive polymer coating described in chapter 4, page 22 has neither, but only a hydroxymethyl group, it has to be prepared first. This preparation can be done by esterification with a dicarboxylic acid. The coupling agent 1-ethyl-3-(3-dimethylaminopropyl)carbodiimide (EDC) can be used to facilitate the formation of an ester between the hydroxyl group of the polymer and succinic acid. The reaction mechanism is analogue with the one described below for the immobilisation of a bioprobe, but instead of obtaining compound **2** (see figure 6.2), the ester with the hydroxyl moiety of the polymer is formed (**March1985** (1985), p. 350 [**March1985**]).

Having a carboxylic acid available on the polymer and an amino group tethered to the 5'-end of the DNA-strand, the probe can be immobilised according to the mechanism shown in figure 6.2. Like in the grafting reaction described above, EDC is used for activation of the carboxylic acid group. This first step yields the stable *O*-acylisourea intermediate (**1**) which then reacts acid catalysed with *N*-hydroxysuccinimide (NHS) to form the ester **2**. This compound is stable and a surface prepared this far can be stored for later functionalisation. The leaving group NHS is cleaved off during the nucleophilic attack of the amine group (aminolysis) and the final compound **3** is formed.

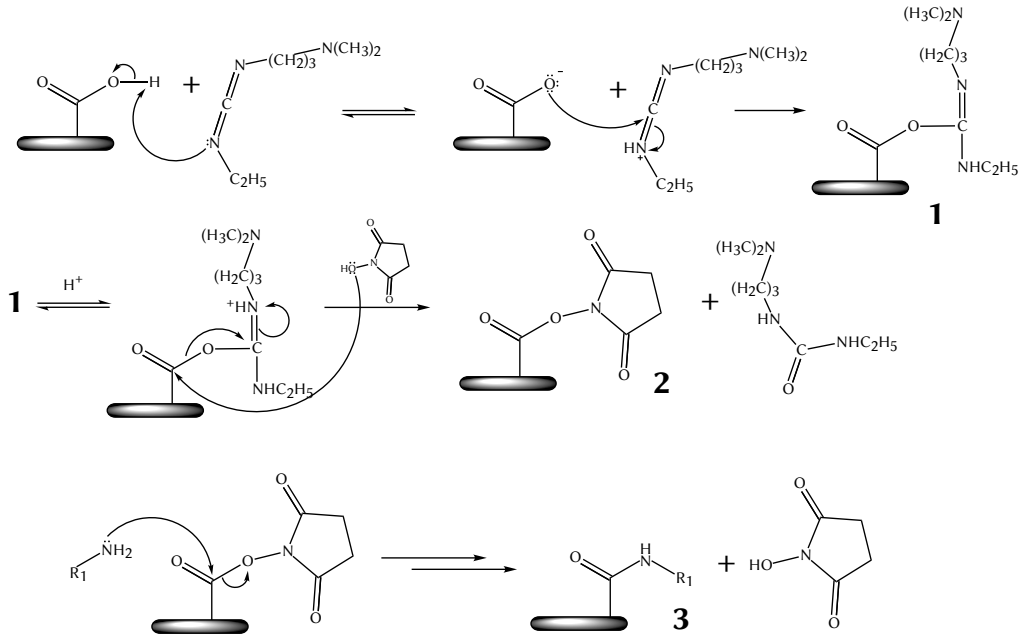

Figure 6.2.: Reaction mechanism of the EDC-mediated coupling of a target molecule R_1 to a solid support (grey).

4-dimethylaminopyridine (DMAP) can be added to the reaction as a catalyst to increase the yield. These carbodiimide reactions can be done in aqueous solutions and at ambient temperature, which makes them favourable over the phosphoramidite mediated reactions described above.

After testing both methods for efficiency and viability it was decided to discontinue the use of phosphoramidite and focus on the carbodiimide method instead. Besides difficulties in handling, the requirement of using organic solvents would be problematic for experiments involving immobilisation of proteins. In the following sections, experimental conditions and results regarding immobilisation efficiency are detailed.

6.2. Experimental part

In this section the experimental procedures relevant for the current chapter are described in detail. First, the two immobilisation methods illuminated in the previous section are presented, then descriptions are given, how the performance and specificity of the reactions was assessed. As a rule, all reactions were carried out under ambient temperature and atmosphere. All chemicals were purchased from Sigma-Aldrich (Schnelldorf, Germany).

6.2.1. Phosphoramidite mediated coupling

Phosphoramidites are susceptible to hydrolysis, so both the solvent acetonitrile and the liquid reagent *N,N*-diisopropylethylamine (DIPEA) needed to be dried over 3 Å molecular sieves prior to use. A PEDOT-OH coated Topas® chip was immersed for 10 minutes in dry acetonitrile containing 70 mM *N,N*-diisopropyl-(cyanoethyl)phosphoramidite chloride and 400 mM DIPEA. The disc was then transferred immediately to a solution of 1 M succinic anhydride and 0.45 mM 1*H*-tetrazole in dry acetonitrile. For this last step different reaction times were tested. The longest time (3 days) proved to be the most efficient for the reaction with succinc anhydride.

6.2.2. Carbodiimide catalysed grafting

Succinic acid was grafted onto surface hydroxyl groups of PEDOT-OH to obtain carboxylic acid groups for further functionalisation steps. Succinic anhydride was hydrolysed in slightly acidic (pH 4) 0.1 M 2-(*N*-morpholino)ethanesulfonic acid (MES) buffer to give a concentration of 100 mM. After addition of 1-ethyl-3-(3-dimethylaminopropyl)carbodiimide (EDC) in equimolar amount the polymer chip was immersed in the solution for 30 minutes. In some experiments 30 mM 4-dimethylaminopyridine (DMAP) were added as catalyst to test its influence on the reaction yield. Due to its toxicity and the minimal effect on the immobilisation performance, this component was not used any more in the final procedure.

6.2.3. Carbodiimide mediated immobilisation of DNA

The surface carboxylic acid groups obtained in the previous step were activated with 50 mM EDC and 40 mM *N*-hydroxysuccinimide (NHS) in MES buffer (0.1 M, pH 4) for 10–15 minutes. After washing with MES buffer, the NHS ester was aminolysed for 3 h by MES buffer containing 100 nM amino terminated DNA. The surface was then rinsed thoroughly with the binding buffer used in the later experiments. For the work in this thesis this was either Dulbecco's phosphate buffered saline (DPBS) or saline sodium citrate buffer (SSC). Details about these biosensor applications can be found in chapter 7.

6.2.4. Determination of carboxylic acid density with toluidine blue

The density of carboxylic acid groups on succinylated PEDOT-OH surfaces was determined by staining a confined area (28.27 mm^2) of the polymer with toluidine blue O (TBO) as described recently by **Luo2008PEDOT** The polymer film was immersed in an aqueous solution containing 0.5 mM TBO at pH 10. Non-specifically bound dye was rinsed off with de-ionised water after 10 minutes. Bound TBO was then eluted from the polymer with 50 % acetic acid. Dye concentration was determined photospectroscopically by calculation of the area under the absorption peaks at 586 nm and 634 nm and comparison with a calibration curve.

6.2.5. Immobilisation of fluorescently labelled DNA

The binding of DNA to the polymer surface was visualised with a simple hybridisation experiment. A 20-mer single stranded oligonucleotide probe was immobilised onto a PEDOT-OH film as described above. Then the polymer was exposed for 30 minutes to 100 nM of another single stranded oligonucleotide with a sequence complementary to the probe and a fluorescent Cy3 label in 2×SSC buffer containing 0.2 % Tween® 20. Bound DNA was detected with a confocal laser scanning microscope (LSM 5 Pascal, Zeiss, Germany) with HeNe laser

excitation (543 nm) and a 560 nm low pass filter. A number of control experiments were carried out to be able to exclude unspecific binding; some of those involved an oligonucleotide strand with 3 mismatching bases and the fluorescent tag fluorescein isothiocyanate (FITC). This fluorophore was detected using Ar-laser excitation at 488 nm and a 505 nm long pass filter. The sequences of the employed strand are listed later in this thesis (table 7.1, page 80), since they were used for other experiments as well.

6.3. Results and discussion

This chapter describes two attempts to immobilise biomolecules on polymers. Hydroxyl groups show a relatively low reactivity, but phosphoramidites have repeatedly been used for coupling reactions on alcohols and are now a standard reagent for automated DNA synthesis [**Nurminen2000**, **Cooke1987**, **Hamblin1987**]. The other class of reactions relies on the activation of carboxylic acid groups by carbodiimides to increase their reactivity towards nucleophilic attacks from hydroxyls or amines [**March1985**].

To compare the efficiency of both methods PEDOT-OH surfaces were coated with succinic acid (a short dicarboxylic acid) and the density of acid groups was determined by a method described by **Luo2008PEDOT** After deciding for one of the methods, immobilisation of DNA was tested employing fluorescently labelled strands.

6.3.1. Toluidine blue O staining

As described in the experimental section on page 64, succinic acid was grafted onto PEDOT-OH using phosphoramidite or EDC as coupling agents. To determine the concentration of the dye in the eluent, a series of different TBO solutions with known concentrations were prepared. Absorption of visible light was measured in the range from 500 nm to 800 nm; figure 6.3 shows the absorption spectra of the concentration series. The spectra have one broad but distinct peak at 631 nm and the absorption decreases with concentration as expected. Plotting the relative peak area against TBO concentration gave a linear dependence (see figure 6.4).

Eluents from experiments on surfaces treated with the different chemicals were measured in the same way and fitted onto the calibration curve. From figure 6.4 it is evident that the TBO concentration from the EDC-sample was much higher than that from the phosphoramidite mediated grafting.

With the measured concentration c_{TBO} and the two known parameters eluent

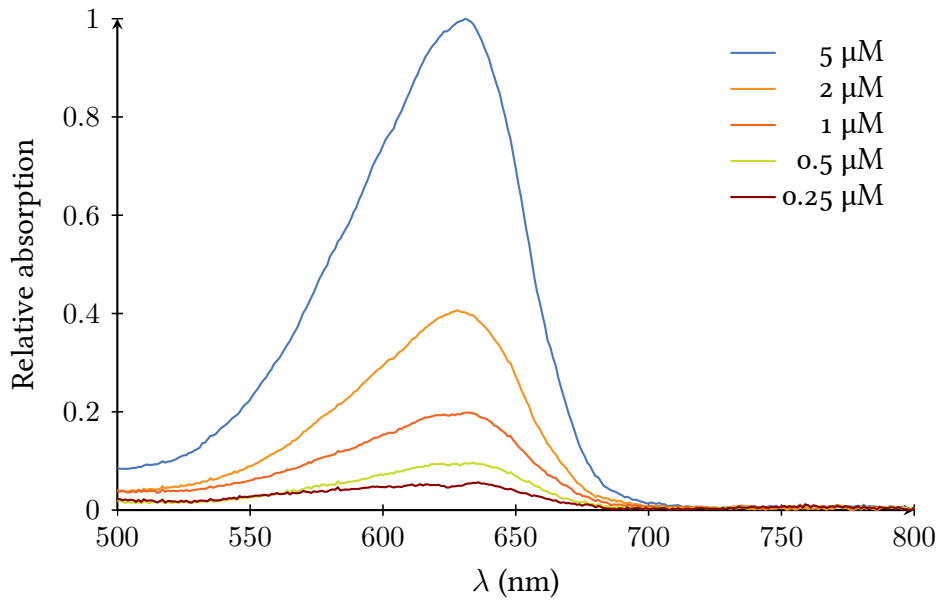

Figure 6.3.: Photospectrometric TBO absorption spectra in acidic pH. The absorption peak was measured at 631 nm.

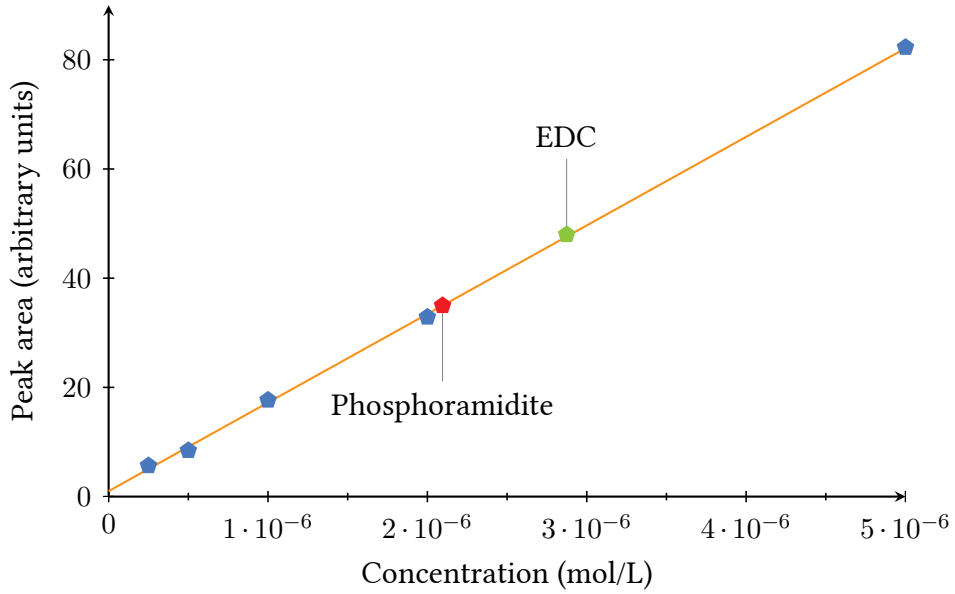

Figure 6.4.: Calibration curve for acid group density calculations. Data points for phosphoramidite and EDC mediated coupling of succinic acid are marked on curve.

volume V and exposed area A the carboxylic acid density ρ_{COOH} was calculated as follows:

$$\rho_{\text{COOH}} = \frac{N_{\text{COOH}}}{A} = \frac{c_{\text{TBO}} \cdot V \cdot N_A}{A} \tag{6.1}$$

where N_{COOH} is the number of acid groups and N_A the Avogadro constant ($6.022 \cdot 10^{23}$). The calculated densities were $2.51 \cdot 10^{14}$ sites/cm² for the phosphoramidite reaction and $3.44 \cdot 10^{14}$ sites/cm² for the EDC assisted coupling.

6.3.2. Immobilisation of DNA to the polymer electrode

DNA hybridisation was made visible by fluorescently tagged oligonucleotide strands and investigation with a confocal laser scanning microscope. The micrograph in figure 6.5 was chosen to illustrate both the successful immobilisation of DNA on the polymer electrodes as well as a small amount of undesirable binding of DNA between two wires. Although the immobilised probe itself had no fluorescent label, the DNA was detectable after hybridisation with the Cy3-tagged complementary strand.

As can be seen in the lower left corner of the image, a small portion of fluorescent DNA was detected between the electrodes. This is most likely due to incomplete removal of over-oxidised PEDOT during the fabrication of the microelectrodes. This remainder of the polymer is not conductive any more and will therefore not disturb the measurements, however, the sensitivity of the device might be diminished due to target DNA binding to insensitive surfaces. A solution for this problem would be to optimise the fabrication protocol, as discussed in chapter 4.

Control experiments using non-functionalised electrodes or the mismatched strand revealed that neither unspecific physisorption nor binding of the mismatched strand occurred to a significant degree. In figure 6.6, a series of micrographs of the control experiments is shown. The boxed letters in the upper left corner of each image list the treatments to which the surfaces were subjected to. The markings read as follows: [A] activated with EDC and NHS, [P] immobilised probe strand, and [C] hybridised with complementary DNA (cDNA). An empty square means that the respective treatment was omitted. As can be seen

in the figure only the surface with all three treatments, i. e. activation with the coupling agents, immobilisation of the DNA probe and hybridisation with cDNA, showed significant fluorescence, while the others show nothing or traces. The weak signal on some of the surfaces where no fluorescence was expected can probably be attributed to spilled DNA from neighbouring spots on the chip.

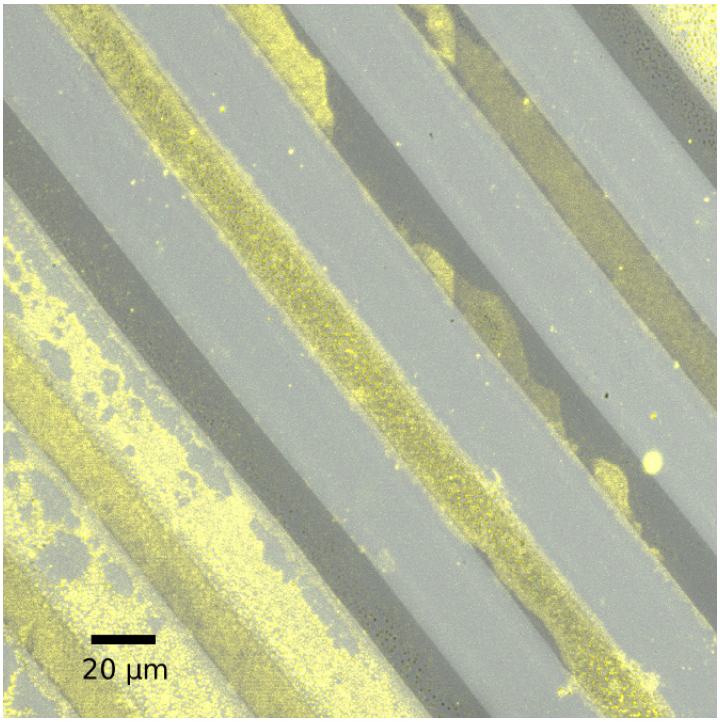

Figure 6.5.: Fluorescence micrograph of conductive polymer microelectrodes with immobilised Cy3-tagged DNA. The fluorescence between the wires could have been caused by DNA binding to over oxidised PEDOT.

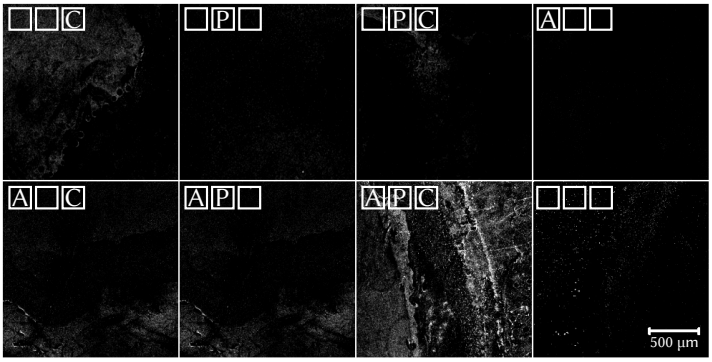

Figure 6.6.: Series of fluorescence micrographs from different control experiments. The symbols explain the surface treatments: A activated with EDC and NHS, P immobilised probe strand, and C hybridised with complementary DNA. An empty square means that the respective treatment was omitted.

6.4. Conclusion

In this chapter different methods for immobilisation of biomolecules on polymer surfaces were discussed. After a theoretical evaluation of the viable options two techniques were studied experimentally and compared regarding their advantages and disadvantages. The experimental results allow the assumption that EDC-coupling is the superior method for immobilisation over the phosphoramidite based reaction. Not only was the density of available immobilisation sites markedly higher, the EDC-activation of the surface was also much faster than the reaction with the phosphoramidite. It should also be mentioned that carbodiimide chemistry can be done in aqueous solutions, while phosphoramidites have to be used in a water-free environment. This limitation would therefore close the doors to any experiments involving proteins as targets for binding.

As a proof of concept, a short single-stranded DNA capture probe was immobilised on the polymer surface and hybridised with a fluorescently labelled complementary strand. This experiment showed that the immobilisation of DNA was possible with the suggested method and control experiments confirmed that the binding was covalent and specific.

Although both methods, phosphoramidite mediated coupling and carbodiimide activation of carboxylic acids, are standard methods in different fields, to the best of the authors knowledge, none have been used for the particular purpose of grafting a bioprobe to a PEDOT-OH electrode so far. However, there are still some weaknesses and further investigations are recommended. One interesting approach would be the directed application of DNA to selected parts of the electrode by ink-jet printing followed by UV-induced crosslinking. This would allow to test for different analytes in a single channel simultaneously and make the use of the costly hydroxymethyl-EDOT monomer obsolete.

7. Biosensor applications

7.1. Introduction

Detection, identification and quantification of pathogens and chemical agents are crucial for water and environmental analysis, clinical diagnosis, food safety, and biodefence. The existing immunological or nucleic acid technologies are either time consuming or require sophisticated equipment and highly trained personnel, hence increasing the analysis costs. Another limitation of these techniques lies in their nature which only allows the detection of certain types of analytes.

Ideally, the assays used in a detection system should enable the detection and quantification of a broad range of different molecules. Furthermore, these techniques should provide reliable, real time, on-field, user-friendly, and inexpensive detection with improved or equivalent sensitivity, specificity and reproducibility compared to state of the art laboratory equipment. Therefore new assay technologies are continuously emerging, and among these, the biosensor technology is the area with fastest growth [1]. These biosensors cover a broad range of detection methods and recognition mechanisms utilising an even broader range of different bioreceptors and physical or chemical transducers. A brief overview was already given in chapter 2 at the beginning of this thesis. Among the technologies described there, label-free biosensors for in situ measurements with high sensitivity and high specificity are of significant interest for the development of diagnostic devices [2–4].

In the preceding chapters the development of an all-polymer electrochemical biosensor for the detection of analytes using single stranded DNA probes was described from the synthesis of the conductive polymer to the covalent attachment of the biomolecules. However, only the involved materials and their

properties have been studied so far; the actual *sensing* part of this technology will therefore be described in this chapter. The biosensor described herein is not limited to one single purpose, but should rather be seen as a modular platform capable of adaptation to the detection of different analytes. Three model applications have been tested so far: hybridisation of DNA, detection of antibiotics using aptamers as probes and detection of influenza A viruses using different aptamers.

7.1.1. Design of the biosensor

Polymer based microfluidic systems meet the requirements of disposable devices for low sample consumption, cost efficiency, reliability, and fast response time, which make the systems ideal for rapid analysis. However, most biosensors for electrochemical detection involve metallic electrodes [5]. To avoid oxidation or participation in electrochemical reactions, noble metals such as gold or platinum are usually employed. These materials have a number of disadvantages, such as high (and still increasing) market prices or comparably low biocompatibility. Apart from that they also require very costly fabrication methods.

Conductive polymers offer very suitable properties to master the specialised task of transducing a binding event between an analyte and a biological probe. They have been used as an alternative to traditional electrode materials because of the additional advantageous properties of inexpensive electrode fabrication and easy electrode functionalisation [6, 7].

Most of these polymers possess a system of conjugated π-bonds which allows them to transport electrons intrinsically. A more thorough discussion of charge transport mechanisms in electrically conductive polymers is given in chapter 3, page 13 et seq. Because of their excellent compatibility with biological samples polypyrrole (PPy) and poly (3,4-ethylenedioxythiophene) (PEDOT) have repeatedly been used for sensors in biological environment [7–14].

For the sensors described in this study, tosylate doped PEDOT was chosen for

its superior stability in phosphate buffers and for its higher conductivity [15–17].

PEDOT can be processed in different ways; popular polymerisation methods are electropolymerisation [9, 15, 18–21] or chemical oxidation polymerisation in liquid [22–26] as well as in vapour phase [27–29]. Chemical oxidation is advantageous because it does not require a conductive substrate.

Micropatterning of conductive polymers is regularly done using cleanroom based photolithographic techniques. However, although such processes are versatile, they are not well-suited for fabricating inexpensive biosensor platforms due to their costs. An alternative micropatterning procedure was developed recently at our institute [25, 30]. It is based on contacting PEDOT thin films with a micro-structured agarose stamp soaked in a solution of aqueous hypochlorite and a non-ionic detergent. Where exposed, PEDOT was over oxidised, i. e. in an irreversibly insulating state, and became more soluble. With this method it was possible to create micro-structured PEDOT for the use as electrode system in a biosensor.

For the intended impedimetric detection an interdigitated electrode design was chosen. The individual wires of the array were 20 µm wide and spaced 20 µm apart. Large contact patches allowed the connection to the measuring equipment. Liquid samples could be directed to the electrodes via a microfluidic channel created during chip assembly.

7.1.2. Sensing of DNA hybridisation

Sensing of DNA hybridisation plays an important role in medical diagnostics, forensics, and food or environmental safety. The strong bond between two complementary DNA (cDNA) strands relies on the unique Watson-Crick base pairing. This selective formation of stable α-helices due to hydrogen bonds and base stacking is used in many popular molecular biology techniques such as PCR amplification, sequencing, genotyping and microarrays. All these techniques are routinely used for detection and analysis of DNA. Among those, hybridisation microarrays have proven to be a valuable tool providing information at genome

level [31, 32]. DNA microarrays use single stranded DNA (ssDNA) probes which are immobilised on the surface of a sensor chip. Usually, arrays consist of short oligonucleotide probes with different sequences, so that multiplex analyses can be performed.

In current applications the sample DNA needs to be labelled with fluorescent tags for detection. This method is quite inconvenient, since samples cannot be used directly and both chemicals for labelling and detection equipment are expensive.

As alternative to fluorescent labelling, label-free methods based on electrical detection are an area of growing interest [33]. Among the electrical DNA sensing methods electrochemical impedance spectroscopy (EIS) is the most often used technique, as it has proven to be a powerful tool capable of detecting changes at electrode/liquid interfaces [34–37]. Conversely to other electrochemical techniques no redox label or other electro-active additives are necessary for detection.

In collaboration with Dorota Kwasny from DTU Nanotech binding of complementary DNA was detected label-free with impedance spectroscopy using the biosensor described in section 7.1.1, page 73. With this sensor we were able to measure picomolar concentrations of cDNA and found a concentration dependence of the impedance for a broad dynamic range.

7.1.3. Detection of antibiotics

The development of novel detection systems for antibiotics is of particular importance. The emergence of pathogens resistant towards important antibiotics occurs at alarmingly high rates. Infections with multidrug resistant pathogens have been reported for a range of potentially lethal pathogens including *Staphylococcus aureus* [38] and *Mycobacterium tuberculosis* [39], leaving few or no options for treatment. In the EU, it is estimated that 25 000 persons die every year from infections with antibiotic resistant microorganisms [40]. Development of novel antibiotics, however, is attracting little attention from the pharmaceutical industry, and for gram-negative pathogens there are few or no late stage clin-

ical trials of new drugs [41]. Besides their use for treating human infections, antibiotics are also utilised as growth promoters in agri- and aquaculture [42, 43].

Due to their short generation time, bacteria can quickly evolve resistance towards all known antibiotics if these are present in sub-lethal concentrations in the environment [44]. To minimise the development of resistance towards antibiotics, it is therefore of critical importance to limit both the use and release of antibiotics into the environment.

Detection of different antibiotics, however, is challenging due to the varied chemical structure of the compounds and the lack of available simple spectroscopic or electrochemical assays. Recently, aptamers targeting a range of antibiotics, including tobramycin [45], kanamycin A [46], ampicillin [47] and chloramphenicol [48] have been developed. In this thesis, a sensor is presented which utilises some of these aptamers to detect the corresponding antibiotic. With this device it was possible to measure picomolar concentrations of the analyte in buffered salt solutions and spiked milk samples.

7.1.4. Virus detection

Influenza is among the main causes of mortality worldwide, resulting in half a million deaths yearly. Moreover it causes serious public health and economic problems. As seen recently, epidemics can spread rapidly around the world and lead to global productivity losses. As usual in February also in this year thousands of patients were hospitalised, bringing the clinics to their limits [49]. The costs for controlling and fighting a large scale infection can be enormous. In 2009 the US alone set aside over US$ 7.65 billion to fight H1N1 [50], while it had been estimated that a H1N1 outbreak in Denmark would cost the Danish economy approximately DKK 3.3 billion [51].

There are several influenza treatments in practice which can reduce severity, duration and complications of the infection, but they must all be started within 48 hours after onset of first symptoms [52]. Current diagnostic methods for the infection are reverse transcription polymerase chain reaction (RT-PCR) or im-

munofluorescence methods. Both methods require extensive instrumentation and highly specific expertise and can therefore mostly be performed only in centralised laboratories in larger clinics or research centres. To meet this clear demand for faster and less expensive solutions, we decided to use our biosensor to detect influenza A virus in human samples.

The experimental work related to these experiments has been carried out by Katrine Kiilerich-Pedersen, a fellow Ph.D. student, and Solène Cherré, who is currently working on her master thesis at the department.

7.2. Experimental part

This section will provide detailed information about the experimental conditions used for testing the three different biosensor devices. At first the assembly of the chip will be described, since it is the same process for all three applications. The following subsections contain information related to the individual experiments and sensors. As the synthesis of the conducting polymer, the patterning of the microelectrodes and the functionalisation of the wires were described in previous chapters already, they will not be repeated here in all detail.

7.2.1. Chip fabrication

The all-polymer microfluidic flow system was fabricated from Topas® grade 5013 polymer (T_g at 130 °C, TOPAS Advanced Polymers GmbH, Germany) using a bilayer composite of tosylate doped poly (3,4-ethylenedioxythiophene) (PEDOT) and its hydroxymethyl derivative PEDOT-OH conducting polymer as electrodes.

Both the top and the bottom part of the chip were made by injection moulding. The injection moulding machine (Engel Victory 80/45 Tech, hydraulic version, Engel Austria GmbH, Austria) was fed with Topas® pellets. The heated polymer was injected into the mould with a temperature of 120 °C. After that, the mould was cooled down to a temperature of 45 °C, and the tool was opened releasing the finished polymer part.

The flat Topas® substrate was covered with conductive thin films of PEDOT or PEDOT-OH respectively by spin coating the reaction solution containing the monomer followed by thermal activation according to the procedure described in section 4.2.1, page 24.

The fabrication of interdigitated microelectrodes by agarose stamping was described in detail in section 4.2.2 on page 25. For the experiments here, typically a solution containing 1 % – 1.5 % sodium hypochlorite in water with 0.1 % of the surfactant Triton™ X-100 and a stamping time of 45 to 60 s were used.

The two parts of the chip, i. e. the flat Topas® disc with the microelectrodes and an injection moulded Topas® cover disc with Luer connectors for simple connection to the electronic equipment and exchange of liquid, were assem-

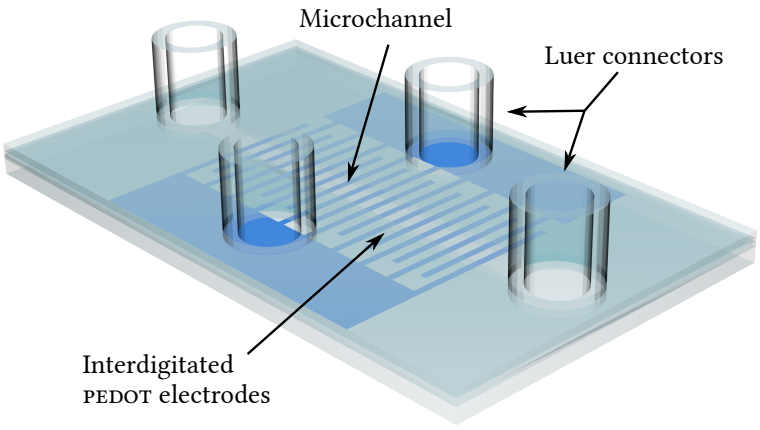

Figure 7.1.: Schematic drawing of the assembled microfluidic chip with interdigitated PEDOT electrodes. The drawing is not to scale.

bled with a 150 µm thick sheet of transfer adhesive (ARcare 90106, Adhesive Research Ireland); a schematic drawing of the chip is presented in figure 7.1. Cavities were cut into the tape by laser ablation to create microfluidic channels. To ensure homogeneous and tight sealing around the channels, the assembled discs were pressed with a force of 500 N at a bonding temperature of 75 °C for 5 minutes. The pressure was released after the chip had cooled down to 40 °C.

This chip could then be functionalised with aptamers or DNA hybridisation probes according to the protocol given in section 6.2.3 on page 64.

7.2.2. Sensing of DNA hybridisation

The aim of this experiment was to detect specific DNA hybridisation with impedance spectroscopy. Short, single stranded oligonucleotides with the sequence marked *probe* in table 7.1 were therefore immobilised on the polymer electrode.

The sensing performance of the device was tested by incubation of the functionalised electrodes with the *target strand* (sequence complementary to the probe) or the *mismatch strand* (three base mismatch in the sequence, see table 7.1).

Table 7.1.: DNA-sequences used in our experiments with their respective modifications or fluorescent labels. Mismatch bases are printed in red colour. The oligonucleotides were synthesised by DNA-Technology (Risskov, Denmark) and Eurofins (Kraainem, Belgium).

Name	Sequence
Probe	5′ TCC ACT ATG GCC TCC ACC AT 3′– NH_2
Target	5′ ATG GTG GAG GCC ATA GTG GA 3′– Cy3
Mismatch	5′ ATG CTG GAT GCC GTA GTG GA 3′– FITC

Hybridisation was done with 100 nM DNA in 2× SSC buffer (saline sodium citrate, pH 7) with 0.2 % Tween® 20 for 30 minutes at room temperature. For the determination of the concentration dependence, hybridisation buffer containing increasing concentrations of DNA was filled into the channels. After the impedance signal had stabilised, the next higher concentration was injected.

Both testing strands were labelled with a different fluorophore (see table 7.1) which was used to asses the immobilisation specificity of the probe and to monitor possible unspecific binding of DNA to electrodes or substrate. Fluorescence of fluorescein isothiocyanate (FITC) and the cyanine Cy3 label was measured with a confocal laser scanning microscope (LSM 5 Pascal, Zeiss, Germany) with Ar- (488 nm) or HeNe-laser (543 nm) excitation and a 505 nm or 560 nm long pass filter, respectively.

For electrochemical impedance spectroscopy two different instruments were used: A VersaStat 3 (Princeton Applied Research, USA) was used for single frequency scans at 501 mHz; all experiments involving only one concentration were carried out with this instrument. The measurement of the concentration dependence was done using a Zahner IM6 potentiostat (Zahner Elektrik, Germany). Wide spectrum sweeps in a frequency range from 100 kHz to 200 mHz (logarithmic scale with ten points per decade for frequencies < 66 Hz and four points per decade for frequencies > 66 Hz) were recorded.

7.2.3. Antibiotics detection

In this study we used short high-affinity aptamers against kanamycin A and ampicillin presented by Song et al. in 2011 and 2012, respectively [46, 47]. The DNA aptamers were synthesised by Integrated DNA Technologies (Denmark) as HPLC purified and lyophilised ssDNA functionalised with a 5′-amino modified C_6 linker. Their sequences from 5′ to 3′ are listed in table 7.2.

Table 7.2.: DNA aptamer sequences used in our experiments for the detection of antibiotics. The strands were synthesised by Integrated DNA Technologies (Denmark).

Target	Aptamer sequence
Ampicillin	5′ GCG GGC GGT TGT ATA GCG G 3′
Kanamycin A	5′ TGG GGG TTG AGG CTA AGC CGA 3′

Electrochemical impedance spectroscopy (EIS) was conducted on chips with and without immobilised aptamers. A potentiostat with integrated frequency generator (Zahner IM6, Zahner Elektrik GmbH, Germany) was connected to the electrodes by spring-loaded (pogo pin) contacts and the impedance of the system was measured with wide spectrum sweeps in a frequency range from 100 kHz to 200 mHz (logarithmic scale with ten points per decade for frequencies < 66 Hz and four points per decade for frequencies > 66 Hz). After the baseline was recorded, the target was added in increasing concentrations and the change of the impedance signal monitored.

7.2.4. Detection of influenza A virus

Like for the antibiotics sensors described above a previously published aptamer sequence was used for this study [53]. The 68-mer DNA aptamer A22 with the sequence 5′ AAT TAA CCC TCA CTA AAG GGC TGA GTC TCA AAA CCG CAA TAC ACT GGT TGT ATG GTC GAA TAA GTT AA 3′ (DNA-Technology, Denmark) binds specifically to influenza A virus and was further functionalised with an amino-terminated C6 linker at the 5′ terminus. The virus used was influenza A (H1N1, strain A/PR/8/34, ATCC cat. no. VR-1469; LOT:59252244) and was aliquoted and stored at −80 °C.

The biosensor chips were prepared as described above and influenza A virus in different concentrations and media was detected using EIS. Spectra in the frequency range from 0.2 Hz to 100 kHz were recorded every 33 s with an amplitude of 10 mV. For later analysis only the values obtained at 251 mHz were used, since the highest signal-to-noise ratio was obtained there. The dynamic range of the sensor was measured by first recording a baseline in PBS until the signal stabilised and then adding increasing concentrations of the virus (10 – 10^6 pfu/mL) in the same medium every 20 minutes. Measurements in saliva were done by recording a baseline with diluted (1:10) and heat-sterilised saliva in PBS and introducing spiked samples after one hour. The sample consisted of non-sterilised saliva which was diluted 1:10 in PBS and contained influenza virus A at a concentration of 10^6 pfu/mL. Control measurements were done with the same samples, but no added virus.

For atomic force microscopy AFM Topas® discs with patterned microelectrodes but withour the channel system and the lid were functionalised with aptamer A22 like before and incubated with PBS containing 10^6 pfu/mL influenza A virus for 20 minutes. Unspecifically attached virus particles were removed by washing the chip three times with PBS. Afterwards the viruses were fixed with 2.5 % glutaraldehyde in PBS for 60 minutes at room temperature and washed with PBS for 15 minutes at 4 °C. Increasing concentrations of ethanol (30 – 99%) were used to dehydrate the samples. AFM images were then recorded with a XE150 (Park Systems, South Korea) in tapping mode at normal environmental conditions.

7.3. Results and discussion

In this section the results from experiments with the all-polymer biosensor will be presented. In the first experiments, the hybridisation of complementary DNA strands was detected with high sensitivity using electrochemical impedance spectroscopy (EIS). For the second experimentation round the same sensor was equipped with aptamers against two structurally different antibiotics, ampicillin and kanamycin A, which were then detected in very low concentration in a buffered solution as well as in a spiked milk sample. The last experiments used the same setup with different aptamers to detect influenza A viruses in saliva. The virus particles caught by the immobilised aptamers were also visualised using atomic force microscopy (AFM).

7.3.1. Sensing of DNA hybridisation

Detection of fluorescently tagged DNA

DNA hybridisation was made visible by using fluorescently tagged oligonucleotide strands and investigation with a confocal laser scanning microscope. The data presented in section 6.3.2, page 68 show both the successful immobilisation of DNA on the polymer electrodes as well as a small amount of undesirable binding of DNA between two wires. Although the immobilised probe itself had no fluorescent label, the DNA was detectable after hybridisation with the Cy3-tagged complementary strand. Control experiments using the mismatch strand or non-functionalised electrodes revealed that neither unspecific physisorption nor binding of the mismatch strand occurred to a significant degree.

Electrochemical sensing of hybridisation

In a number of studies involving sensing of DNA hybridisation via electrochemical impedance spectroscopy electro-active reactants such as the redox pair ferro-/ferricyanide ($[Fe(CN_6)]^{3-/4-}$) are added for detection [34–37]. In those experiments it was found that DNA hybridisation causes stronger repulsion of the

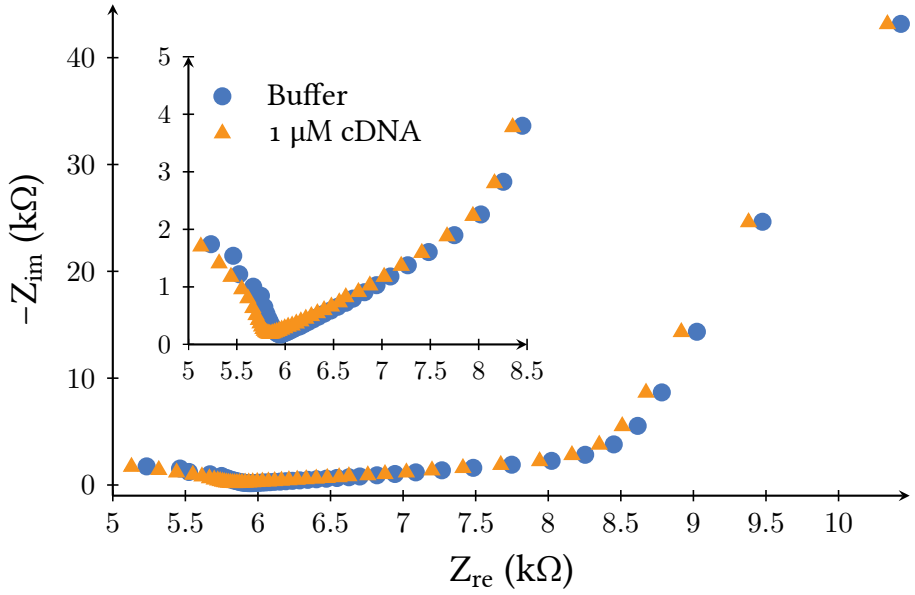

Figure 7.2.: Nyquist plot of two impedance spectra before (●) and after (▲) injection of complementary DNA. The inset shows the high frequency part of the spectra in detail.

negatively charged $[Fe(CN_6)]^{3-/4-}$ ions due to the likewise anionic DNA on the surface, resulting in an increased charge transfer resistance. In an impedance spectrum – displayed as Nyquist plot – this leads to an increase of the diameter of the characteristic semicircle. Contrary to those results, we observed that in our experiments the impedance decreased after addition of complementary DNA. As is evident from figure 7.2 the real component of the complex impedance signal was shifted to lower values in the entire frequency range as a result of hybridisation, while the imaginary component only changed in the high frequency part of the spectrum.

To understand these findings, we suggest a model as illustrated in figure 7.3: after immobilisation the single stranded DNA chains cover most of the electrode surface, thus reducing the area available for charge transfer. When the immobilised DNA hybridises with complementary strands, α-helices are formed, which require less space and therefore expose more of the electrode surface. It is reasonable to suppose that this effect could cause a reduction of the charge

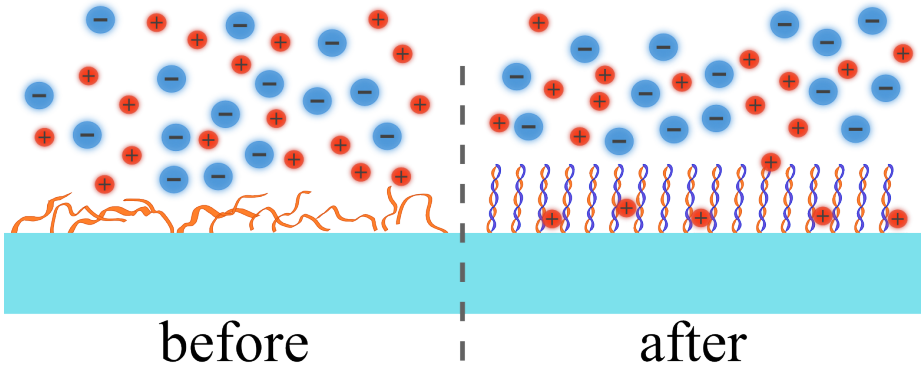

Figure 7.3.: Schematic drawing of the possible surface model suggesting a reduced charge transfer resistance caused by conformational changes of the immobilised DNA due to hybridisation.

transfer resistance and might therefore lead to the decrease of the absolute impedance as observed in the spectra.

The model was also corroborated by the comparison of impedance measured before and after immobilisation of the DNA probe (see figure 7.4). Without the DNA probe the surface of the electrodes could interact with ions from the solution, thus the impedance was lower. The immobilisation of probes created an insulating layer, blocking the surface as described above. The addition of a strand with three mismatching bases did not affect the signal significantly, while cDNA reduced it markedly. This proves the specificity of the biosensor.

The detection limits of the sensor were assessed by recording impedance spectra continuously while changing the DNA concentration in the channel after the signal stabilised. Starting at a concentration as low as 100 pM and increasing it logarithmically until 1 µM, we were able to obtain the calibration curve presented in figure 7.5. The first concentration (100 pM) was already enough to cause a statistically significant ($p = 0.04$) impedance decrease. Increasing the concentration led to a fairly linear decrease of impedance in the logarithmic plot. The highest concentration tested (1 µM) did not result in a further signal decrease, so it can be assumed that the sensor was saturated at this point.

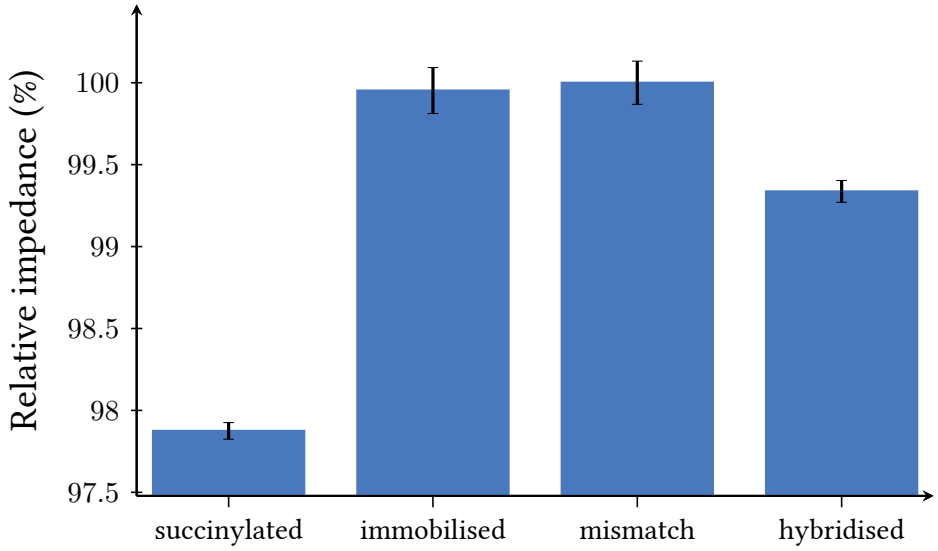

Figure 7.4.: Comparison of impedance values measured at 501 mHz with succinylated electrodes, with immobilised DNA probe, after addition of mismatch strand and after hybridisation with complementary DNA. Error bars show standard deviation.

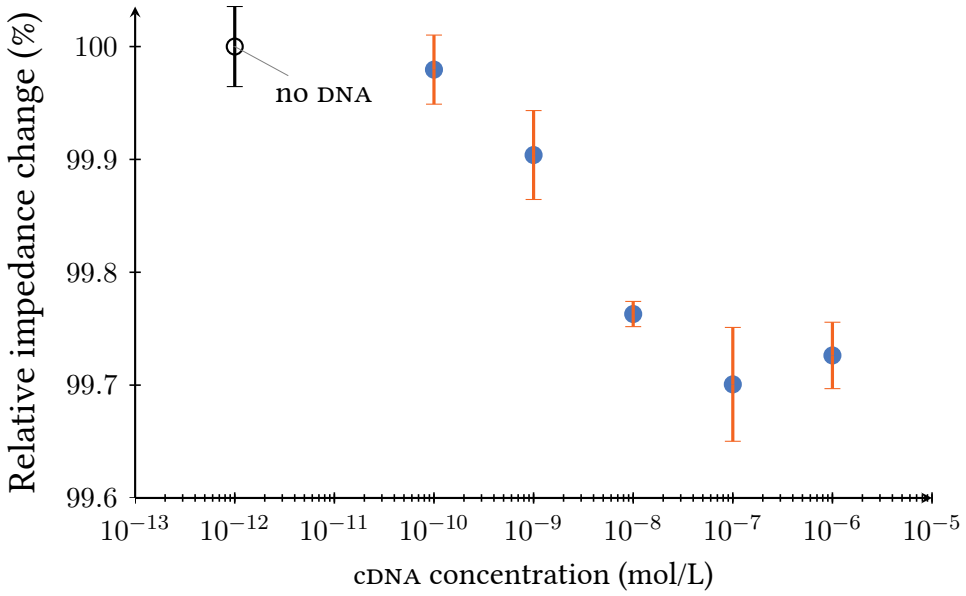

Figure 7.5.: Impedance values measured at 356 mHz for a concentration series from 100 pM to 1 µM complementary DNA. The first value represents the impedance level before addition of DNA. Error bars show standard deviation.

7.3.2. Detection of antibiotics

Impedimetric characterisation of the aptasensor

It was already shown in section 7.3.1 that the presented biosensor was capable of detecting minute amounts of DNA strands binding to their counterparts immobilised on the surface of the electrodes. It was suggested that the conformational change caused by these binding events is responsible for the observed signal change. In this study we show that the above described all-polymer biosensor can also be used as a sensitive and selective platform for detection of different antibiotics. We have chosen already published aptamers against kanamycin A and ampicillin as biological recognition entities for our experiments [46, 47].

The immobilisation of the aptamers alone provoked an increase in the impedance as was expected due to the increased charge transfer resistance at the electrode/liquid interface. Binding of the target molecules to the corresponding aptamer caused a further increase in the impedance measured at frequencies below 1 Hz. A logarithmic correlation of analyte concentration and impedance response was found for a broad dynamic range and both analytes. In the following the individual aptasensors will be discussed in more detail.

Analyte concentrations starting from 10 pM were tested with the ampicillin-aptamer. Figure 7.6 shows the relative change of absolute impedance with increasing analyte concentrations. The first statistically significant ($p < 0.05$) signal was observed at 100 pM. Further increase of analyte concentration showed a fairly linear dependence in the logarithmic plot.

As described in section 4.3.4, page 40, the patterning of the chips was subject to uncertainties which resulted in variation in the width of the electrodes in the range of several micrometers. It was found that there was a very good correlation between impedance change and wire size (see figure 7.7, page 89), so that a better reproducibility can be expected from electrodes fabricated with higher accuracy. These results are also in accordance with the conductivity loss reported for the single wire pattern in section 4.3.3, page 35.

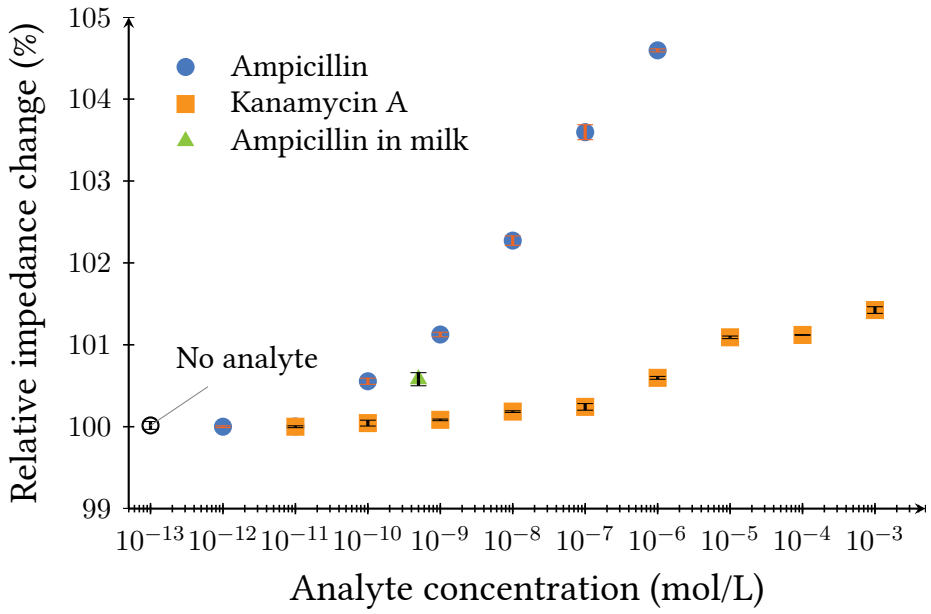

Figure 7.6.: A typical impedance response for increasing concentrations of ampicillin or kanamycin, respectively. The empty symbol illustrates the measured baseline level before the first injection. The green triangle represents the obtained impedance change in the case of 500 pmol/L ampicillin in milk sample. The error bars show the average of the signal noise.

With a dissociation constant of k_D = 78.8 nM the kanamycin A aptamer establishes a weaker bond to its target than the ampicillin aptamer (k_D = 13.4 nM) [46, 47]. It is therefore likely that an aptasensor based on this probe would be less sensitive. As shown in figure 7.6 our findings verify this presumption. Typically a concentration of 10 nM was necessary to obtain a statistically significant increase ($p < 0.05$) of the impedance modulus. Lower concentrations, starting from 10 pM, caused little or no effect on the signal. We believe that the relatively low limit of detection (LOD) and wide dynamic range of the biosensor is also due to specific device properties and not exclusively related to affinity of the probes used in this study. In addition, sensors and assays for ochratoxin A (OTA) have shown that using the same aptamer in different assays and sensors can result in over a 1000-fold difference in LOD [54]. The lower detection limit found with the ampicillin aptamer indicates that a high affinity for target compounds will facilitate higher device sensitivity.

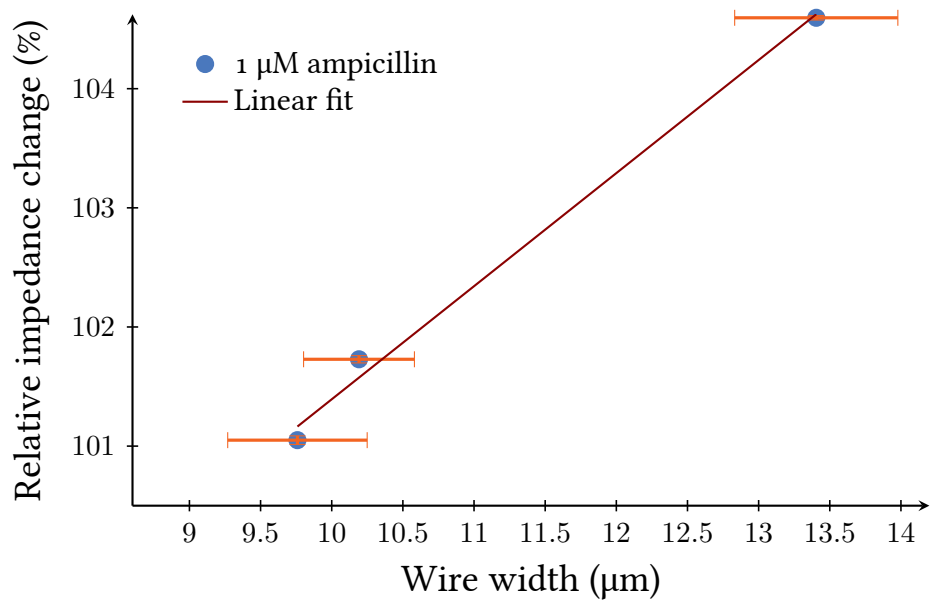

Figure 7.7.: Correlation of impedance response and wire width based on measurements performed on three different chips using 1 µM ampicillin and electrodes functionalised with the anti-ampicillin aptamer.

Control experiments, where the antibiotics were reacted with mismatching aptamers, gave no changes in the impedance signal compared to the baseline. After that, injecting the matching antibiotics into the biosensor resulted in the expected increase of impedance. This shows that the immobilisation of the aptamers on the electrodes did not affect the selectivity of the aptamers towards their targets.

With the described experimental setup (see section 7.2.3) it was possible to obtain one full impedance spectrum in 2:35 min. Figure 7.8 shows the impedance data at a single frequency (356 mHz) which were taken from the full spectra. As can be seen in the graph, the impedance change occurs within the sampling time, i. e. within 2:35 minutes and stabilises at a new level. We have also conducted impedance measurements at a single frequency, where the instrument-determined minimum sampling time was ca. 17 s (data not shown), but also this higher temporal resolution was insufficient to determine the reac-

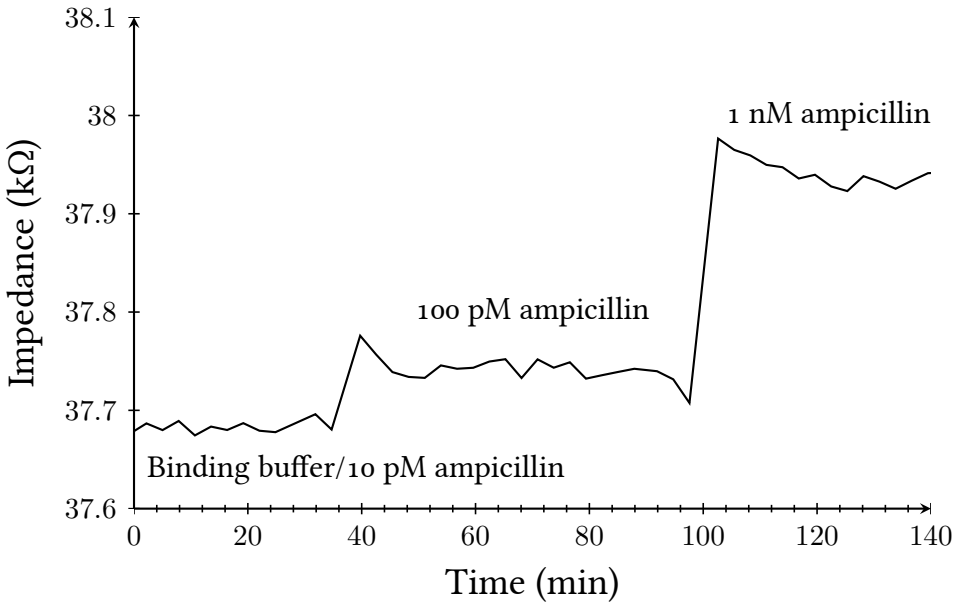

Figure 7.8.: Increase of impedance at a frequency of 356 mHz is shown after addition of the analyte in different concentrations.

tion rate of the target-aptamer complex formation. However, this shows that the analysis time is reasonably short for a number of real-life applications.

EU regulation no. 675/92 (as amendment to regulation no. 2377/90) lays down a maximum residue limit (MRL) for ampicillin of 4 µg/L in milk, which is equivalent to a concentration of 11.45 nM. Our experiments shown above proved that we were able to detect much lower concentrations of ampicillin in buffer solution. In order to prove the reliability of the sensor detecting analytes in real samples, a 10 % solution of ultra-high temperature treated (UHT) low fat milk in DPBS containing 5 mM $MgCl_2$ was prepared and spiked with 500 pM ampicillin. Impedance spectra were measured as before. In these experiments we were able to measure a relative increase of impedance of 0.58 ± 8 % (the value was inserted in figure 7.6 for comparison with measurements in buffer solution). These data are well in accordance with the concentration dependence reported above. We can therefore claim that our sensor is capable of reproducibly detecting an ampicillin concentration in milk that is far below the MRL set by the EU.

Equivalent circuit modelling of the EIS results

An equivalent circuit model fitting the electrical properties of the sensor is shown in figure 7.9. This model was used to simulate impedance spectra while changing certain parameters to understand the effects observed in our experiments; it satisfactorily fits the experimental data over the measured frequency range.

In the model, R_1 is the intrinsic resistance of the electrodes. The parallel resistance (R_2) and the constant phase element (CPE_1) with coefficients P_1 and n_1 represent the electrode-solution interface, where R_2 is the charge transfer resistance and CPE_1 the electrical double layer on the surface. The following Warburg impedance (W_1) indicates the diffusion limited electrochemical processes specified by the coefficient A_{w1}. The impedance spectrum includes a semicircle portion at high frequencies corresponding to bulk solution resistance (R_3) and the geometrical capacitance (C_1) of the interdigitated electrodes. Finally, the capacitance C_2 is the limiting capacitance, which reflects the limited solid state diffusion of charges inside the conducting polymer.

The intrinsic resistance of the electrode (R_1), the solution resistance (R_3) and electrode geometrical capacitance (C_1) are not changing during the aptamer-target binding process. The Warburg coefficient (A_{w1}) represents the impedance due to the diffusion of charges to and from the electrode surface. The temperature and the viscosity of the solution were constant during the binding process, however, conformational changes and rearrangements of the surface bound aptamers during complex formation are likely to alter the electrode surface area available for charge transfer, influencing A_{w1}. Modifications

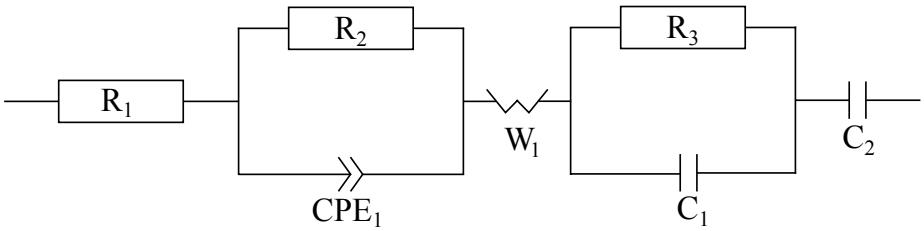

Figure 7.9.: Equivalent circuit model for fitting the experimental spectra (see description in the text).

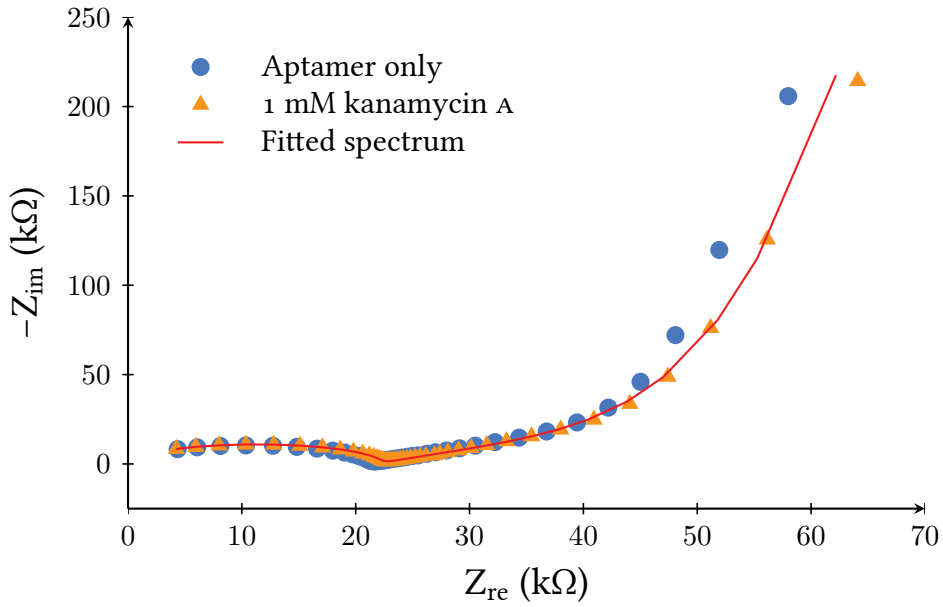

Figure 7.10.: Nyquist plots from impedance spectra before (●) and after (▲) addition of kanamycin A. In the low frequency region (right side) of the spectra a clear shift towards higher resistance is visible. The solid red line represents a simulated spectrum based on the fitting parameters from table 7.3. The curve is calculated from the values after analyte addition.

of the electrode surface can inflict changes to the electrolytic double layer at the electrode/electrolyte interface with its non-ideal capacitance (reflected as the constant phase element CPE_1) and the reaction rate of the transfer of charges between electrode and electrolyte (expressed as the charge transfer resistance R_2). Both factors are dependent on the change of the ionic concentration near the electrode surface, which is influenced by the binding event of an analyte molecule to an immobilised aptamer. We can therefore assume that both the constant phase element, the charge transfer resistance and the Warburg element will be the most interesting parameters for investigations of target binding to surface-bound probes. The surface coverage with aptamers could have an influence on the sensitivity of such a device as described here, but the size of the antibiotics is much less than that of the aptamers, therefore it is not likely that steric hindrance would affect the results.

Impedance spectra recorded at different stages of the experiment were fitted

Table 7.3.: Comparison of parameters corresponding to elements in the equivalent circuit model fitted to the spectra shown in figure 7.10.

Parameter	Aptamer only (error/%)	Kanamycin (error/%)	Unit
C_1	$1.59 \cdot 10^{-10}$ (2.8)	$1.58 \cdot 10^{-10}$ (2.3)	F
C_2	$4.11 \cdot 10^{-6}$ (2.3)	$4.06 \cdot 10^{-6}$ (3.0)	F
R_1	$3.34 \cdot 10^{2}$ (41.3)	$3.07 \cdot 10^{2}$ (46.7)	Ω
R_2	$2.51 \cdot 10^{4}$ (7.8)	$2.41 \cdot 10^{4}$ (9.3)	Ω
R_3	$2.06 \cdot 10^{4}$ (0.8)	$2.16 \cdot 10^{4}$ (0.8)	Ω
A_{w1}	$1.44 \cdot 10^{4}$ (12.8)	$2.13 \cdot 10^{4}$ (9.0)	$\Omega/\sqrt{s}$
P_1	$5.75 \cdot 10^{-6}$ (6.2)	$6.80 \cdot 10^{-6}$ (6.9)	$1/\Omega$
n_1	0.58 (1.9)	0.57 (2.2)	–

with the "EIS spectrum analyser" software[1]. An example of the fitted curves is shown together with two measured spectra represented as a Nyquist plot in figure 7.10. The curve was calculated from parameters which were fitted to the impedance data obtained from the kanamycin aptasensor after the analyte was added. The result indicates a good agreement with the measured data, especially in the lower frequency range.

A comparison of parameters obtained from fitting the model to the data recorded before analyte addition and after injection of kanamycin A at a concentration of 1 mM is made in table 7.3. As expected, only slight changes were observed for the capacitances C_1 and C_2 as well as the material or solution related resistances R_1 and R_3. Elements describing the electrode/liquid interface experienced a larger change. The strongest deviation from the original value was found for the Warburg coefficient A_{w1}.

7.3.3. Virus detection

As seen in the previous experiments with the antibiotics, the biosensor can detect minute changes in the vicinity of the electrode surface. It is a fair assumption to suggest that a larger target will have a stronger effect on the measured impedance, because it causes a greater disruption of the electrochemical

[1] A.S. Bondarenko and G.A. Ragoisha, http://www.abc.chemistry.bsu.by/vi/analyser/

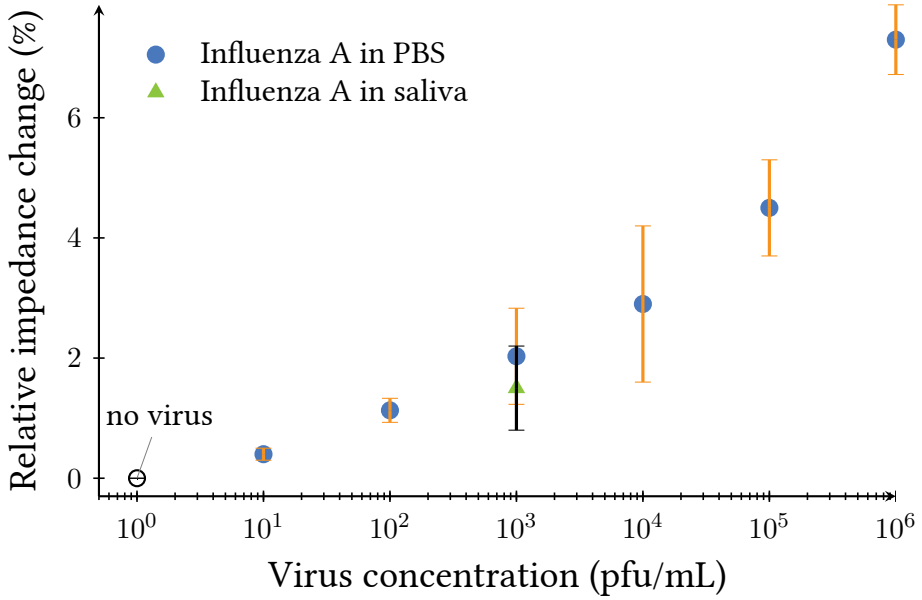

Figure 7.11.: Concentration dependent impedance response for virus detection. The sensor shows a broad dynamic range and it was possible to detect down to 2 plaque-forming units in a sample of approx. 200 µL. Error bars show the deviation between three different chips. These deviations are in line with deviations of wire widths for these chips.

environment near the electrodes. Figure 7.11 shows the broad dynamic range of the sensor from $10 - 10^6$ plaque forming units/mL. The highest tested concentration caused an increase in the impedance signal of almost 8 % and thus corroborates the hypothesis that a larger target will give a more distinct signal. The lowest tested concentration was 10 pfu/mL, which corresponds to approximately 2 pfu/sample, since the microfluidic channel can hold a volume of less than 200 µL. This means that the detection limit is clearly low enough for practical purposes. The broad dynamic range can be a useful feature, but very often no information about the pathogen concentration is required for the diagnosis and a simple yes/no answer is sufficient. The seemingly strong deviations visualised as error bars stem from the different wire widths of the tested chips. As shown above, the differences in width could be directly correlated to the signal deviations (data not shown).

To test the usability of the biosensor in a realistic environment saliva was

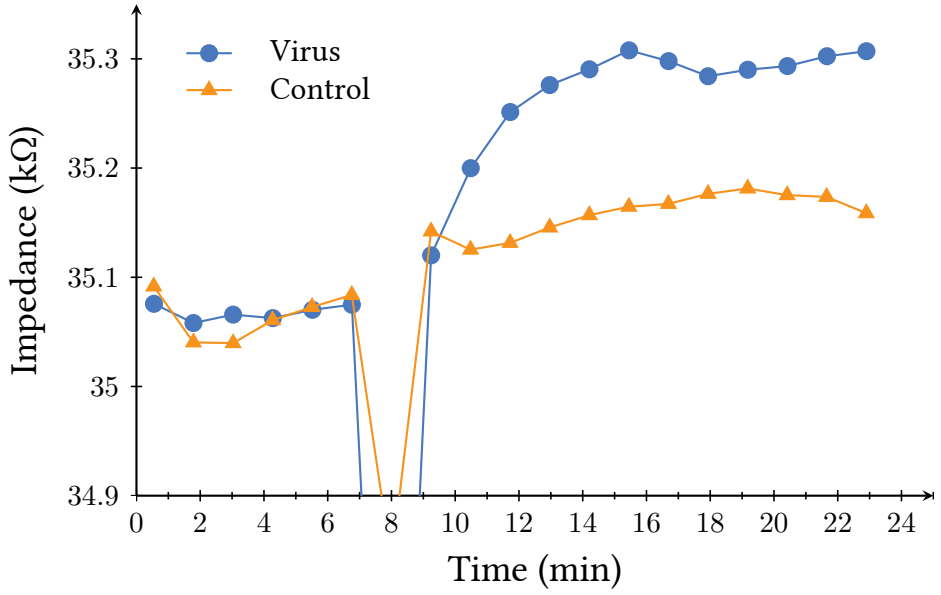

Figure 7.12.: Impedance detection in a spiked saliva sample. It was possible to detect 10^3 pfu/mL influenza A virus in a saliva sample. The outliers at minute 8 originate from the disturbance caused by sample injection.

diluted 1:10 in PBS and spiked with 10^3 pfu/mL influenza A virus. This concentration is, bearing in mind the dilution, on the lower end of typical virus loads found in saliva of infected patients. Figure 7.12 shows a distinct increase in the measured impedance after the injection of the sample. The control experiment (only saliva) remained unchanged, considering the slightly skewed baseline. The injection of the sample at minute 8 in this graph naturally caused a big disturbance in the system, hence the observed outliers. With the detection performance shown here this sensor is a viable alternative to conventional methods. Apart from requiring less expertise in handling the device and being less expensive, this sensor should have the capability to discriminate between viable and non-viable virus units, a feature RT-PCR cannot deliver.

The size of the influenza A virus (ca. 100 nm) allowed us to record AFM images of the successfully immobilised particles on the surface of the polymer electrodes. Figure 7.13 a shows the small spherical objects scattered on the electrode surface which was previously functionalised with the A22 aptamer, while there are no particles on the electrode in figure 7.13 b, where no probes

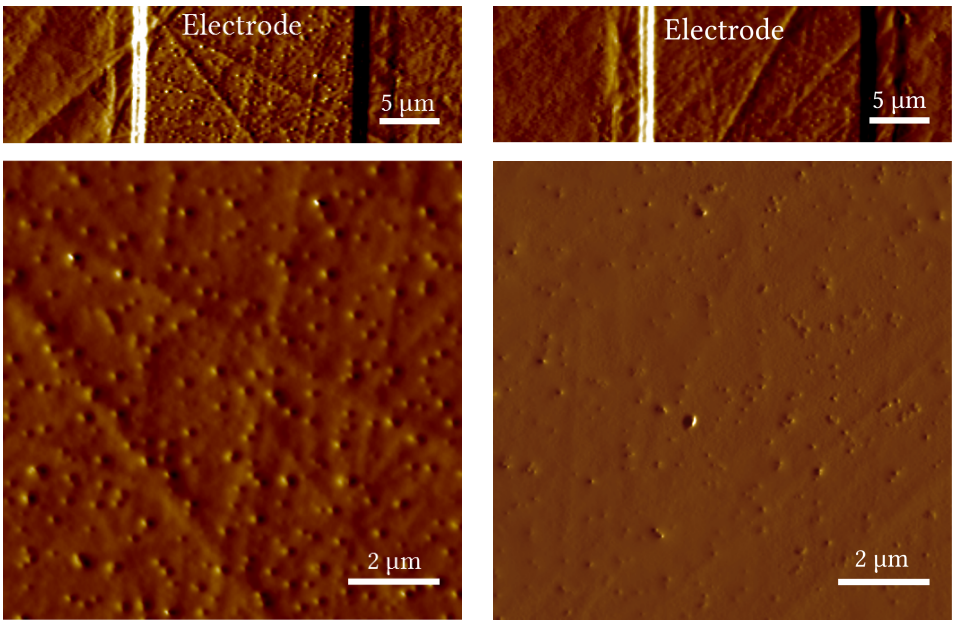

(a) Sample with immobilised aptamer: virus particles captured by the probes.

(b) Sample without immobilised aptamer: no virus particles captured by the probes.

Figure 7.13.: AFM images of stamped PEDOT-OH microwires with (a) and without (b) immobilised aptamers and after incubation with 10^5 pfu/mL influenza A virus in PBS.

were immobilised. The small, irregular indentations visible on both samples in the high resolution images could originate from the glutaraldehyde treatment used to fix the bound viruses.

7.4. Conclusion

In this chapter three different applications for the all-polymer biosensor developed during this PhD project were presented. They all have in common that, given some further optimisations, they could replace, or at least compete with, today's state of the art equipment in terms of sensitivity and specificity.

With the DNA hybridisation sensor it was possible to detect picomolar concentrations of complementary DNA, while strands with three mismatching bases did not show any effect. In contrast to most other published biosensors of this kind no markers had to be attached to analytes or probes and no electroactive additives were required. Future work on this particular sensor could involve the introduction of additional probes to enable multiplex detection of a large number of different DNA sequences in parallel. A manuscript containing the results presented here is currently in preparation and will soon be submitted to a scientific journal.

The second sensor application involved aptamers as recognition elements. These DNA sequences were selected for high affinity and selectivity towards the two antibiotics ampicillin and kanamycin A. Both systems proved to be very effective and concentrations in the sub-nanomolar range could be measured. Using the anti-ampicillin aptamer it was also possible to detect the antibiotic in a milk sample at a concentration far below the maximum residue limit in the EU. Theoretical simulations gave an insight into a possible surface model explaining the observed phenomena. The model suggested that larger targets might enhance the impedance signal and thus allow higher sensitivity.

This hypothesis was confirmed by the third biosensor system. Again, an aptamer was immobilised onto the electrode surface. This aptamer, however, showed high affinity towards a surface protein of the influenza A (H1N1) virus. The biosensor was used to detect a broad dynamic range of 10 – 10^6 plaque forming units/mL, which corresponds to a lower detection limit of only 2 pfu/sample. The system was also tested with spiked saliva samples where it was possible to detect clinically relevant concentrations of the virus. As mentioned before, multiplexing would be a desirable future goal also for this sensor type.

An article about the successful detection of antibiotics with this sensor was recently published in Biosensors & Bioelectronics [55]. Another manuscript containing the results from the virus experiments is currently in preparation.

8. General conclusion

This thesis described the development of an all-polymer biosensor from the synthesis of the monomer to formation of a conductive polymer layer, over the patterning and characterisation of this layer, the selection of aptamers, the chemical immobilisation of these bioprobes onto the polymer all the way to the application of the sensor in three different settings.

The path towards this goal was often stony and some detours or even full turnabouts were inevitable. The synthesis of the monomer as described at length in chapter 3 for instance turned out rather unsuccessful and also the selection of aptamers had to be discontinued after several failed attempts. However, these setbacks did not jeopardise the overall success of the project. The monomer from the failed synthesis became commercially available and the aptamers were replaced by available sequences. While testing the different selection methods we also came to the conclusion that capillary electrophoresis is probably the most promising approach for future experiments. Plans were made to create a microfluidic device which integrates this technique and allows semi-automatic selection of anti-virus aptamers.

The thorough characterisation of spin coated tosylate doped PEDOT thin films revealed that, unlike some other PEDOT formulations, the tosylate doped polymer does not show improved conductive behaviour after different heat treatments. The investigation of the micropatterning by agarose stamping provided new insights into the parameters governing the process. It was found that prolonged exposure causes the conductivity of stamped wires to diminish, while their physical shape and size remains mostly intact. We learned further that the stamping is not suitable for any large scale applications. Even if we had an automated stamping robot to ensure constant and even pressure on the gel, we could not overcome the fast degradation of the agarose. The necessity for spin

coating prior to stamping renders the entire process quite uneconomic and only allows a low throughput. For future large scale production of a finalised chip, other fabrication methods should therefore be considered. There exist several roll-to-roll methods, which are already used in the production of polymer solar cells. Other alternatives might also be two component injection moulding or ink-jet printing.

After the fabrication of the microelectrodes was accomplished, the possibilities for their functionalisation were studied. After an initial selection two promising candidates were chosen and compared. Carbodiimide catalysed coupling performed in general better than phosphoramidite mediated reactions. Carbodiimide reactions are also more flexible since they are done in aqueous solutions, while phosphoramidites can only be used in anhydrous environments. Bearing in mind faster production methods, the functionalisation technique should be reconsidered, however. The need for hydroxyl or carboxylic acid groups for the grafting adds complications to the production or calls for compromises. A highly interesting method for future applications would be direct UV-crosslinking of certain repetitive DNA sequences onto a polymer. The main advantages of this process are that it can be performed in nearly dry conditions and that it is relatively fast. It could therefore easily be integrated into a high-throughput work flow.

The last phase of the project was the testing of the device. Three different analytical experiments were designed for the sensor: DNA hybridisation, detection of antibiotics with aptamer probes and detection of influenza A virus using another aptamer probe. In all three settings the sensor showed an extraordinary performance, being able to specifically detect picomolar amounts of analytes or single virus particles, respectively.

However, the device can certainly be improved in many aspects. Apart from the issues with the fabrication mentioned above, the electrode material PEDOT reacts very sensitive to many environmental factors such as temperature or pH. The easiest way to overcome this would perhaps be the introduction of a third electrode into the existing system, thus allowing differential measure-

ments where only the signal change caused by the interaction of the analyte with the probe would be registered.

In summary it can be said that a novel biosensor platform based on electrochemical impedimetric sensing was developed. Three prototypes of specialised sensors were tested and they performed very well under laboratory conditions. Together with the mentioned improvements and a suitable manufacturing solution this system has the potential for several marketable applications in the health care sector as well as for environmental monitoring or food safety.

Bibliography

[1] Olivier Lazcka, F. Javier Del Campo, and F. Xavier Muñoz, *Pathogen detection: A perspective of traditional methods and biosensors.* Biosensors & Bioelectronics, 22 (7) **2007**, pp. 1205–1217.

[2] Manju Gerard, Asha Chaubey, and B.D. Malhotra, *Application of conducting polymers to biosensors.* Biosensors & Bioelectronics, 17 (5) **2002**, pp. 345–359.

[3] W. Liao, S. Guo, and X.S. Zhao, *Novel probes for protein chip applications.* Frontiers in Bioscience, 11 **2006**, pp. 186–197.

[4] S. Cosnier, *Biosensors based on electropolymerized films: new trends.* Analytical and Bioanalytical Chemistry, 377 (3) **2003**, pp. 507–520.

[5] Kagan Kerman, Masaaki Kobayashi, and Eiichi Tamiya, *Recent trends in electrochemical DNA biosensor technology.* Measurement Science and Technology, 15 (2) **2004**.

[6] Noemi Rozlosnik, *New directions in medical biosensors employing poly(3,4-ethylenedioxy thiophene) derivative-based electrodes.* Analytical and Bioanalytical Chemistry, 395 (3) **2009**, pp. 637–45.

[7] K. Kiilerich-Pedersen, C.R. Poulsen, T. Jain, and N. Rozlosnik, *Polymer Based Biosensor for Rapid Electrochemical Detection of Virus Infection of Human Cells.* Biosensors & Bioelectronics **2011**, pp. 386–392.

[8] A. Balamurugan and Shen-Ming Chen, *Poly(3,4-ethylenedioxythiophene-co-(5-amino-2-naphthalenesulfonic acid)) (PEDOT-PANS) film modified glassy carbon electrode for selective detection of dopamine in the presence of ascorbic acid and uric acid.* Analytica Chimica Acta, 596 (1) **2007**, pp. 92–8.

[9] Hong Xie, Shyh-Chyang Luo, and Hsiao-Hua Yu, *Electric-field-assisted growth of functionalized poly(3,4-ethylenedioxythiophene) nanowires for label-free protein detection.* Small, 5 (22) **2009**, pp. 2611–7.

[10] Anil Kumar Sarma, Preety Vatsyayan, Pranab Goswami, and Shelley D. Minteer, *Recent advances in material science for developing enzyme electrodes.* Biosensors & Bioelectronics, 24 (8) **2009**, pp. 2313–22.

[11] Juan C. Vidal, Silvia Méndez, and Juan R. Castillo, *Electropolymerization of pyrrole and phenylenediamine over an organic conducting salt based amperometric sensor of increased selectivity for glucose determination.* Analytica Chimica Acta, 385 (1-3) **1999**, pp. 203–211.

[12] Marie-Pierre Dubois, Chantal Gondran, Olivier Renaudet, Pascal Dumy, Hugues Driguez, Sébastien Fort, and Serge Cosnier, *Electrochemical detection of Arachis hypogaea (peanut) agglutinin binding to monovalent and clustered lactosyl motifs immobilized on a polypyrrole film.* Chemical Communications, (34) **2005**, pp. 4318–20.

[13] G. Bidan, M. Billon, T. Livache, G. Mathis, A. Roget, and L. Torresrodriguez, *Conducting polymers as a link between biomolecules and microelectronics.* Synthetic Metals, 102 (1-3) **1999**, p. 1363.

[14] L. Sasso, I. Vedarethinam, J. Emnéus, W.E. Svendsen, and J. Castillo-León, *Self-assembled diphenylalanine nanowires for cellular studies and sensor applications.* Journal of Nanoscience and Nanotechnology, 12 (4) **2012**, pp. 3077–3083.

[15] Hitoshi Yamato, Masaki Ohwa, and Wolfgang Wernet, *Stability of polypyrrole and poly(3,4-ethylenedioxythiophene) for biosensor application.* Journal of Electroanalytical Chemistry, 397 (1-2) **1995**, pp. 163–170.

[16] V. Syritski, R.E. Gyurcsányi, A. Öpik, and K. Tóth, *Synthesis and characterization of inherently conducting polymers by using Scanning Electrochemical Microscopy and Electrochemical Quartz Crystal Microbalance.* Synthetic Metals, 152 (1–3) **2005**, pp. 133–136.

[17] L. Groenendaal, F. Jonas, D. Freitag, H. Pielartzik, and J.R. Reynolds, *Poly(3,4-ethylenedioxythiophene) and Its Derivatives: Past, Present, and Future*. Advanced Materials, 12 (7) **2000**, p. 481.

[18] Y. Shi, S. Luo, W. Fang, K. Zhang, E. Ali, F. Boey, J. Ying, J. Wang, H. Yu, and L. Li, *Work function engineering of electrodes via electropolymerization of ethylenedioxythiophenes and its derivatives*. Organic Electronics, 9 (5) **2008**, p. 859.

[19] Alexander Kros, Roeland J.M. Nolte, and Nico A.J.M. Sommerdijk, *Poly(3,4-ethylenedioxythiophene)-based copolymers for biosensor applications*. Journal of Polymer Science Part A: Polymer Chemistry, 40 (6) **2002**, p. 738.

[20] A. Lima, P. Schottland, S. Sadki, and C. Chevrot, *Electropolymerization of 3,4-ethylenedioxythiophene and 3,4-ethylenedioxythiophene methanol in the presence of dodecylbenzenesulfonate*. Synthetic Metals, 93 (1) **1998**, pp. 33–41.

[21] G.A. Sotzing, J.R. Reynolds, and P.J. Steel, *Electrochromic conducting polymers via electrochemical polymerization of bis(2-(3,4-ethylenedioxy)thienyl) monomers*. English. Chemistry of Materials, 8 (4) **1996**, pp. 882–889.

[22] K.E. Aasmundtveit, E.J. Samuelsen, L.A.A. Pettersson, O. Inganäs, T. Johansson, and R. Feidenhans'l, *Structure of thin films of poly(3,4-ethylenedioxythiophene)*. Synthetic Metals, 101 (1–3) **1999**, pp. 561–564.

[23] Bjørn Winther-Jensen and Keld West, *Stability of highly conductive poly-3,4-ethylene-dioxythiophene*. Reactive and Functional Polymers, 66 (5) **2006**, pp. 479–483.

[24] Thomas Steen Hansen, Keld West, Ole Hassager, and Niels B. Larsen, *Integration of conducting polymer network in non-conductive polymer substrates*. Synthetic Metals, 156 (18-20) **2006**, p. 1203.

[25] Thomas S. Hansen, Keld West, O. Hassager, and Niels B. Larsen, *Direct Fast Patterning of Conductive Polymers Using Agarose Stamping*. Advanced Materials, 19 (20) **2007**, p. 3261.

[26] Thomas Steen Hansen, Keld West, Ole Hassager, and Niels B. Larsen, *An all-polymer micropump based on the conductive polymer poly (3,4-ethylenedioxythiophene) and a polyurethane channel system*. Journal of Micromechanics and Microengineering, 17 (5) **2007**, p. 860.

[27] T.T. Le, D.W. Kim, Y. Lee, and J.D. Nam, *Vapor-phase thin-film coating of PEDOT on polymeric substrate for electroluminescence device*. [Accessed online 25.11.2010]. **2005**.

[28] Bjørn Winther-Jensen and Keld West, *Vapor-phase polymerization of 3,4-ethylenedioxythiophene: A route to highly conducting polymer surface layers*. Macromolecules, 37 (12) **2004**, pp. 4538–4543.

[29] Dhiman Bhattacharyya and Karen K. Gleason, *Single-Step Oxidative Chemical Vapor Deposition of –COOH Functional Conducting Copolymer and Immobilization of Biomolecule for Sensor Application*. Chemistry of Materials, 23 (10) **2011**, p. 2600.

[30] Johan Ulrik Lind, Canet Acikgoz, Anders Egede Daugaard, Thomas L. Andresen, Soeren Hvilsted, Marcus Textor, and Niels Bent Larsen, *Micropatterning of functional conductive polymers with multiple surface chemistries in register*. Langmuir, 28 (15) **2012**, pp. 6502–6511.

[31] E.M. Blalock, ed., *A beginner's guide to microarrays*. Kluwer Academic Publishers, 2003.

[32] B.S. Emanuel and S.C. Saitta, *From microscopes to microarrays: dissecting recurrent chromosomal rearrangements*. Nature Reviews Genetics, 8 (11) **2007**, pp. 869–883.

[33] Kannan Balasubramanian, *Label-free indicator-free nucleic acid biosensors using carbon nanotubes*. Engineering in Life Sciences, 12 (2) **2012**, pp. 121–130.

[34] D. Berdat, A.C.M. Rodríguez, F. Herrera, and M.A.M. Gijs, *Label-free detection of DNA with interdigitated micro-electrodes in a fluidic cell.* Lab on a Chip, 8 (2) **2008**, pp. 302–308.

[35] M. Gebala, L. Stoica, S. Neugebauer, and W. Schuhmann, *Label-Free Detection of DNA Hybridization in Presence of Intercalators Using Electrochemical Impedance Spectroscopy.* Electroanalysis, 21 (3-5) **2009**, pp. 325–331.

[36] D. Li, X. Zou, Q. Shen, and S. Dong, *Kinetic study of DNA/DNA hybridization with electrochemical impedance spectroscopy.* Electrochemistry communications, 9 (2) **2007**, pp. 191–196.

[37] Y. Yusof, Y. Yanagimoto, S. Uno, and K. Nakazato, „Electrical characteristics of biomodified electrodes using nonfaradaic electrochemical impedance spectroscopy". In: *Proceedings of World Academy of Science, Engineering and Technology.* Vol. 73. 2011, pp. 295–299.

[38] R Monina Klevens et al., *Invasive methicillin-resistant Staphylococcus aureus infections in the United States.* JAMA-Journal of the American Medical Association, 298 (15) **2007**, pp. 1763–1771.

[39] Centers for Disease Control and Prevention (CDC), *Emergence of Mycobacterium tuberculosis with extensive resistance to second-line drugs–worldwide, 2000-2004.* MMWR. Morbidity and mortality weekly report, 55 (11) **2006**, pp. 301–305.

[40] A.R White et al., *Effective antibacterials: at what cost? The economics of antibacterial resistance and its control.* Journal of Antimicrobial Chemotherapy, 66 (9) **2011**, pp. 1948–1953.

[41] E.J. Septimus and K.M. Kuper, *Clinical challenges in addressing resistance to antimicrobial drugs in the twenty-first century.* Clinical Pharmacology & Therapeutics, 86 (3) **2009**, pp. 336–339.

[42] Felipe C. Cabello, *Heavy use of prophylactic antibiotics in aquaculture: a growing problem for human and animal health and for the environment.* Environmental Microbiology, 8 (7) **2006**, pp. 1137–1144.

[43] Wolfgang Witte, *Medical Consequences of Antibiotic Use in Agriculture.* Science, 279 (5353) **1998**, pp. 996–997.

[44] Erik Gullberg, Sha Cao, Otto G. Berg, Carolina Ilbäck, Linus Sandegren, Diarmaid Hughes, and Dan I. Andersson, *Selection of Resistant Bacteria at Very Low Antibiotic Concentrations.* PLoS Pathogens, 7 (7) **2011**, e1002158.

[45] Eva González-Fernández, Noemí de-los-Santos-Álvarez, María Jesús Lobo-Castañón, Arturo José Miranda-Ordieres, and Paulino Tuñón-Blanco, *Impedimetric aptasensor for tobramycin detection in human serum.* Biosensors & Bioelectronics, 26 (5) **2011**, pp. 2354–2360.

[46] Kyung-Mi Song, Minseon Cho, Hunho Jo, Kyoungin Min, Sung Ho Jeon, Taisun Kim, Min Su Han, Ja Kang Ku, and Changill Ban, *Gold nanoparticle-based colorimetric detection of kanamycin using a DNA aptamer.* Analytical Biochemistry, 415 (2) **2011**, pp. 175–181.

[47] Kyung-Mi Song, Euiyoung Jeong, Weejeong Jeon, Minseon Cho, and Changill Ban, *Aptasensor for ampicillin using gold nanoparticle based dual fluorescence–colorimetric methods.* Analytical and Bioanalytical Chemistry, 402 (6) **2012**, pp. 2153–2161.

[48] Jaytry Mehta, Bieke Van Dorst, Elsa Rouah-Martin, Wouter Herrebout, Marie-Louise Scippo, Ronny Blust, and Johan Robbens, *In vitro selection and characterization of DNA aptamers recognizing chloramphenicol.* Journal of Biotechnology, 155 (4) **2011**, pp. 361–369.

[49] Robert Koch Institut: Arbeitsgemeinschaft Influenza. [Accessed online: February 13, 2013]. **2013**.

[50] PBS Newshour, *How Much Will the H1N1 Flu Cost the U.S.?* [Accessed online: February 13, 2013]. **2009**.

[51] EPN.dk, *Ny influenza koster milliarder.* [Accessed online: February 13, 2013]. **2009**.

[52] Katrine Kiilerich-Pedersen, Johannes Daprà, Solène Cherré, and Noemi Rozlosnik, *High Sensitivity Point-of-Care Device for Direct Virus Diagnostics.* In preparation for Biosensors & Bioelectronics **2013**.

[53] Sung Ho Jeon, Basak Kayhan, Tamar Ben-Yedidia, and Ruth Arnon, *A DNA aptamer prevents influenza infection by blocking the receptor binding region of the viral hemagglutinin.* Journal of Biological Chemistry, 279 (46) **2004**, pp. 48410–48419.

[54] L.H. Lauridsen, J.A. Rothnagel, and R.N. Veedu, *Enzymatic Recognition of 2´-Modified Ribonucleoside 5´-Triphosphates: Towards the Evolution of Versatile Aptamers.* ChemBioChem, 13 (1) **2012**, pp. 19–25.

[55] Johannes Daprà, Lasse Holm Lauridsen, Alex Toftgaard Nielsen, and Noemi Rozlosnik, *Comparative study on aptamers as recognition elements for antibiotics in a label-free all-polymer biosensor.* Biosensors & Bioelectronics **2013**.

Index

A. Publications

Papers & book chapters

Johannes Daprà, Katrine Kiilerich-Pedersen, Nikolaj Ormstrup Christiansen, Claus Riber Poulsen, Noemi Rozlosnik *Conductive Polymers in Medical Diagnostics* in: "Nanomedicine in Diagnostics", **2012**, 96

Johannes Daprà, Lasse Holm Lauridsen, Alex Toftgaard Nielsen, Noemi Rozlosnik *Comparative study on aptamers as recognition elements for antibiotics in a label-free all-polymer biosensor* Biosensors & Bioelectronics, **2013** (Published online ahead of print)

Johannes Daprà, Dorota Kwasny, Johan U. Lind, Niels B. Larsen, Winnie E. Svendsen, Noemi Rozlosnik *All-polymer electrochemical DNA hybridisation biosensor based on poly (3,4-ethylenedioxythiophene* (Manuscript in preparation)

Patents

Noemi Rozlosnik, Johannes Daprà *Biosensor for point-of-care diagnostic and on-site measurements*, **2012** PCT/EP2012/067508

Conference proceedings

Johannes Daprà, Dorota Kwasny, Winnie E. Svendsen, Noemi Rozlosnik *All-polymer Chip for electrochemical detection of DNA hybridisation* Poster at: "Nanotoday Conference 2011", Waikoloa, HI, USA, **2011**

Johannes Daprà, Noemi Rozlosnik *Application of aptamers for label-free all-polymer biosensors* Oral presentation at: "International Conference and Exhibition on Biosensors & Bioelectronics", Las Vegas, NV, USA, **2012**

Johannes Daprà, Noemi Rozlosnik *Application of Label-free Aptasensors in Environmental Monitoring* Poster at: "Micro- and Nanotechnology in Medicine Conference 2012", Lahaina, HI, USA, **2012**

5

Conductive Polymers in Medical Diagnostics

Johannes Daprà,[1] *Katrine Kiilerich-Pedersen,*[1] *Nikolaj Ormstrup Christiansen,*[1] *Claus Riber Poulsen*[1] and *Noemi Rozlosnik*[1,*]

INTRODUCTION

The demand is growing in the field of medical diagnostics for cost efficient and disposable devices, which demonstrate high sensitivity, reliability and simplicity. Lately, biosensors—in particular conducting polymer-based electrochemical sensors—have demonstrated numerous advantages in areas related to human health, such as diagnosis of infectious disease, genetic mutations, drug discovery, forensics, and food technology, due to their simplicity and high sensitivity.

The major processes involved in any biosensor system are analyte recognition, signal transduction, and readout. Due to their specificity, speed, portability, and low cost, biosensors offer exciting opportunities for numerous decentralized clinical applications—point of care systems.

The ongoing trend in biomedicine is to go smaller. For almost a decade, the buzz word has been *nano*, and the analytical micro devices are now appearing in the clinic. The progress within microfluidic technologies has enabled miniaturization of biomedical systems and biosensors. The down-scaling has several advantages: refined control of fluidics, low sample consumption, applicability to point of care, and low cost.

[1]Department of Micro- and Nanotechnology, Technical University of Denmark, Denmark.
*Corresponding author

Point of care is an emerging field within medical diagnostics and disease monitoring, and eventually disease control. Employing specially designed micro systems, a patient can be monitored continuously at the bed side, and save precious time on commuting between home, doctor and hospital. The technological advancements in the biosensor technology within recent years have accelerated the R&D in point of care devices.

Cost benefit is always an important factor in development of novel medical devices. To reduce the expenses of biosensors, the use of noble metals and cleanroom processing should be kept at a minimum. Therefore, we predict a shift in the usage of gold and platinum to degradable polymer materials. Polymer based microfluidic devices meet the requirements of low cost and mass production, and they are suitable for biosensor applications. One of the most promising conductive polymers is poly(3,4-ethylenedioxythiophene) (PEDOT) and its derivatives due to their attractive properties: high stability, high conductivity (up to 400–600 S/cm) and high transparency.

This chapter will look further into the advantages and applications of all-polymer microfluidic devices for biomedical diagnostics and compare with traditional systems. In many biosensor applications, only one analyte is of interest, and preferentially it should be isolated from an inhomogeneous patient sample. Section 2 provides the reader with an overview of the different novel microfluidic separation techniques in polymeric devices.

Different detection methods are applied in biosensors, some of the promising techniques will be summarized in Section 3. Conductive polymers—primarily PEDOT—are the focus of Section 4. They have many excellent properties and in fact, they can compete with gold in many applications. The focus of Section 5 is sensitivity and specificity of biosensors. High sensitivity and specificity is crucial and can be achieved by functionalization with different molecules. The section will primarily focus on the use of aptamers which is favourable above antibodies. Finally, Section 6 gives an overview of the current status in biosensor development while focusing on ongoing research.

NOVEL MICROFLUIDIC SEPARATION TECHNIQUES FOR SAMPLE PREPARATION

The progress in micro fabrication and lab-on-a-chip technologies is a major field for development of new approaches to bioanalytics and cell biology. Microfluidics has proven successful for cell and particle handling, and the interest in micro devices for separation of particles or cells has increased significantly (Giddings 1993, Nolan & Sklar 1998, Toner & Irimia 2005).

Biological samples comprise a heterogeneous population of cells or particles, which is inconvenient for many biomedical applications, where the objective of study is often just one species. For example, the isolation of CD4+ T-lymphocytes from whole blood is essential to diagnoze human immunodeficiency virus (HIV) (Kuntaegowdanahalli et al. 2009), the isolation of leukocytes is important in drug screening assays, and the isolation of specific micro particles from blood plasma is critical for our understanding of inflammatory diseases. Thus, separation of cells or particles has a wide range of applications within different areas of medicine such as diagnostics, therapeutics, drug discovery, and personalized medicine (Gossett et al. 2010).

Flow cytometry has remained the preferred method for cell sorting by many biologists because the technique is well established and has both high sensitivity and high throughput. Recently, fluorescence based sorting of cells and particles has also been implemented in microfluidic devices.

The microfluidic separation techniques are broadly classified as being either passive or active, depending on the operating principles (Table 5.1). Active separation of particles requires an external force (i.e., electrical power, mechanical pressure or magnetic force), whereas passive separation techniques rely on channel geometry and inherent hydrodynamic forces for functionality (i.e., pillars, pressure field gradient or hydrodynamic force). The following section will introduce a couple of novel separation principles with application in biomedical sensors. For further reading on continuous separation of particles, see review papers by Lenshof and Laurell (2010), Gossett et al. (2010), and Bhagat et al. (2010).

Table 5.1: Active and passive separation technique with application in biomedical sensors.

	Method	**Mechanism**
Active	Acoustophoresis	Acoustic waves
	Optical tweezers	Optical
	Dielectrophoresis	Electric field
Passive	Obstacles	Laminar flow
	Induced lift	Inertial force

Active Separation Techniques

Acoustophoresis

Acoustophoresis is the separation of particles using high intensity sound waves. In a microfluidic system, particles with an induced acoustic standing wave will experience a force towards a node or anti node dependent on their physical properties (Lenshof and Laurell 2010). If two

particles suspended in a fluid have opposite acoustic contrast, a separation will occur gathering one at node and the other at anti-node. Generally, rigid particles will have a negative *phase* and move toward the node, whereas air bubbles and lipid vesicles gather at the anti-node (Lenshof and Laurell 2010). After separation, the properties of the laminar flow in the microfluidic channel ensure that particles remain at their position in the channel, hence they can be collected separately with a flow splitter.

Both particles with opposite and similar acoustic contrast can be separated using this technique. The size of particles will influence the time scale. Large particles experience a higher force than smaller ones, and thus gather at the node faster than the small particles. Peterson et al. (2007) described a microfluidic system with three inlets (Fig. 5.1), where a sample composed of different sized particles was introduced at the sides of a microfluidic channel with a sheath fluid in the middle to keep particles in close proximity to channel walls. The system is designed such that an ultrasonic transducer induces a force on the particles, which forces them towards the middle of the channel. Since the larger particles experience a higher force than small particles, the large particles immediately gather at the centre of the channel. Particles are thus allocated proportional to their size. Making use of a flow splitter, particles are separated according to their size. Applying this technique, Peterson et al. (2007) demonstrated separation of a mixture of different sized particles.

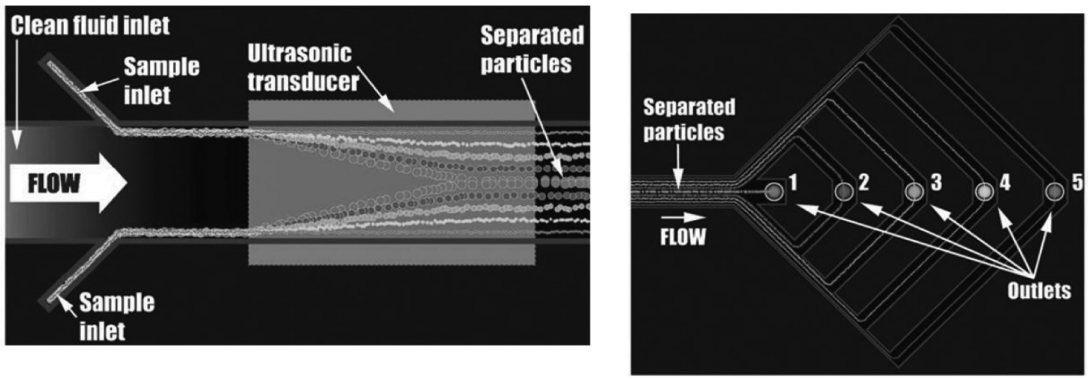

Figure 5.1: Acoustophoresis. (a) Particles entering main channel from two side inlets. Particles are positioned near channel walls because clean sheath fluid is introduced at a third inlet. The flow of particles is controlled by the acoustic waves, which are introduced by an ultrasonic transducer. After this point, the particles distribute proportional to size. (b) Flow splitters are used for separation of different sized particles. Nine fractions of the flow can be gathered at five outlets (Adapted from Peterson et al. 2007).

Color image of this figure appears in the color plate section at the end of the book.

Ion Depletion

Ion depletion is a microfluidic technique for separation and concentration of proteins. As the name indicates, the method is based on ion transfer in a nanofluidic channel (approximately 50 nm in depth). Counter-ions will migrate from the Debye layer through the nanochannel to a higher extent than co-ions, so that a net transfer of counter-ions is transferred from the anodic side to the cathodic side. Thus, the concentration of counter-ions decreases on the anodic side and an increase is achieved on the cathodic side. If a protein in solution is part of the co-ion population, this protein will be trapped in a plug on either side of the ion depletion region, and is hence separated from the bulk solution. The principle of ion depletion is illustrated on Figs. 5.2 and 5.3 (Wang et al. 2005).

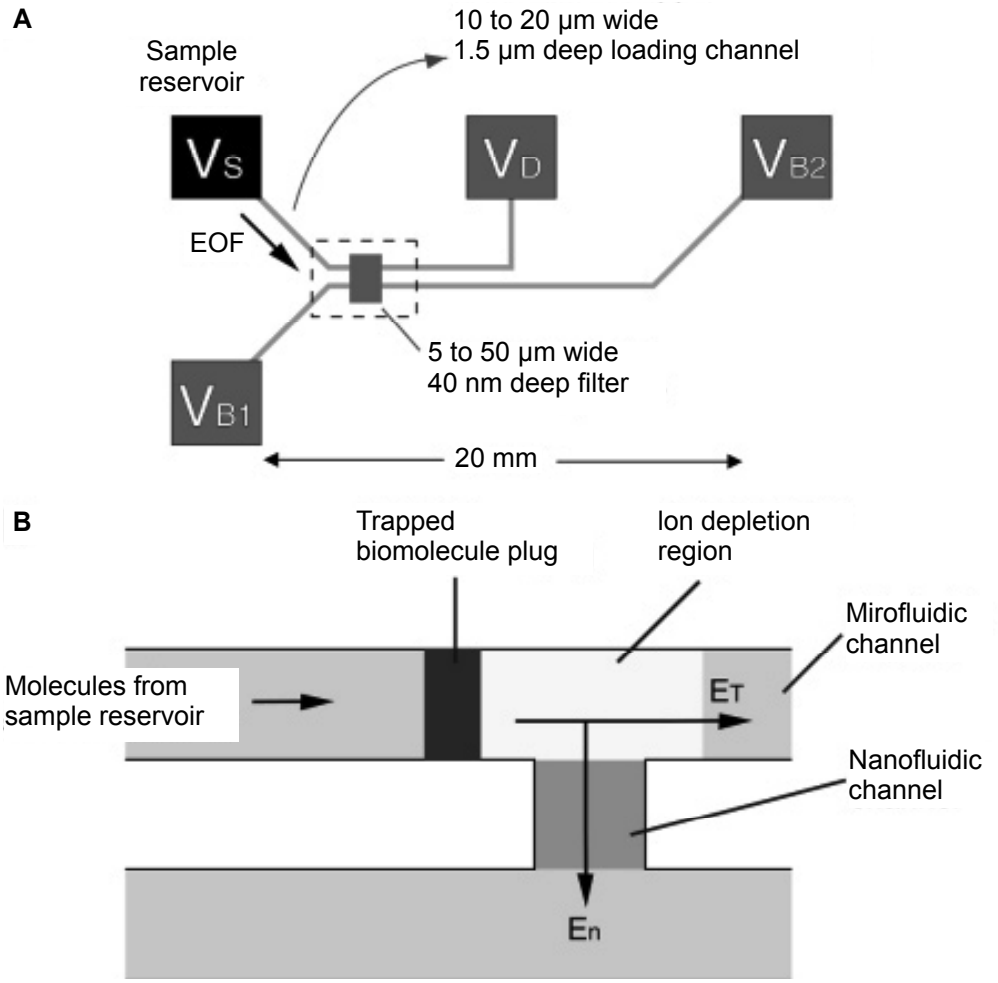

Figure 5.2: Nanofluidic protein concentrating device by ion depletion: (A) Layout of the device. (B) Schematic diagram showing the concentration mechanism. Once proper voltages are applied, the trapping region and depletion region will be formed as indicated. The E_T specifies the electrical field applied across the ion depletion region, while the E_n specifies the cross nanofilter electrical field (Adapted from Wang et al. 2005).

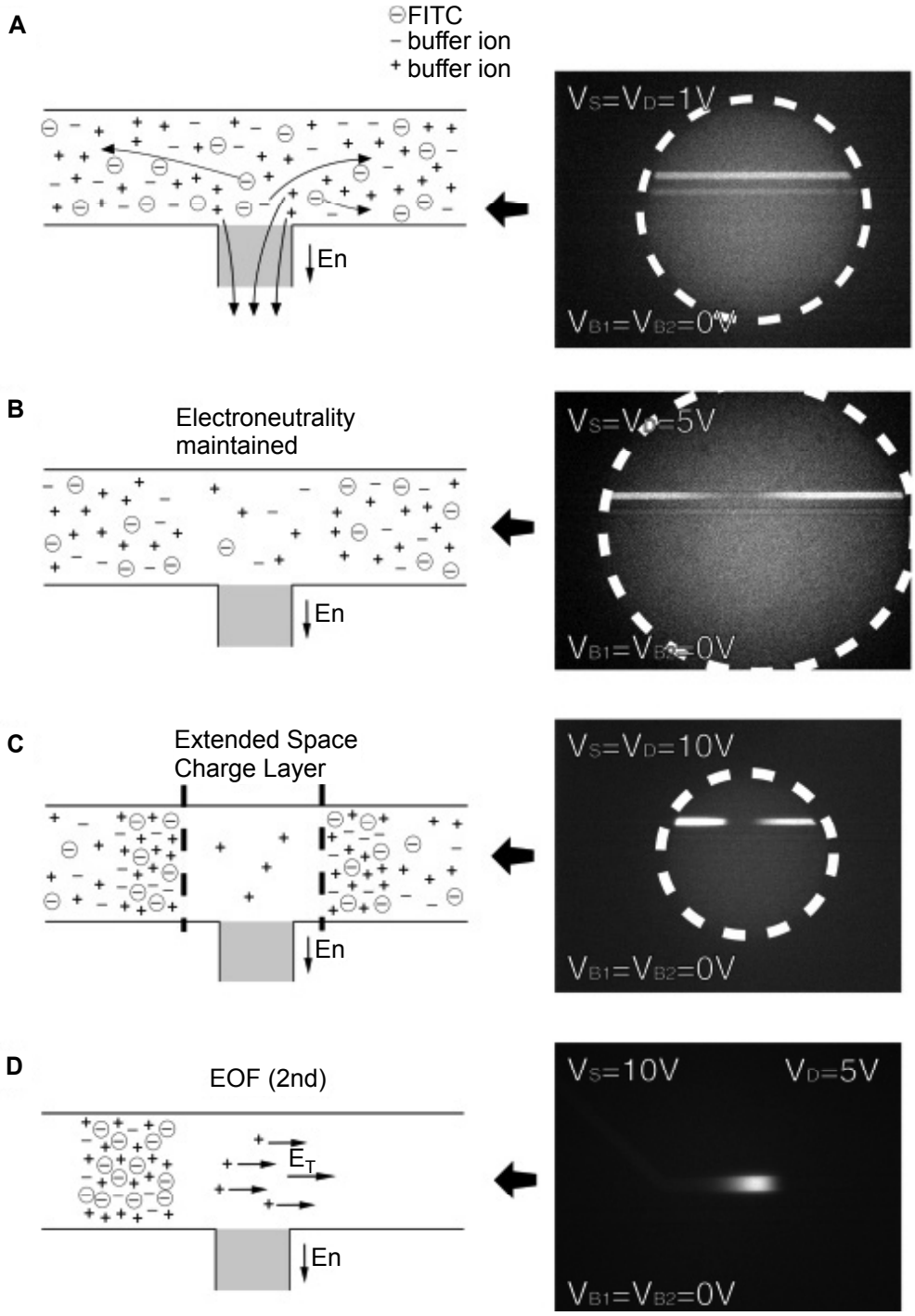

Figure 5.3: Mechanism of preconcentration in the nanofilter device (A) No concentration polarization is observed when a small electrical field (E_n) is applied across the nanofilter. (B) As the E_n increases, the transport of ions becomes diffusion-limited and generates the ion depletion zone. However, the region maintains its electroneutrality. (C) Once a strong field (E_n) is applied, the nanochannel will develop an induced space charge layer, where electroneutrality is no longer maintained. (D) By applying an additional field (E_T) along the microfluidic channel in the anodic side (from V_S to V_D), a nonlinear electrokinetic flow (called electroosmosis of the second kind) is induced, which results in fast accumulation of biomolecules in front of the induced space charge layer (Adapted from Wang et al. 2005).

Passive Separation Techniques

Obstacles

Obstacles arranged in microfluidic channels are commonly applied for preventing particles from entering certain areas or used to manipulate the flow of fluid in a microchannel. Deterministic lateral displacement is a method for size separation of particles or cells, accomplished by placing posts asymmetrically in a microchannel (Fig. 5.4) and thus forcing particles of different sizes to follow different flow paths.

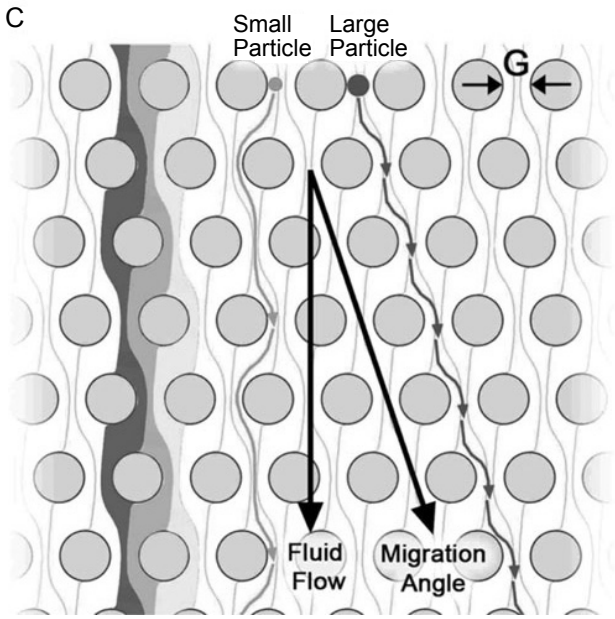

Figure 5.4: Deterministic lateral displacement (Adapted from Gossett et al. 2010).

Spiral Microchannels

Separation of particles in a spiral microchannel was described by Kuntaegowdanahalli and colleagues (2009) (see Fig. 5.5).

It is a passive separation technique based on the centrifugal force. Centrifugal based techniques have been demonstrated using flows in curvilinear microchannels (Gregoratto et al. 2007, Seo et al. 2007). In general, the flow of fluid through a curvilinear channel experiences a centrifugal acceleration, directed radially outward. The channel geometry gives rise to vortices, which are exploited for separation of different sized particles. Particles in the centre of the channel will experience a drag away from the centre, whereas particles in the proximity of the channel walls experience repulsion from the walls. Consequently, particles align at four equilibrium positions in the channel and different sized particles can thus be collected at different outlets (Bhagat et al. 2008, Di Carlo et al. 2007).

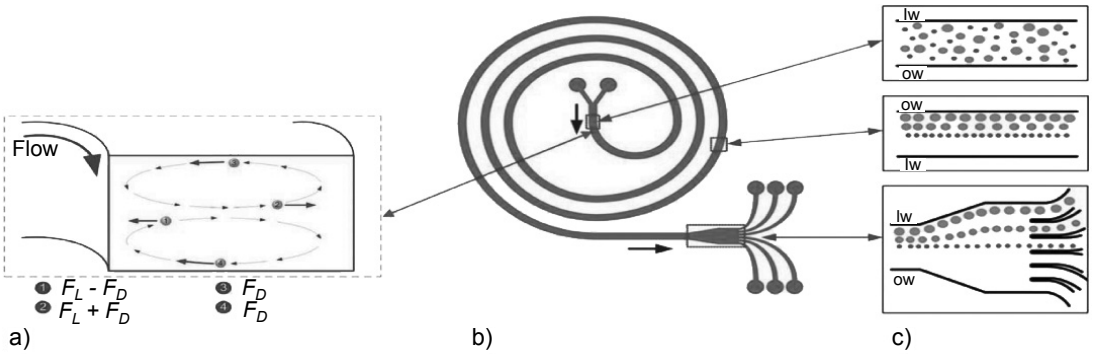

Figure 5.5: Spiral microchannel. (a) Neutral buoyant particles suspended in a medium in a spiral shaped channel experience forces and drag. Resultantly, particles redistribute within the microchannel. (b) Schematic representation of spiral channel for particle separation. (c) Different sized particles equilibrate at different positions in microchannel, and are collected at different outlets (Adapted from Kuntaegowdanahalli et al. 2009 and Bhagat et al. 2008).

Color image of this figure appears in the color plate section at the end of the book.

ELECTRICAL DETECTION METHODS

Modern biosensors for medical diagnostics must be specific, quick, and reproducible at reasonable cost. Electrical sensing is one of the simplest detection methods in microsystems. The electrical detection has traditionally received the major share of the attention in biosensor development. Such devices produce a simple, inexpensive and yet accurate and sensitive platform for patient diagnosis.

The name 'electrochemical biosensor' is applied to a molecular sensing device which intimately couples a biological recognition element to an electrode transducer. The purpose of the transducer is to convert the biological recognition event into a useful electrical signal at the electrode-solution interfaces.

Microelectrodes are powerful and versatile tools in the study of electrochemical processes of mechanistic and/or analytical interest. They experience high mass transport rates but little interference from interfacial capacitance or solution resistance effects. These advantageous properties are due to the small size of these devices. Microelectrodes can work with very small sample volumes enabling the detection of very small amounts of material. The improved mass transport properties facilitate the measurement of higher exchange current densities and electron transfer rate constants and also allow the study of fast coupled chemical reactions.

Electrochemical systems are extremely sensitive to the processes that take place on the surfaces of the electrodes, and in this sense the electrodes are direct transducers in biomedical applications. Several types

of electrochemical methods are used in biosensors; the two most common ones are the amperometry and impedance spectroscopy (EIS) (Lazcka et al. 2007). Recently, all-polymer field effect transistors for biosensing have been introduced (Lee et al. 2010).

Amperometry

Amperometry is a method of electrochemical analysis in which the signal of interest is a current that is linearly dependent upon the concentration of the analyte. As certain chemical species are oxidized or reduced (redox reactions) at the electrodes, electrons are transferred from the analyte to the working electrode or to the analyte from the electrode. The direction of flow of electrons depends upon the properties of the analyte and can be controlled by the electric potential applied to the working electrode.

Amperometric biosensors operate by applying a constant potential and monitoring the current associated with the reduction or oxidation of an electroactive species involved in the recognition process. The amperometric biosensor is attractive because of its high sensitivity and wide linear range.

Conductivity and Impedance Spectroscopy

Electrochemical impedance spectroscopy (EIS) combines analyses of both the resistive and capacitive properties of materials, based on the perturbation of the system by a small-amplitude sinusoidal AC signal. The impedance of the system can be scanned over a wide range of AC signal frequencies. The amplitude of the current, potential signals and the resulting phase difference between voltage and current dictates the system impedance. Therefore, the impedance signal is dependent on the nature of the system under study.

Equivalent circuit models fitted to the impedance curves are useful tools for characterizing the system. Although this methodology is widely accepted because of ease of use, extreme care must be taken to ensure that the equivalent circuit obtained makes physical sense. An advantage of EIS compared to amperometry is that redox labels are no longer necessary, which simplifies the sensor preparation.

Organic Field Effect Transistors

Organic field effect transistors (Organic FETs) have a potential of being the active matrix for many electronic devices, including biosensors for biological material. An organic field-effect transistor consists of a source and drain electrode, an organic semiconductor (which is in this case a conductive polymer), a gate dielectric, and a gate electrode. A number

of different studies have demonstrated conductance-based sensors employing a molecular receptor layer immobilized on the surface of a semiconductor device. The receptor molecules provide the means to achieve highly selective sensing because they can be engineered to have much higher binding affinities with the desired target molecules than the other species in the analyte solution (see Section 4). Although the organic FET is a promising candidate for biosensor applications, optimization of the device structure and operating conditions is still required.

CONDUCTIVE POLYMERS FOR SENSING

A major cost factor in electrochemical biosensors is the electrode material—often noble metal—demanding extensive production steps in cleanroom facilities. To cut down on these expenses there is a trend to utilize conductive polymers for sensing. This section will give an introduction to advantages of conductive polymers compared to noble metals, and guide through the considerations associated with selecting an appropriate polymer material for biosensor applications.

Polymers or Metals?

The application of polymers as supporting materials in microfluidic systems is well established; however the electronic sensing units in most chips are fabricated from metallic conductors such as platinum or gold.

Biocompatibility, high sensitivity and specificity are a demand in modern medical biosensors. Biocompatibility is required because some biological applications involve living cells, bacteria or virus. High specificity and sensitivity is essential for detecting highly diluted analytes in biological samples, because the samples contain a cocktail of similar components, which can influence a measurement. All of these requirements can be fulfilled by the metal electrode materials such as solid platinum or gold (Prodromidis and Karayannis 2002). Though, a major disadvantage of the noble metals is the high cost, which is continuously increasing.

Conjugated polymers are an alternative to the traditional electrode materials. The electronic structure of these compounds gives them properties similar to inorganic semiconductors. In 1977, Shirakawa et al. discovered that doping polyacetylene with halogens increased the conductivity by up to four orders of magnitude. The following research on this topic by Shirakawa, MacDiarmid and Heeger was awarded with the Nobel Prize in chemistry in 2000.

Over the years, electronically conductive polymers have been proposed for many applications (Jagur-Grodzinski 2002, Olson et al. 2010)—from biomedical sensors to nanowire integration in photovoltaic

cells or printable RFID antennae—yet only few have made it to the market. Among those are electrochromic coatings for windows, antistatic coatings, organic light emitting diodes (OLEDs), and corrosion protection for metals or surface finish for printed circuit boards (Groenendaal et al. 2000, Gustafsson et al. 1994, Wessling 2001).

The immediate advantage of conductive polymer electrodes is the much lower cost of raw materials and the inexpensive production steps. Certain polymers offer high biocompatibility and options for modifying the properties by varying side groups. This can be useful for probe immobilization, which is a crucial procedure in biosensors. Conductive polymers allow a broad range of chemical modifications for covalent attachment of enzymes, antibodies, DNA or other bioprobes (Sarma et al. 2009, Teles and Fonseca 2008).

In summary, replacing metals with polymers as electrode material does not only limit the cost on the materials themselves, but also allows for the inexpensive mass production by modern ink-jet printing methods (Loffredo et al. 2009, Mabrook et al. 2006) or agarose stamping (Hansen et al. 2007).

Polymer Selection

As mentioned in Section 3.1, biocompatibility is a very important factor in selecting an appropriate polymer. Biocompatibility is mainly influenced by the intrinsic toxicity of a material but also by hydrophilicity. Many conjugated polymers suffer from degradation because of irreversible oxidation processes, or they lose their conductive properties over time. A constant and reliable signal is crucial for sensor devices, and accordingly the polymer should be stable over a certain period of time.

In order to provide a good signal to noise ratio in electrochemical measurements, a low ohmic resistance (i.e., high conductivity) is preferred. Currently, these requirements are met by few polymers on the market.

Polypyrrole

The physical properties of polypyrrole (PPy, Fig. 5.6(a)) make it suitable for biosensor applications. PPy has high decomposition temperature (180–237°C), glass transition temperature (Tg, 160–170°C), and relatively high conductivity of up to 3 $S{\cdot}cm^{-1}$ (Biswas and Roy 1994). Besides, PPy has a good environmental stability and different facile processing methods (Wang et al. 2001).

In 2005, Dubois et al. developed a PPy based biosensor for label-free detection of peanut agglutinin. The lactosyl probe unit was immobilized on a biotinylated PPy film via avidin bridges. Their findings demonstrated

that the bioprobe could be immobilized directly on the functionalized electrode surface, facilitating label-free detection by electrochemical methods.

There are different strategies to functionalize the electrode surface, and another approach was described by Campbell et al. (1999). They incorporated human erythrocytes into the PPy matrix, and upon capture and binding of Anti-Rhesus (D) antibody, a resistance change could be detected. Other techniques will be discussed in Section 4.

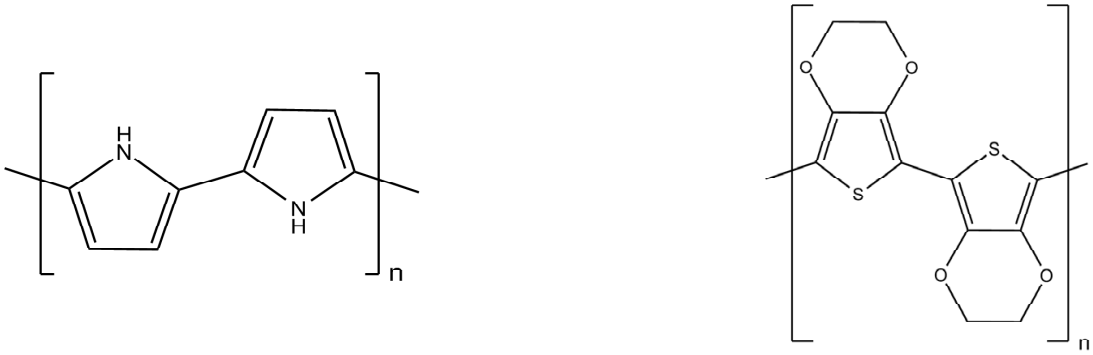

Figure 5.6: Monomer units of (a) polypyrrole (PPy) and (b) poly(3,4-ethylenedioxythiophene) (PEDOT).

Poly(3,4-ethylenedioxythiophene)

Improved properties compared to PPy were found for poly(3,4-ethylenedioxythiophene) or PEDOT. It is either chemically or electrically polymerized from the commercially available monomer 3,4-ethylenedioxythiophene. As can be seen in Fig. 5.6(b), it has some structural similarities with PPy. PEDOT has exceptional high conductivity (up to 600 $S{\cdot}cm^{-1}$), high environmental stability and is biocompatible and transparent for visible light. The most common dopants used for PEDOT are poly(styrene sulphonate) (PSS) and tosylate. Several new methods have been also used to enhance the sensitivity, applicability and/or specificity of these sensors based on PEDOT, for example the incorporation of nanoparticles into the polymer matrix, ink jet printing/patterning of the conducting polymers, molecular imprinting for specific detection, the creation of organic transistors from conducting polymers to improve sensor sensitivity, or the embedding of cells into the conducting polymer matrix for direct stimulation (Rozlosnik 2009).

The works by Balamurugan and Chen (2007) and Vasantha and Chen (2006) show the high potential and superior qualities of PEDOT, and this conductive polymer has been employed in a number of biosensor micro devices.

An interesting study was presented by Kumar et al. (2006). A biosensor was developed to determine the concentration of the important mammalian neurotransmitter, dopamine via an electrochemical process. Since the concentration of ascorbic acid is around a thousand times higher than dopamine in a biological sample, and the two analytes have similar electrochemical potentials, the challenge was to measure the concentration of dopamine in the presence of ascorbic acid. Kumar et al. (2006) employed glassy carbon electrodes coated with PEDOT, and their findings demonstrated significant peak separation and improved anti-fouling properties compared to the more common electrode material glassy carbon, making PEDOT a good candidate for further applications in this field.

Glucose detection for blood sugar monitoring of diabetes patients is a huge and growing market for disposable biosensors. The established commercial systems make use of metal electrodes (typically Pt) coated with a gel containing the enzyme glucose oxidase, and the effectively measured agent is thus the oxidation product, hydrogen peroxide (H_2O_2). In contrast to the direct oxidation of dopamine on the electrodes in the example above, this indirect detection of glucose is more complicated. Considering the current market price of platinum of about 41 €/g (http://platinumprice.org), replacing the electrode material with a low cost polymer such as PEDOT seems sensible. Park et al. (2008) imprisoned glucose oxidase in hollow PEDOT micro-tubules on an indium-tin-oxide (ITO) glass surface (Fig. 5.7). In this configuration, the enzymes are surrounded by the electrode, and therefore their activity is not constrained by immobilization on a surface or incorporation into a polymer. Although the performance of this biosensor cannot meet the requirements of a classic system, it can be refined by increasing the enzyme density or improving the conductivity.

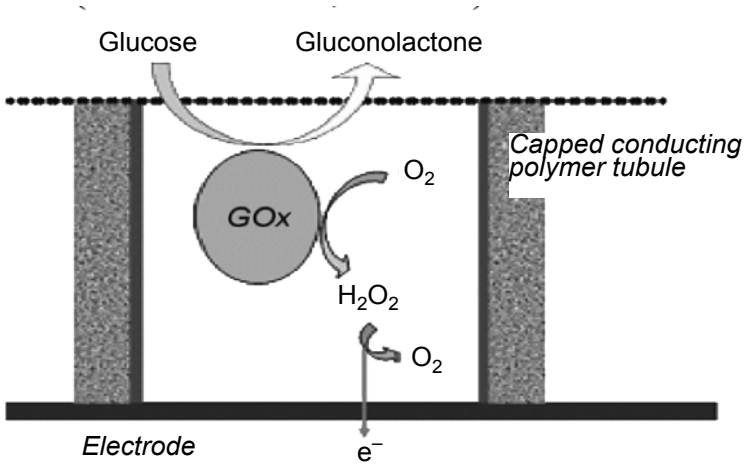

Figure 5.7: Glucose oxidase is imprisoned inside a PEDOT microtube covered with a non-conductive polymer (Park et al. 2008).

Many biosensors for pathogen detection are based on antibodies as probes, and deliver an indirect signal. These immunosensors require a fluorescently tagged second antibody, which reacts with occupied immobilized antibodies in a so-called sandwich assay.

A different approach was tested by Kim et al. (2010), who worked on the development of a point of care system for prostate specific antigen/α1-antichymotropsin (PSA-ACT) complex detection. This cancer marker is associated with prostate tumours and important for preoperative diagnosis and screening. Instead of using the conventional optical methods, they constructed an organic electrochemical transistor (OECT) based on PEDOT. The antigen was captured by immobilized antibodies on the conductive polymer. For signal enhancement, a secondary antibody with a covalently tethered gold nanoparticle was used. The system provided a detection limit as low as 1 $pg \cdot mL^{-1}$ and is thus sensitive enough for reliable PSA-ACT analysis.

PEDOT Derivatives

A field effect transistor (FET) based biosensor was demonstrated by Xie et al. (2009). The working principle is fundamentally different, considering it uses conductive polymer nanowires, which were electropolymerized between two gold electrodes. For minimizing the distance between polymer and binding event it was necessary to couple the probe (an aptamer, see also Section 4.3) directly to the electrode material. Normal PEDOT offers no possibility for covalent bonding of other molecules, so a derivative bearing a carboxylic acid group was used. With this functional group the oligonucleotide for thrombin detection was attached with a simple 1-ethyl-3-(3-dimethylaminopropyl)car-bodiimide/*N*-hydroxysuccinimide procedure (see Section 4.3, (EDC/NHS)). Thrombin binds specifically to the aptamers and becomes immobilized on the surface. The positively charged protein influences the transistor, so that the current flow changes. This type of biosensor has a broad dynamic range covering the physiologically interesting thrombin concentration range from a few to several hundred nanomoles.

Other PEDOT derivatives have also been investigated (Akoudad and Roncali 2000, Ali et al. 2007, Daugaard et al. 2008). The structural formulas of the most commonly used monomers are shown in Fig. 5.8; PEDOT-OH is more hydrophilic than normal PEDOT, and the azide modified PEDOT-N3 polymerizes slowly and has decreased conductivity. The only commercially available monomer is (2,3-dihydrothieno[3,4-*b*][1,4]dioxin-2-yl)methanol (commonly known as hydroxymethyl-EDOT or EDOT-OH) (8(a)), and it can be used as a basis for further modifications.

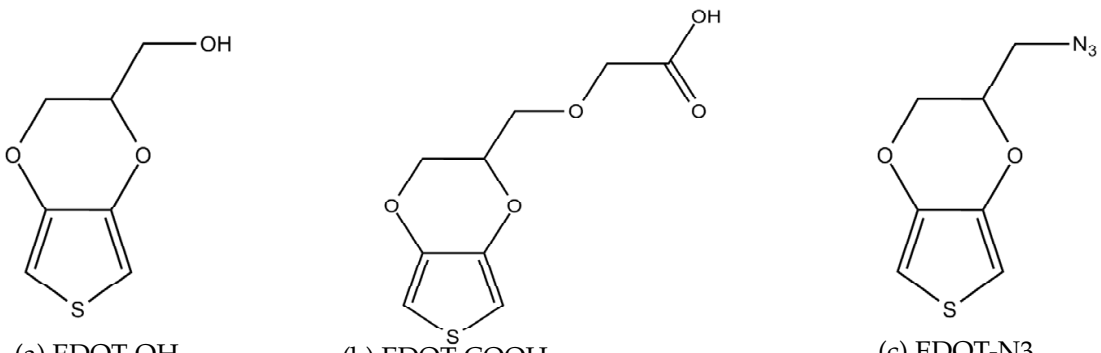

(a) EDOT-OH (b) EDOT-COOH (c) EDOT-N3

Figure 5.8: Different derivatives of 3,4-ethylenedioxythiophene (Ali et al. 2007, Daugaard et al. 2008).

Immobilization Methods

There are different techniques for immobilization of biomolecules (e.g., DNA) on an electrode surface. The most popular methods are formation of a biotin-streptavidin complex, formation of different covalent bonds like esters or amides, or click chemistry.

Biotin-Streptavidin Complex

Streptavidin is a protein consisting of four identical subunits, each of which has an extremely high affinity for biotin. A biotinylated surface can be coated with streptavidin so it offers reactive sites for fixation of likewise biotin tagged (bio)molecules. The biotin-streptavidin interaction is one of the strongest non-covalent bonds in nature and it is very specific. Moreover, the system is easy to handle and very biocompatible.

Despite the many advantages of streptavidin, a major drawback is the instability at low or high pH values, and high temperature. For some detection methods the rather thick protein layer between electrode and probe can substantially decrease the sensitivity of the sensor.

Covalent Bonding

Different activation methods have been used for a long time in chemistry, which require the availability of certain functional groups on the surface. The activation of a carboxylic acid group with 1-ethyl-3-(3-dimethylaminopropyl) carbodiimide (EDC) and *N*-hydroxysuccinimide (NHS) is often applied for amide-bond formation under mild conditions and can be used for binding molecules bearing free amino groups (Balamurugan et al. 2008, Xie et al. 2009).

For hydroxyl functionalized polymers and target molecules, a technique from DNA synthesis can be employed. The alcohol groups are activated with phosphoramidites to form a phosphoester, which

then reacts with another hydroxyl moiety and links the target molecules covalently to the surface (Pirrung 2002).

Click Chemistry

A very elegant approach for probe immobilization is the usage of so called 'click-chemistry'. In the Cu-catalysed Huisgen-type 1,3-cycloaddition suggested by Daugaard et al. (2008) an azide reacts in high yield with an alkyne to form a five-membered heterocycle. This bond is very stable and also the precursors have advantages such as stability toward hydrolysis and dimerization or ease of introduction (Kolb et al. 2001).

However, the azide functionalization of PEDOT downgraded its conductive properties significantly and the remaining Cu catalyst could influence biological systems.

ELECTRODE FUNCTIONALIZATION

Functionalization of electrodes is essential for achieving high sensitivity and specificity of electrochemical biosensors. This section provides an overview of the current trend in electrochemical sensors for medical diagnostics.

Recognition of Pathogens

Point of care diagnostic devices present a viable option for rapid and sensitive detection and analysis of pathogens. Biosensors can play an important role in the early diagnosis of acute viral disease and confine the spread of virulent disease outbreaks. Biosensors can also play an important role in early detection and diagnosis of cancer and autoimmune disorders based on specific biochemical markers.

As discussed in Section 2, separation and isolation of large quantities of a specific analyte would be preferable for many medical applications.

Patient samples comprise of a heterogeneous population of particles and cells, hence challenging the isolation of a single species in a high background concentration. For this reason, biosensors must be very specific and sensitive, allowing precise detection of very small quantities.

Antibodies

Many techniques for preparing functional biological surfaces for studies of cells, viruses or disease markers have been described in the literature. Refer to Section 4.3 for an overview of different coupling methods.

Immunoglobulins (IgG) are large Y-shaped proteins produced by the immune system, and are most abundant in blood plasma. Two identical antigen binding sites are formed from several loops of the polypeptide chain. These loops allow many chemical groups to close in on a ligand and link to it with many weak (non-covalent) reversible bonds. An antibody-antigen bond is highly specific because of the molecular structure of the protein.

Antibodies are the most common recognition molecules in biosensors. It is a naturally occurring protein and can only be produced in a host against immunogenic substances, giving rise to batch variation and a limited target range. For research purposes, monoclonal or polyclonal antibodies can be applied as a recognition molecule. Typically, monoclonal antibodies will ensure a higher specificity than polyclonal antibodies.

In medical sensor applications, functional orientation of the antibodies on the surface is crucial to ensure high sensitivity and specificity. It can be achieved by immobilizing the proteins on a supporting layer of protein A.

Aptamers

For many years, antibodies have been applied for surface functionalization in biosensors, ensuring specificity and sensitivity of sensors. Artificial nucleic acid ligands—known as aptamers—can cover the same field of application as antibodies. In the recent years, the use of aptamers has increased (Han et al. 2010, Syed and Pervaiz 2010), and they are in many ways superior to antibodies, as will be discussed in this section.

The Properties of Aptamers

Aptamers are oligonucleotides with a typical length of 40 to 80 base pairs, and were discovered in the 1980's as naturally occurring regulation elements in prokaryotic cells. They showed high affinity for viral and cellular proteins.

In 1990, Tuerk and Gold developed a convenient process for *in vitro* aptamer production, the so-called systematic evolution of ligands by exponential enrichment (SELEX, see in Section 5.3.2).

Aptamers are in many ways better than antibodies as is summarized in Table 5.2. The affinity for the target molecules of aptamers is similar to antibodies, and in some cases even higher compared to antibodies. The specificity is also higher for aptamers, as they can distinguish between targets of the same family, like it was shown for the molecules caffeine and theophylline (Zimmermann et al. 2000). Selection and production of the nucleic acid ligands can be done *in vitro*, and once the correct sequence has been determined, the oligonucleotide can be synthesized in an automated

Table 5.2: Differences between aptamers and antibodies. Advantages are emphasized (Lee et al. 2008).

	Aptamers	**Antibodies**
Affinity	Low nM—pM	Low nM – pM
Specificity	High	High
Production	In vitro chemical process	In vivo biological process
Target range	Wide: ions—whole cells	Narrow: immunogenic compounds
Batch to batch variation	Little or no	Significant
Chemical modification	Easy and straightforward	Limited
Thermal denaturation	Reversible	Irreversible
Shelf life	Unlimited	Limited

chemical procedure. The range for possible target molecules is very wide and—in comparison with the mentioned biomolecules—comprises all kinds of smaller ions, organic compounds and even whole cells. Contrary to antibodies, aptamers can be selected against toxic compounds.

Due to the chemical synthesis, there is no significant batch variation and it allows for easy chemical modification, like attachment of certain end groups for surface immobilization.

Reversible thermal denaturation makes aptamers potentially recyclable and their very high stability promises a long shelf life (Lee et al. 2008).

The SELEX Process

Aptamer production is accomplished in the SELEX (**S**ystematic **E**volution of **L**igands by **Ex**ponential Enrichment) process (see Fig. 5.9). A pool of single stranded oligonucleotides with a random section of about 25 to 70 base pairs (the library) is incubated with the target molecule. Some nucleic acid strands will interact with the target molecule and form strong non-covalent bonds. Target-DNA-complexes are partitioned from unbound DNA. After dissolution of the complex, the selected oligonucleotides are amplified in a standard PCR process. DNA strands are separated and the whole procedure is repeated up to 20 times in order to select the best fitting sequences.

If RNA is used, a transcription step must be inserted before and after PCR. In order to increase specificity for the target molecule and exclude unspecific binding, counter selection steps can be employed. In those selection rounds no target is used and DNA strands with affinity to the support and container material are removed from the pool.

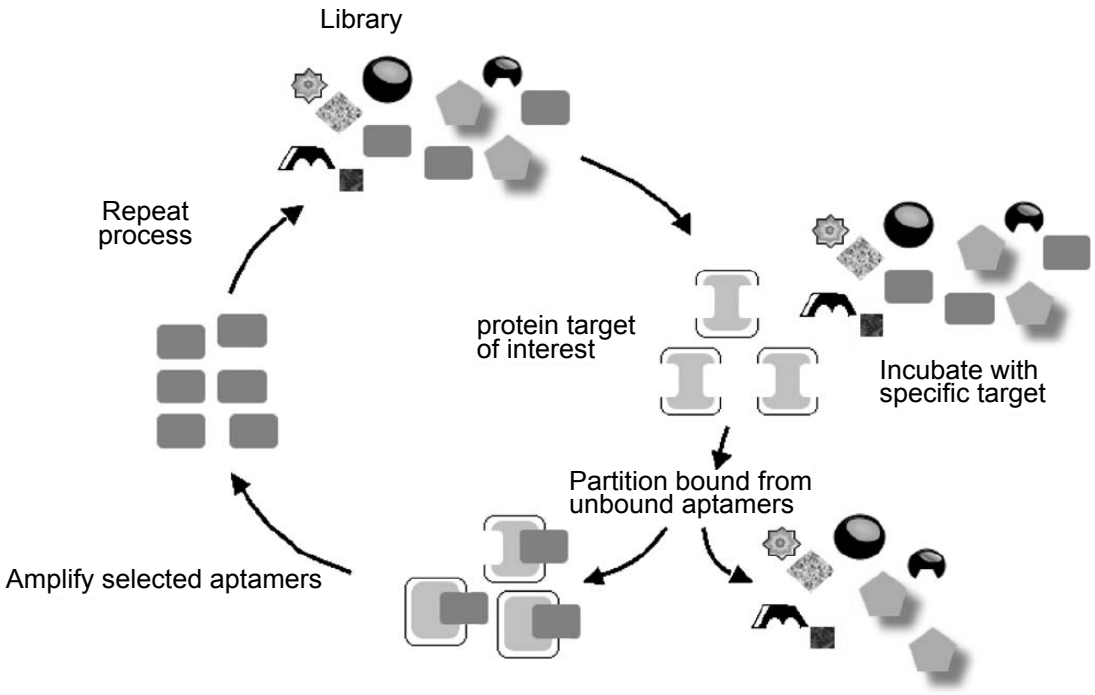

Figure 5.9: The SELEX process for use with a DNA library (Lee et al. 2008).

Biosensor Applications

In order to eliminate systematic problems with sandwich assays, the development of label free biosensors is an interesting topic. Xiao et al. (2005) modified a thrombin specific aptamer with a thiol group for immobilization on a gold surface. The strand was partially hybridized with a not fully complementary strand bearing a methylene blue (MB) tag.

In the presence of thrombin, the strands separated and the MB redox tag was approximated to the Au surface Fig. 5.10(a).

Similar signal-on detectors were developed by Baker et al. (2006) and Lai et al. (2006). The single stranded aptamer had the ability to hybridize with itself and form three loops upon target binding (see Fig. 5.10(b)). The conformational change brings the MB tag in proximity to the gold surface and allows for an electrical measurement. Both systems could be regenerated to a high degree, and thus are potentially reusable. Baker's system could detect cocaine concentrations as low as 500 μM in biological fluids even in the presence of contaminants.

So et al. (2005) attached thrombin binding aptamer to a single walled carbon nanotube (SWNT) which connected two electrodes.

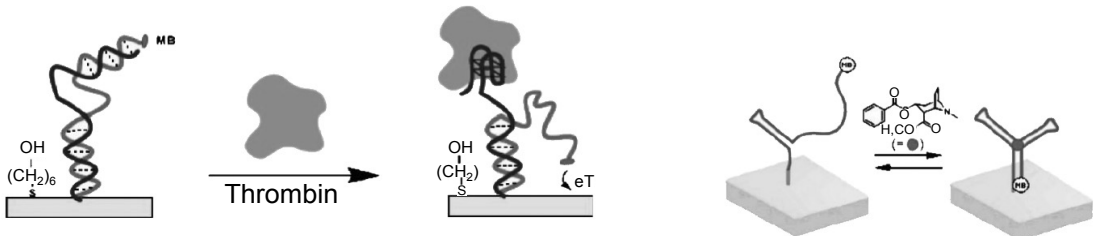

Figure 5.10: Aptamers with a methylene blue redox tag for thrombin (a) and cocaine detection (b). The binding event induces a conformational change in the aptamer and brings the redox active tag closer to the gold surface Baker et al. (2006); Lai et al. (2006). An analogue sensor was described earlier in Section 3.2. Xie et al. (2009) used carboxylic acid modified PEDOT nanowires instead of SWNTs as FET.

Color image of this figure appears in the color plate section at the end of the book.

Binding the charged protein induced an electrostatic gate potential and changed the source-drain current. The field effect transistor (FET) biosensor was able to detect thrombin in a concentration range of 10–100 nM.

OUTLOOK

In recent years, a fascinating development in the application of conductive polymers in medical diagnostics occurred. Elegant research on new sensing concepts has opened the door to a wide variety of microsystem based biosensors for clinical applications. Such devices are extremely useful for delivering diagnostic information in a fast, simple, and low cost fashion, and are thus uniquely qualified for meeting the demands of point of care systems, e.g., for cancer screening. The high sensitivity of the modern biosensors should facilitate early detection and treatment of diseases, and lead to increased patient survival rates.

In the future, one of the main challenges is to bring the new biosensor techniques to the bedside for use by non-laboratory personnel without compromising accuracy and reliability. The internal calibration and reference is also a major requirement, and provokes researchers to reshape the existing methods. From a clinical point of view, the *in vivo* biosensors that are biocompatible and can remain in the body for weeks or months will also be a demand. Special attention should be given to non-specific adsorption issues that commonly control the detection limits of electrochemical bioaffinity assays. The stability of biosensors remains an important issue in the fabrication and use of these devices for many application areas.

By measuring abnormalities within few minutes, disposable cartridges containing electrode strips and simple sample processing could offer early and fast screening of diseases in a point of care setting.

It has become apparent that the field of polymer biosensors has reached a new level of maturity. In the near future it is highly likely that pathogen detection will undoubtedly benefit from the integration of biosensors into all-polymer micro devices, and thus in some regards revolutionize the medical diagnostics.

ACKNOWLEDGEMENTS

This work was supported by the Danish Research Council for Technology and Production Sciences and the Technical University of Denmark.

REFERENCES

Akoudad, S. and J. Roncali. 2000. Modification of the electrochemical and electronic properties of electrogenerated poly(3,4-ethylene-dioxythiophene) by hydroxymethyl and oligo(oxyethylene) substituents. Electrochemistry Communications 2(1): 72.

Ali, E.M. and E.A.B. Kantchev, H-H. Yu and J.Y. Ying. 2007. Conductivity shift of polyethylenedioxythiophenes in aqueous solutions from side-chain charge perturbation. Macromolecules 40(17): 6025–6027.

Baker, B.R. and R.Y. Lai, M.S. Wood, E.H. Doctor, A.J. Heeger and K.W. Plaxco. 2006. An electronic, aptamer-based small-molecule sensor for the rapid, label-free detection of cocaine in adulterated samples and biological fluids. J Am Chem Soc 128(10): 3138–9.

Balamurugan, A. and S.-M. Chen. 2007. Poly(3,4-ethylenedioxythiophene-co-(5-amino-2-naphthalenesulfonic acid)) (pedot-pans) film modified glassy carbon electrode for selective detection of dopamine in the presence of ascorbic acid and uric acid. Anal Chim Acta 596(1): 92–8.

Balamurugan, S. and A. Obubuafo, S.A. Soper and D.A. Spivak. 2008. Surface immobilization methods for aptamer diagnostic applications. Anal Bioanal Chem 390(4): 1009–21.

Bhagat, A.A.S. and S.S. Kuntaegowdanahalli and I. Papautsky. 2008. Continuous particle separation in spiral microchannels using dean flows and differential migration. Lab on a Chip 8(11): 1906–1914.

Bhagat, A.A.S. and H. Bow, H.W. Hou, S.J. Tan, J. Han and C.T. Lim. 2010. Microfluidics for cell separation. Medical & Biological Engineering & Computing 48(10, Sp. Iss. SI): 999–1014.

Biswas, M. and A. Roy. 1994. Thermal, stability, morphological, and conductivity characteristics of polypyrrole prepared in aqueous medium. Journal of Applied Polymer Science 51(9): 1575.

Campbell, T.E. and A.J. Hodgson and G.G. Wallace. 1999. Incorporation of erythrocytes into polypyrrole to form the basis of a biosensor to screen for rhesus (d) blood groups and rhesus (d) antibodies. Electroanalysis 11(4): 215.

Daugaard, A.E. and S. Hvilsted, T.S. Hansen and N.B. Larsen. 2008. Conductive polymer functionalization by click chemistry. Macromolecules 41(12): 4321.

Di Carlo, D. and D. Irimia, R. Tompkins and M. Toner. 2007. Continuous inertial focusing, ordering, and separation of particles in microchannels. PNAS 104(48): 18892–18897.

Dubois, M-P. and C. Gondran, O. Renaudet, P. Dumy, H. Driguez, S. Fort and S. Cosnier. 2005. Electrochemical detection of arachis hypogaea (peanut) agglutinin binding to monovalent and clustered lactosyl motifs immobilized on a polypyrrole film. Chem Commun (Camb) (34): 4318–20.

Giddings, J. 1993. Field-flow fractionation: analysis of macromolecular, colloidal, and particulate materials. Science 260(5113): 1456–465.

Gossett, D.R. and W.M. Weaver, A.J. Mach, S.C. Hur, H.T.K. Tse, W. Lee, H. Amini and D. Di Carlo. 2010. Label-free cell separation and sorting in microfluidic systems. Analytical and Bioanalytical Chemistry 397(8): 3249–3267.

Gregoratto, I. and C. McNeil and M. Reeks. 2007. Micro-devices for rapid continuous separation of suspensions for use in micro-total-analysis-systems. SPIE.

Groenendaal, L. and F. Jonas, D. Freitag, H. Pielartzik and J.R. Reynolds. 2000. Poly(3,4-ethylenedioxythiophene) and its derivatives: Past, present, and future. Advanced Materials 12(7): 481.

Gustafsson, J. and B. Liedberg and O. Inganäs. 1994. In situ spectroscopic investigations of electrochromism and ion transport in a poly (3,4-ethylenedioxythiophene) electrode in a solid state electrochemical cell. Solid State Ionics 69(2): 145.

Han, K. and Z. Liang and N. Zhou. 2010. Design Strategies for Aptamer-Based Biosensors. Sensors 10(5): 4541–4557.

Hansen, T. and K. West, O. Hassager and N. Larsen. 2007. Direct fast patterning of conductive polymers using agarose stamping, Advanced Materials 19(20): 3261.

Jagur-Grodzinski, J. 2002. Electronically conductive polymers. Polymers for Advanced Technologies 13(9): 615.

Kim, D-J. and N-E. Lee, J-S.Park, I-J. Park, J-G. Kim and H.J. Cho. 2010. Organic electrochemical transistor based immunosensor for prostate specific antigen (psa) detection using gold nanoparticles for signal amplification., Biosens Bioelectron 25(11): 2477–82.

Kolb, H.C. and M.G. Finn and K.B. Sharpless. 2001. Click Chemistry: Diverse Chemical Function from a Few Good Reactions. Angewandte Chemie International Edition 40(11): 2004.

Kumar, S.S. and J. Mathiyarasu, K.L.N. Phani and V. Yegnaraman. 2006. Simultaneous determination of dopamine and ascorbic acid on poly (3,4-ethylenedioxythiophene) modified glassy carbon electrode. Journal of Solid State Electrochemistry 10(11): 905.

Kuntaegowdanahalli, S.S. and A.A.S. Bhagat, G. Kumar and I. Papautsky. 2009. Inertial microfluidics for continuous particle separation in spiral microchannels, Lab on a Chip 9(20): 2973–2980.

Lai, R.Y. and D.S. Seferos, A.J. Heeger, G.C. Bazan and K.W. Plaxco. 2006. Comparison of the signaling and stability of electrochemical dna sensors fabricated from 6- or 11-carbon self-assembled monolayers. Langmuir 22(25): 10796–800.

Lazcka, O. and F.J.D. Campo and F.X. Muñoz. 2007. Pathogen detection: A perspective of traditional methods and biosensors, Biosensors and Bioelectronics 22(7): 1205–1217.

Lee, J.-O. and H-M. So, E-K. Jeon, H. Chang, K. Won and Y.H. Kim. 2008. Aptamers as molecular recognition elements for electrical nanobiosensors. Anal Bioanal Chem 390(4): 1023–32.

Lee, M-W. and M-Y. Lee, J-C. Choi, J-S. Park and C-K. Song. 2010. Fine patterning of glycerol-doped pedot:pss on hydrophobic pvp dielectric with ink jet for source and drain electrode of otfts. Organic Electronics 11(5): 854–859.

Lenshof, A. and T. Laurell. 2010. Continuous separation of cells and particles in microfluidic systems. Chemical Society Reviews 39(3): 1203–1217.

Loffredo, F. and A.D.G.D. Mauro, G. Burrasca, V. La Ferrara, L. Quercia, E. Massera, G. Di Francia and D.D. Sala. 2009. Ink-jet printing technique in polymer/carbon black sensing device fabrication. Sensors and Actuators B: Chemical 143(1): 421.

Mabrook, M. and C. Pearson and M. Petty. 2006. Inkjet-printed polypyrrole thin films for vapour sensing. Sensors and Actuators B: Chemical 115(1): 547.

Nolan, J. and L. Sklar. 1998. The emergence of flow cytometry for sensitive, real-time measurements of molecular interactions. Nat Biotechnol 16(7): 633–8.

Olson, T.S. and S. Pylypenko, P. Atanassov, K. Asazawa, K. Yamada and H.Tanaka. 2010. Anion-exchange membrane fuel cells: Dual-site mechanism of oxygen reduction reaction in alkaline media on cobalt–polypyrrole electrocatalysts. The Journal of Physical Chemistry C 114(11): 5049.

Park, J. and H.K. Kim and Y. Son. 2008. Glucose biosensor constructed from capped conducting microtubules of pedot. Sensors and Actuators B: Chemical 133(1): 244.

Peterson, F. and L. Åberg, A. Swård-Nilsson and T. Laurell. 2007. Free Flow Acoustophoresis: Microfluidic-Based Mode of Particle and Cell Separatio. Anal Chem 79(14): 5117–5123.

Pirrung, M.C. 2002. How to make a DNA chip. Angew. Chem. Int Ed Engl 41(8): 1276–89.

Prodromidis, M. and M. Karayannis. 2002. Enzyme based amperometric biosensors for food analysis. Electroanalysis 14(4): 241.

Rozlosnik, N. 2009. New directions in medical biosensors employing poly(3,4-ethylenedioxy thiophene) derivative-based electrodes. Analytical and Bioanalytical Chemistry 395(3): 637–45.

Sarma, A.K. and P. Vatsyayan, P. Goswami and S.D. Minteer. 2009. Recent advances in material science for developing enzyme electrodes. Biosens Bioelectron 24(8): 2313–22.

Seo, J. and M. Lean and A. Kole. 2007. Membrane-free micro-filtration by asymmetric inertial migration. Appl Phys Lett 91(033901).

Shirakawa, H. and E.J. Louis, A.G. MacDiarmid, C.K. Chiang and A.J. Heeger. 1977. Synthesis of electrically conducting organic polymers: halogen

derivatives of polyacetylene, (CH) x . Journal of the Chemical Society, Chemical Communications (16): 578.

So, H.-M. and K. Won, Y.H. Kim, B.-K. Kim, B.H. Ryu, P.S. Na, H. Kim and J-O. Lee. 2005. Single-walled carbon nanotube biosensors using aptamers as molecular recognition elements. J Am Chem Soc 127(34): 11906–7.

Syed, M.A. and S. Pervaiz. 2010. Advances in Aptamers. Oligonucleotides 20(5): 215–224.

Teles, F. and L. Fonseca. 2008. Applications of polymers for biomolecule immobilization in electrochemical biosensors. Materials Science and Engineering: C 28(8): 1530.

Toner, M. and D. Irimia. 2005. Blood on a Chip. Annu. Rev. Biomed Eng. pp. 77–103.

Tuerk, C. and L. Gold. 1990. Systematic evolution of ligands by exponential enrichment: Rna ligands to bacteriophage t4 dna polymerase. Science 249(4968): 505.

Vasantha, V. and S. Chen. 2006. Electrocatalysis and simultaneous detection of dopamine and ascorbic acid using poly(3,4-ethylenedioxy)thiophene film modified electrodes. Journal of Electroanalytical Chemistry 592(1): 77.

Wang, L-X. and X-G.Li and Y-L. Yang. 2001. Preparation, properties and applications of polypyrroles. Reactive and Functional Polymers 47(2): 125–139.

Wang, Y. and A. Stevens and J. Han. 2005. Million-fold preconcentration of proteins and peptides by nanofluidic filter. Analytical Chemistry 77(14): 4293–4299.

Wessling, B. 2001. From conductive polymers to organic metals. Chemical Innovation USA 31(1): 34–40.

Xiao, Y. and B.D. Piorek, K.W. Plaxco and A.J. Heeger. 2005. A reagentless signal-on architecture for electronic, aptamer-based sensors via target-induced strand displacement. J Am Chem Soc 127(51): 17990–1.

Xie, H. and S-C. Luo and H-H. Yu. 2009. Electric-field-assisted growth of functionalized poly(3,4-ethylenedioxythiophene) nanowires for label-free protein detection. Small 5(22): 2611–7.

Zimmermann, G.R. and C.L. Wick, T.P. Shields, R.D. Jenison and A. Pardi. 2000. Molecular interactions and metal binding in the theophylline-binding core of an rna aptamer, RNA-A Publication of the RNA Society 6(5): 659–667.

Biosensors and Bioelectronics 43 (2013) 315–320

Contents lists available at SciVerse ScienceDirect

Biosensors and Bioelectronics

journal homepage: www.elsevier.com/locate/bios

Comparative study on aptamers as recognition elements for antibiotics in a label-free all-polymer biosensor

Johannes Daprà [a], Lasse Holm Lauridsen [b], Alex Toftgaard Nielsen [b], Noemi Rozlosnik [a,*]

[a] Department of Micro- and Nanotechnology, Technical University of Denmark, Produktionstorvet 423, DK-2800 Kgs. Lyngby, Denmark
[b] The Novo Nordisk Foundation Center for Biosustainability, Scion-DTU, Fremtidsvej 3, DK-2970 Hørsholm, Denmark

ARTICLE INFO

Article history:
Received 9 November 2012
Received in revised form
19 December 2012
Accepted 20 December 2012
Available online 7 January 2013

Keywords:
Aptamer
Conductive polymer
Electrochemical impedance spectroscopy
Antibiotics

ABSTRACT

We present an all-polymer electrochemical microfluidic biosensor using Topas® as substrate and a conductive polymer bilayer as electrode material. The conductive bilayer consists of tosylate doped poly(3,4-ethylenedioxythiophene) (PEDOT:TsO) and the hydroxymethyl derivative PEDOT-OH:TsO, which was covalently functionalized with two aptamer probes with affinity to ampicillin or kanamycin A, respectively. Using electrochemical impedance spectroscopy (EIS) we were able to detect ampicillin in a concentration range from 100 pM to 1 μM and kanamycin A from 10 nM to 1 mM. The obtained EIS spectra were fitted with an equivalent circuit model successfully explaining the impedance signal. Real samples from regular ultra-high temperature treated low-fat milk spiked with ampicillin were successfully tested to assess the functionality of the sensor with real samples. In conclusion, we have demonstrated the applicability of the newly developed platform for real time, label-free and selective impedimetric detection of commonly used antibiotics. Additionally it was possible to detect ampicillin in a milk sample at a concentration below the allowed maximum residue limit (MRL) in the European Union.

1. Introduction

Detection, identification and quantification of pathogens and chemical agents are crucial for water and environmental analysis, clinical diagnosis, food safety, and biodefence. The existing immunological or nucleic acid technologies are mostly time consuming and require both sophisticated equipment as well as highly trained personnel, hence increasing the analysis costs. Another limitation of these techniques lies in their nature, which only allows the detection of certain types of analytes.

Therefore, new assay technologies are continuously emerging, and among these, the biosensor technology is the area with fastest growth (Lazcka et al., 2007). Ideally, the assays used in a detection system should enable the detection and quantification of a broad range of different molecules. Furthermore, the technique should provide reliable, real time, on-site, user-friendly, and inexpensive detection with adequate sensitivity, specificity and reproducibility.

Label-free biosensors for in situ measurements with high sensitivity and high specificity are of significant interest for the development of diagnostic devices (Cosnier, 2003; Gerard et al., 2002; Liao et al., 2006).

1.1. Impedimetric biosensors

Impedance spectroscopy is a powerful method to analyse the complex electrical resistance of a system and it is sensitive to surface phenomena and changes of bulk properties. Electrochemical detection using electrochemical impedance spectroscopy (EIS) is advantageous because of its label-free and reagentless character and high sensitivity, as recently reviewed by Pänke et al. (2008). Thus impedance detection is particularly suited to follow binding events in the field of biosensors.

The tools that allow for specific detection (generally referred to as affinity tools) are highly selective binders of the target. At present, antibodies of mammals are the best characterised and most widely used affinity tools, i.e. biological recognition elements in biosensor platforms. However, antibodies do have their limitations: they are sensitive to pH changes and can easily be inactivated (e.g. through elevated temperatures, proteases) (Binz et al., 2005; Hoogenboom, 2005). Moreover, producing antibodies is generally difficult and expensive.

1.2. Aptamers as recognition elements

As alternatives to antibodies, aptamers have recently attracted increasing attention due to their capability to bind a wide range of targets: nucleic acids, proteins, metal ions and other molecules

* Corresponding author. Tel.: +45 27148902.
E-mail addresses: noro58@gmail.com, noro@nanotech.dtu.dk (N. Rozlosnik).

0956-5663/$ - see front matter © 2013 Elsevier B.V. All rights reserved.
http://dx.doi.org/10.1016/j.bios.2012.12.058

with high affinity and sensitivity (Hong et al., 2012; Song et al., 2012b).

Aptamers are peptides or oligonucleotides (RNA or single-stranded DNA; ssDNA) that bind to a specific target molecule. The aptamers typically fold into a three-dimensional structure, whose conformation is changing upon ligand binding. Aptamer-like structures can also be found in nature: riboswitches in bacteria and eukaryotes control translation depending on ligand binding (Winkler et al., 2002).

Novel aptamers can be developed using a process called systematic evolution of ligands by exponential enrichment (SELEX) (Ellington and Szostak, 1990; Tuerk and Gold, 1990). It enables the selection of high-affinity nucleic acid sequences from a random pool of candidates.

The oligonucleotide aptamers can easily be modified with signal moieties and can be produced at low cost. Up to now, a variety of assays have been successfully developed for aptamer-based analysis of biomolecules (Centi et al., 2007; Guo et al., 2008; Wu et al., 2011; Yan et al., 2010).

Efforts have been made to develop aptamer-based biosensors (aptasensors) for sandwich assays in recent years. Although these biosensors could detect the target, the detection limits still need to be improved (Wang et al., 2007; Zuo et al., 2009).

1.3. Detection of antibiotics

The development of novel detection systems for antibiotics is of particular importance. The emergence of microorganisms resistant towards important antibiotics occurs at alarmingly high rates. Infections with multidrug-resistant pathogens have been reported for a range of potentially lethal bacteria including *Staphylococcus aureus* (Klevens et al., 2007) and *Mycobacterium tuberculosis* (Centers for Disease Control and Prevention (CDC), 2006), leaving few or no options for treatment. In the European Union (EU), it is estimated that 25 000 persons die every year from infections with antibiotic-resistant micro-organisms (White et al., 2011). Development of novel antibiotics, however, is attracting little attention from the pharmaceutical industry, and for gram-negative pathogens there are few or no late stage clinical trials of new drugs (Septimus and Kuper, 2009). Besides their use for treating human infections, antibiotics are also utilised as growth promoters in agri- and aquaculture (Cabello, 2006; Witte, 1998).

Due to their short generation time, bacteria can quickly evolve resistance towards all known antibiotics if these are present in sub-lethal concentrations in the environment (Gullberg et al., 2011). To minimise the development of resistance towards antibiotics, it is, therefore, of critical importance to limit both the use and the release of antibiotics into the environment.

Detection of different antibiotics, however, is challenging due to the varied chemical structure of the compounds and the lack of available simple spectroscopic or electrochemical assays.

Recently, aptamers targeting a range of antibiotics, including tobramycin (González-Fernández et al., 2011), kanamycin (Song et al., 2011), ampicillin (Song et al., 2012a) and chloramphenicol (Mehta et al., 2011) have been developed.

1.4. Design of the aptasensor

Polymer-based microfluidic systems meet the requirements of disposable devices for low sample consumption, cost efficiency, reliability, and fast response time, which make the systems ideal for rapid analysis. However, most biosensors for electrochemical detection involve metallic electrodes (Kerman et al., 2004). To avoid oxidation or participation in electrochemical reactions, noble metals such as gold or platinum are usually employed. These materials have a number of disadvantages, such as high (and still increasing) market prices or comparably low biocompatibility. Apart from that they also require very costly fabrication methods.

Conductive polymers offer very suitable properties to master the specialized task of transducing a binding event between an analyte and a biological probe. They have been used as alternative to traditional electrode materials because of the additional advantageous properties of inexpensive electrode fabrication and easy electrode functionalization (Kiilerich-Pedersen et al., 2011; Rozlosnik, 2009).

Because of their excellent compatibility with biological samples, polypyrrole (PPy) and poly(3,4-ethylenedioxythiophene) (PEDOT) have repeatedly been used for sensors in biological environments (Balamurugan and Chen, 2007; Bidan et al., 1999; Dubois et al., 2005; Kiilerich-Pedersen et al., 2011; Sarma et al., 2009; Vidal et al., 1999; Xie et al., 2009).

Even though pyrrole is the less expensive monomer compared to 3,4-ethylenedioxythiophene (EDOT), and PPy shows equally good air stability, PEDOT was used exclusively in this study for its superior stability in phosphate buffers and for its higher conductivity (Groenendaal et al., 2000; Syritski et al., 2005; Yamato et al., 1995).

PEDOT can be processed in different ways. Popular polymerization methods are electropolymerization (Kros et al., 2002; Lima et al., 1998; Shi et al., 2008; Sotzing et al., 1996; Xie et al., 2009; Yamato et al., 1995) or chemical oxidation polymerization in liquid (Aasmundtveit et al., 1999; Hansen et al., 2006, 2007a, 2007b; Winther-Jensen and West, 2006) as well as in vapor phase (Bhattacharyya and Gleason, 2011; Le et al., 2005; Winther-Jensen and West, 2004). Chemical oxidation is advantageous because it does not require a conductive substrate.

Micropatterning of conductive polymers is regularly done using cleanroom-based photolithographic techniques. However, although such processes are versatile, they are not well-suited for fabricating inexpensive biosensor platforms due to their costs. As an alternative, we have recently developed a simple micropatterning procedure, which is based on contacting PEDOT thin films with a micro-structured agarose stamp soaked in a solution of aqueous hypochlorite and a non-ionic detergent (Hansen et al., 2007b; Lind et al., 2012). Where contacted, PEDOT is removed and the underlying substrate exposed. By applying a cyclic-olefin-copolymer (COC) substrate we were able to fabricate nucleotide-functionalized PEDOT microelectrodes on a COC background with a low degree of unspecific binding of DNA, in a simple and inexpensive manner. This sensor has been used to specifically detect picomolar concentrations of antibiotics.

2. Materials and methods

2.1. Chemicals

All chemicals were purchased from Sigma-Aldrich (Schnelldorf, Germany) if not stated otherwise.

2.1.1. Chip material

The substrate and the top part of the microfluidic chip were fabricated from Cyclic Olefin Copolymer (COC) Topas® grade 5013 (T_g at 130 °C, TOPAS Advanced Polymers GmbH, Germany).

2.1.2. Electrode material

For the electrodes, the conducting polymer poly(3,4-ethylene-di-oxy-thio-phene) doped with tosylate (PEDOT:TsO) was used.

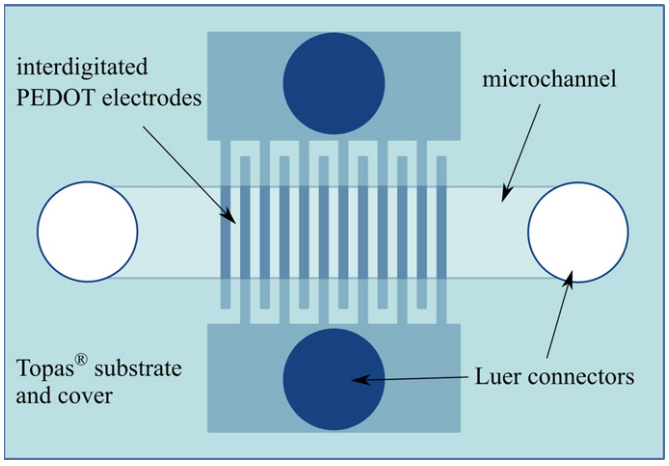

Fig. 1. Schematic drawing of the assembled microfluidic chip with interdigitated PEDOT:TsO electrodes. Drawing is not to scale.

2.1.3. Antibiotics and aptamers

In this study, we used short high-affinity aptamers against kanamycin A and ampicillin presented by Song et al. (2011, 2012a, 2012b), respectively. The DNA aptamers were synthesized by Integrated DNA Technologies (Denmark) as high performance liquid chromatography (HPLC) purified and lyophilized ssDNA functionalized with a 5′-amino modified C_6 linker. Their sequences from 5′ to 3′ are:

Ampicillin	GCG GGC GGT TGT ATA GCG G
Kanamycin A	TGG GGG TTG AGG CTA AGC CGA

2.2. Chip fabrication

The all-polymer microfluidic flow system was fabricated from Topas® polymer using a bilayer composite of PEDOT:TsO and PEDOT-OH:TsO conducting polymer as electrodes (Fig. 1).

Both the top and the bottom part of the chip were made by injection moulding using Topas® pellets.

2.2.1. Conducting polymer film deposition

Conductive thin films of PEDOT:TsO were made by spin coating the reaction solution containing the monomer and thermal activation according to the following procedure:

About 260 μL Baytron C (40% $Fe^{(III)}$ tosylate in butanol), 80 μL butanol, 6 μL pyridine and 8.8 μL EDOT were thoroughly mixed and spun on a 50.8 mm Topas® 5013 disc with 1000 rpm for 60 s. Coated polymer discs were then heated to 70 °C for 5 min. The inhibitor pyridine evaporated and the progress of polymerization was observable by a colour change from yellow to green. After rinsing the discs with de-ionized water to remove excess reactants and by-products, they obtained the characteristic blue colour of PEDOT:TsO. A second polymer layer was applied in the same way using the monomer ((2,3-dihydrothieno[3,4-*b*][1,4]-dioxin-2-yl)methanol) also known as hydroxymethyl-EDOT or EDOT-OH instead of EDOT. This yielded a PEDOT-OH:TsO coating of the same thickness, where the hydroxymethyl group of each monomer provides a possible grafting site for later functionalization.

2.2.2. Microelectrode preparation

Interdigitated microelectrodes were fabricated by agarose stamping, as described in detail by Hansen et al. (2007b) and more recently by Lind et al. (2012).

In short, a stamp was prepared by casting a 10% w/w agarose gel into a mould with a relief of the electrode design etched in silicon. After solidification, the stamp was soaked in the etching solution and applied manually to the PEDOT:TsO/PEDOT-OH:TsO bilayer.

For etching a 1–1.5% w/v solution of sodium hypochlorite in water containing 0.1% v/v of the surfactant TritonX100 was used. The stamping time depends on the thickness of the conductive polymer layer or bilayer, respectively. To etch through approximately 200 nm we needed between 45 and 60 s. After stamping, over-oxidized PEDOT was removed by washing with water. The conducting polymer layers were re-doped by immersion in 4% w/v $Fe^{(III)}$ tosylate solution for a few seconds. During this process, the colour of the polymer changed from dark to light blue indicating the conversion from a reduced state to a more conductive oxidized state with higher degree of doping. The stamp design comprised interdigitated electrodes with a width of 20 μm. The spacing between the single wires was the same as their width.

2.2.3. Chip assembly

The chip consisted of two parts: the flat Topas® disc with the microelectrodes and an injection molded Topas® cover disc with Luer connectors for simple connection to the electronic equipment and exchange of liquids. Both parts were assembled with a 150 μm thick sheet of transfer adhesive (ARcare 90106, Adhesive Research Ireland). Cavities were cut into the tape by laser ablation to create microfluidic channels. To ensure homogeneous and tight sealing around the channels, the assembled discs were pressed with a force of 500 N at a bonding temperature of 75 °C for 5 min. Pressure was released after the chip had cooled down to 40 °C. A schematic drawing of the chip is presented in Fig. 1.

2.2.4. Electrode functionalization

Succinic acid was grafted onto surface hydroxymethyl groups by filling the channels with 0.1 M 2-(*N*-morpholino)ethanesulfonic acid (MES) buffer at pH 4.0 with 50 mM of the coupling agent 1-ethyl-3-(3-dimethylaminopropyl)carbodiimide (EDC) and succinic anhydride for 30 min.

The new surface carboxylic acid groups were activated with 50 mM EDC and 40 mM NHS (*N*-hydroxy succinimide) in MES buffer (0.1 M, pH=4.0) for 5 min. After washing with MES buffer, the 5′-amino modified aptamer (100 nM in MES) was added to form a stable amide bond.

After a reaction time of 3 h, the channels were rinsed with several millilitres of binding buffer (DPBS; Dulbecco's phosphate buffered saline, containing 5 mM $MgCl_2$).

To verify the success of the immobilization, the grafting method was tested with fluorescently labeled DNA. Control experiments without activation reagents showed that no non-specifically adsorbed DNA remained after washing. Fluorescence micrographs are shown in Fig. S1 in the electronic supplementary information.

2.3. Electrochemical impedance measurements

Electrochemical impedance spectroscopy (EIS) was conducted on chips with and without immobilized aptamers. A potentiostat with integrated frequency generator (Zahner IM6, Zahner Elektrik GmbH, Germany) was connected to the electrodes by spring-loaded (Pogo Pin) contacts and the impedance of the system was measured with wide spectrum sweeps in a frequency range from 100 kHz to 200 mHz (logarithmic scale with 10 points per decade for frequencies <66 Hz and four points per decade for frequencies >66 Hz). After the baseline was recorded, the target was

added in increasing concentrations and the change of the impedance signal monitored.

3. Results and discussion

3.1. Film characterization

As has been reported in previous publications, the conductivity of both PEDOT:TsO and PEDOT-OH:TsO is, compared to other conjugated polymers, very high. Surface conductivity values of up to 700 S/cm have been found for PEDOT:TsO (Hansen et al., 2007b; Winther-Jensen and West, 2006), while for tosylate doped hydroxymethyl-PEDOT a value of 83 S/cm has been reported (Hsiao et al., 2010).

Our findings for PEDOT:TsO were 424 ± 57.2 S/cm and for PEDOT-OH:TsO 81 ± 10.7 S/cm. The double layer composite showed a conductance of 275 ± 61.2 S/cm. The conductances of our polymer films are, therefore, within the expected range.

3.2. Micropatterning

After stamping, the actual width of the micro-electrode wires was determined by optical microscopy. Despite being designed with a width of 20 μm, the mean width of the wires was measured to be 9.7 ± 2.2 μm. The large deviation from the original wire size can be explained by diffusion processes occurring during stamping. Shortening the exposure time would certainly reduce the effect; however, then the etching of the desired areas would not be complete, resulting in residual conductivity between the wires. Uniform pressure control by automation of the stamping process would improve the reproducibility significantly.

3.3. Impedimetric characterization of the aptasensor

In this study, we show that the above-described all-polymer biosensor is a sensitive and selective platform for detection of different antibiotics. We have chosen already published aptamers against kanamycin A and ampicillin for our experiments (Song et al., 2011, 2012a).

The immobilization of the aptamers alone provoked an increase in the impedance, as was expected due to the increased charge transfer resistance at the electrode/liquid interface.

Binding of the target molecules to the corresponding aptamer caused a further increase in the impedance measured at frequencies below 1 Hz. A logarithmic correlation of analyte concentration and impedance response was found for a broad dynamic range and both analytes. In the following, the individual aptasensors will be discussed in more detail.

Analyte concentrations starting from 10 pM were tested with ampicillin-aptamer. Fig. 2 shows the relative change of absolute impedance with increasing concentrations. The first statistically significant ($p < 0.05$) signal was observed at 100 pM. Further increase of analyte concentration showed a fairly linear dependence in the logarithmic plot.

As described above, the patterning of the chips was subject to uncertainties, which resulted in variation in the width of the electrodes in the range of several micrometers.

There was a very good correlation between impedance change and wire size (see Fig. S2 in the electronic supplementary information), so that a better reproducibility can be expected from electrodes fabricated with higher accuracy.

With a dissociation constant $k_D = 78.8$ nM the kanamycin A aptamer establishes a weaker bond to its target than the ampicillin aptamer ($k_D = 13.4$ nM) (Song et al., 2011, 2012a). It is, therefore, likely that an aptasensor based on this probe would be less sensitive. As shown in Fig. 2 our findings verify this presumption. Typically a concentration of 10 nM was necessary to obtain a statistically significant increase ($p < 0.05$) of the impedance modulus. Lower concentrations, starting from 10 pM, caused little or no effect on the signal. We believe that the relatively low limit of detection (LOD) and wide dynamic range of the biosensor is also due to specific device properties and not exclusively related to affinity of the probes used in this study. In addition, sensors and assays for Ochratoxin A (OTA) have shown that using the same aptamer in different assays and sensors can result in over a 1000-fold differences in LOD (Lauridsen and Veedu, 2012). The lower detection limit found with the ampicillin aptamer indicates that a high affinity for target compounds will facilitate higher devise sensitivity.

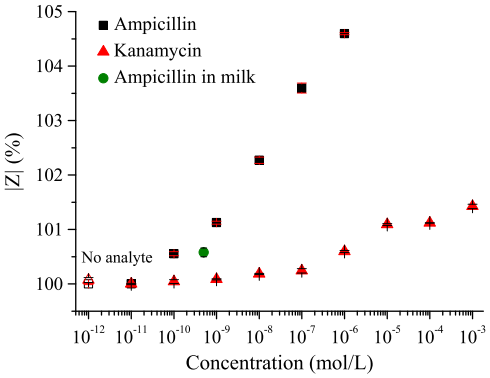

Fig. 2. A typical impedance response for increasing concentrations of ampicillin or kanamycin, respectively. The empty symbols illustrate the measured baseline level before the first injection. The green circle represents the obtained impedance change in the case of 500 mol/L ampicillin in milk sample. The error bars show the average of the signal noise. (For interpretation of the references to color in this figure caption, the reader is referred to the web version of this article.)

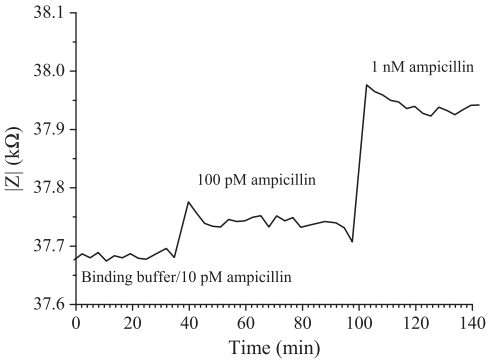

Fig. 3. Increase of impedance at a frequency of 356 mHz is shown after addition of the analyte in different concentrations.

Control experiments, where the antibiotics were reacted with the mismatching aptamers, gave no changes in the impedance signal compared to the baseline. After that, injecting the matching antibiotics into the biosensor resulted in the expected increase of impedance. This shows that the immobilization of the aptamers on the electrodes did not affect the selectivity of the aptamers towards their targets.

With the described experimental setup (see Section 2.3) we were able to obtain one full impedance spectrum in 2:35 min. Fig. 3 shows the impedance data at a single frequency (356 mHz), which was taken from the full spectra. As can be seen in the graph, the impedance change occurs within the sampling time, i.e. within 2:35 min and stabilizes at a new level. We have also conducted impedance measurements at a single frequency, where

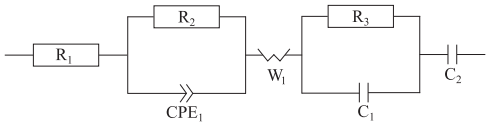

Fig. 4. Equivalent circuit model for fitting the experimental spectra (see description in the text).

the instrument-determined minimum sampling time was ca. 17 s (data not shown), but also this higher temporal resolution was insufficient to determine the reaction rate of the target-aptamer complex formation. However, this shows that the analysis time is reasonably short for a number of real-life applications.

EU regulation no. 675/92 (as amendment to regulation no. 2377/90) lays down a maximum residue limit (MRL) for ampicillin of 4 μg/L in milk, which is equivalent to a concentration of 11.45 nM. Our experiments shown above proved that we were able to detect much lower concentrations of ampicillin in buffer solution. In order to prove the reliability of the sensor detecting analytes in real samples, a 10% solution of ultra-high temperature treated (UHT) low fat milk in DPBS containing 5 mM $MgCl_2$ was prepared and spiked with 500 pM ampicillin. Impedance spectra were measured as before. In these experiments, we were able to measure an increase of impedance of $0.58 \pm 8\%$. These data are in well accordance with the concentration dependence reported above. We can, therefore, claim that our sensor is capable of reproducibly detecting an ampicillin concentration in milk that is far below the MRL set by the EU.

3.4. Equivalent circuit modeling of the EIS results

An equivalent circuit model fitting the electrical properties of the sensor is shown in Fig. 4. This model was used to simulate impedance spectra while changing certain parameters to understand the effects observed in our experiments; it satisfactorily fits the experimental data over the measured frequency range.

In the model, R_1 is the intrinsic resistance of the electrodes. The parallel resistance (R_2) and the constant phase element (CPE_1) with coefficients P_1 and n_1 represent the electrode–solution interface, where R_2 is the charge transfer resistance and CPE_1 the electrical double layer on the surface. The following Warburg impedance (W_1) indicates the diffusion limited electrochemical processes specified by the coefficient A_{w1}. The impedance spectrum includes a semicircle portion at high frequencies corresponding to bulk solution resistance (R_3) and the geometrical capacitance (C_1) of the interdigitated electrodes. Finally, the capacitance C_2 is the limiting capacitance, which reflects the limited solid state diffusion of charges inside the conducting polymer.

The intrinsic resistance of the electrode (R_1), the solution resistance (R_3) and electrode geometrical capacitance (C_1) are not changing during the aptamer-target binding process. The Warburg coefficient (A_{w1}) represents the impedance due to the diffusion of charges to and from the electrode surface. The temperature and the viscosity of the solution were constant during the binding process; however, conformational changes and rearrangements of the surface bound aptamers during complex formation are likely to alter the electrode surface area available for charge transfer, influencing A_{w1}. Modifications of the electrode surface can inflict changes to the electrolytic double layer at the electrode/electrolyte interface with its non-ideal capacitance (reflected as the constant phase element CPE_1) and the reaction rate of the transfer of charges between electrode and electrolyte (expressed as the charge transfer resistance R_2). Both factors are dependent on the change of the ionic concentration near the electrode surface, which is influenced by the binding event of an analyte molecule to an immobilized aptamer. We can, therefore, assume that both the constant phase element, the charge transfer resistance and the Warburg element will be the most interesting parameters for investigations of target binding to surface-bound probes. The surface coverage with aptamers could have an influence on the sensitivity of such a device as described here, but the size of the antibiotics is much less that than the aptamers, therefore, it is not likely that steric hindrance would affect the results.

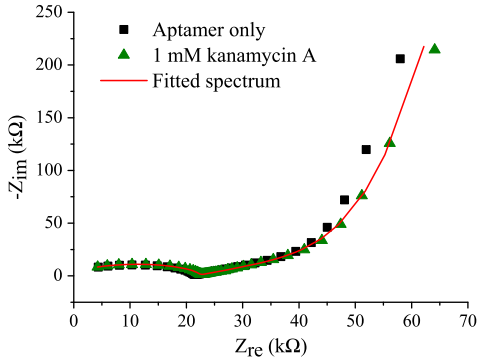

Fig. 5. Nyquist plots from impedance spectra before (■) and after (▲) addition of kanamycin A. In the low frequency region (right side) of the spectra a clear shift towards higher resistance is visible. The solid red line represents a simulated spectrum based on the fitting parameters from Table 1. The curve is calculated from the values after analyte addition. (For interpretation of the references to color in this figure caption, the reader is referred to the web version of this article.)

Table 1
Comparison of parameters corresponding to elements in the equivalent circuit model fitted to the spectra shown in Fig. 5.

Parameter	Aptamer only (error/%)	Kanamycin (error/%)	Unit
C_1	1.59×10^{-10} (2.8)	1.58×10^{-10} (2.3)	F
C_2	4.11×10^{-6} (2.3)	4.06×10^{-6} (3.0)	F
R_1	3.34×10^{2} (41.3)	3.07×10^{2} (46.7)	Ω
R_2	2.51×10^{4} (7.8)	2.41×10^{4} (9.3)	Ω
R_3	2.06×10^{4} (0.8)	2.16×10^{4} (0.8)	Ω
A_{w1}	1.44×10^{4} (12.8)	2.13×10^{4} (9.0)	$\Omega/\sqrt{s}$
P_1	5.75×10^{-6} (6.2)	6.80×10^{-6} (6.9)	$1/\Omega$
n_1	0.58 (1.9)	0.57 (2.2)	–

Impedance spectra recorded at different stages of the experiment were fitted with the "EIS Spectrum Analyser" software.[1] An example of the fitted curves is shown together with two measured spectra represented as a Nyquist plot in Fig. 5. The curve was calculated from parameters which were fitted to the impedance data obtained from the kanamycin aptasensor after the analyte was added. The result indicates a good agreement with the measured data, especially in the lower frequency range.

A comparison of parameters obtained from fitting the model to the data recorded before analyte addition and after injection of kanamycin A at a concentration of 1 mM is made in Table 1. As expected, only slight changes were observed for the capacitances C_1 and C_2 as well as the material or solution related resistances R_1 and R_3. Elements describing the electrode/liquid interface experienced a larger change. The strongest deviation from the original value was found for the Warburg coefficient A_{w1}.

4. Conclusion

We have successfully developed the first prototype of an all-polymer electrochemical biosensor using Topas® as microfluidic

[1] A.S. Bondarenko and G.A. Ragoisha, http://www.abc.chemistry.bsu.by/vi/analyser/.

system and a bilayer of tosylate doped poly(3,4-ethylenedioxythiophene) (PEDOT:TsO) and its hydroxymethyl derivative PEDOT-OH:TsO as electrode material covalently functionalized with aptamers. The newly developed inexpensive biosensor has high sensitivity and selectivity for the tested targets, which makes it a promising platform for detection of analytes from complex samples by a fast, label-free and reliable method. The device was tested with real samples from milk, where it was possible to detect ampicillin in concentrations below the MRL defined in EU regulation no. 675/92.

Acknowledgement

This project was financially supported by funding from the Danish Research Council, The Novo Nordisk Foundation and the Technical University of Denmark.

Appendix A. Supplementary data

Supplementary data associated with this article can be found in the online version at http://dx.doi.org.10.1016/j.bios.2012.12.058.

References

Aasmundtveit, K.E., Samuelsen, E.J., Pettersson, L.A.A., Inganäs, O., Johansson, T., Feidenhans'l, R., 1999. Synthetic Metals 101 (1–3), 561–564.
Balamurugan, A., Chen, S.-M., 2007. Analytica Chimica Acta 596 (1), 92–98.
Bhattacharyya, D., Gleason, K.K., 2011. Chemistry of Materials 23 (10), 2600.
Bidan, G., Billon, M., Livache, T., Mathis, G., Roget, A., Torresrodriguez, L., 1999. Synthetic Metals 102 (1–3), 1363.
Binz, H., Amstutz, P., Plückthun, A., 2005. Nature Biotechnology 23 (10), 1257–1268.
Cabello, F.C., 2006. Environmental Microbiology 8 (7), 1137–1144.
Centers for Disease Control and Prevention (CDC), March 2006. MMWR. Morbidity and Mortality Weekly Report 55(11), 301–305.
Centi, S., Tombelli, S., Minunni, M., Mascini, M., 2007. Analytical Chemistry 79 (4), 1466–1473.
Cosnier, S., 2003. Analytical and Bioanalytical Chemistry 377 (3), 507–520.
Dubois, M.-P., Gondran, C., Renaudet, O., Dumy, P., Driguez, H., Fort, S., Cosnier, S., 2005. Chemical Communications (Cambridge) (34), 4318–4320.
Ellington, A.D., Szostak, J.W., 1990. Nature 346 (6287), 818–822.
Gerard, M., Chaubey, A., Malhotra, B., 2002. Biosensors and Bioelectronics 17 (5), 345–359.
González-Fernández, E., de-los Santos-Álvarez, N., Lobo-Castañón, M.J., Miranda-Ordieres, A.J., Tuñón-Blanco, P., 2011. Biosensors and Bioelectronics 26 (January (5)), 2354–2360.
Groenendaal, L., Jonas, F., Freitag, D., Pielartzik, H., Reynolds, J.R., 2000. Advanced Materials 12 (7), 481.
Gullberg, E., Cao, S., Berg, O.G., Ilbäck, C., Sandegren, L., Hughes, D., Andersson, D.I., 2011. PLoS Pathogens 7 (July (7)).
Guo, W., Yuan, J., Li, B., Du, Y., Ying, E., Wang, E., 2008. Analyst 133 (9), 1209–1213.
Hansen, T.S., West, K., Hassager, O., Larsen, N.B., 2006. Synthetic Metals 156 (18–20), 1203.
Hansen, T.S., West, K., Hassager, O., Larsen, N.B., 2007a. Journal of Micromechanics and Microengineering 17 (5), 860.
Hansen, T.S., West, K., Hassager, O., Larsen, N.B., 2007b. Advanced Materials 19 (20), 3261.
Hong, P., Li, W., Li, J., 2012. Sensors 12 (2), 1181–1193.
Hoogenboom, H., 2005. Nature Biotechnology 23 (9), 1105–1116.
Hsiao, A.-E., Tuan, C.-S., Lu, L.-H., Liao, W.-S., Teng, W.-J., 2010. Synthetic Metals 160 (21–22), 2319.
Kerman, K., Kobayashi, M., Tamiya, E., 2004. Measurement Science and Technology 15 (2).
Kiilerich-Pedersen, K., Poulsen, C.R., Jain, T., Rozlosnik, N., 2011. Biosensors and Bioelectronics, 386–392.
Klevens, R.M., Morrison, M.A., Nadle, J., Petit, S., Gershman, K., Ray, S., Harrison, L.H., Lynfield, R., Dumyati, G., Townes, J.M., Craig, A.S., Zell, E.R., Fosheim, G.E., McDougal, L.K., Carey, R.B., Fridkin, S.K., 2007. JAMA—Journal of the American Medical Association 298 (15), 1763–1771.
Kros, A., Nolte, R.J.M., Sommerdijk, N.A.J.M., 2002. Journal of Polymer Science. Part A—Polymer Chemistry 40 (6), 738.
Lauridsen, L., Veedu, R., 2012. Nucleic Acid Therapeutics. 22 (6), 371–379, http://dx.doi.org/10.1089/nat.2012.0377.
Lazcka, O., Campo, F.J.D., Muñoz, F.X., 2007. Biosensors and Bioelectronics 22 (7), 1205–1217.
Le, T.T., Kim, D.W., Lee, Y., Nam, J.D., 2005. Accessed online 25.11.2010 〈http://gralib.hcmuns.edu.vn/gsdl/collect/hnkhbk/index/assoc/HASH01f3/8a663927.dir/doc.pdf〉.
Liao, W., Guo, S., Zhao, X., 2006. Frontiers in Bioscience 11, 186–197.
Lima, A., Schottland, P., Sadki, S., Chevrot, C., 1998. Synthetic Metals 93 (February (1)), 33–41.
Lind, J.U., Acikgoz, C., Daugaard, A.E., Andresen, T.L., Hvilsted, S., Textor, M., Larsen, N.B., 2012. Langmuir 28 (15), 6502–6511.
Mehta, J., Van Dorst, B., Rouah-Martin, E., Herrebout, W., Scippo, M.-L., Blust, R., Robbens, J., 2011. Journal of Biotechnology 155 (4), 361–369.
Pänke, O., Balkenhohl, T., Kafka, J., Schäfer, D., Lisdat, F., 2008. Biochemical Engineering & Biotechnology 109, 195–237.
Rozlosnik, N., 2009. Analytical and Bioanalytical Chemistry 395 (3), 637–645.
Sarma, A.K., Vatsyayan, P., Goswami, P., Minteer, S.D., 2009. Biosensors and Bioelectronics 24 (8), 2313–2322.
Septimus, E.J., Kuper, K.M., 2009. Clinical Pharmacology & Therapeutics 86 (September (3)), 336–339.
Shi, Y., Luo, S., Fang, W., Zhang, K., Ali, E., Boey, F., Ying, J., Wang, J., Yu, H., Li, L., 2008. Organic Electronics 9 (5), 859.
Song, K.-M., Cho, M., Jo, H., Min, K., Jeon, S.H., Kim, T., Han, M.S., Ku, J.K., Ban, C., 2011. Analytical Biochemistry 415 (2), 175–181.
Song, K.-M., Jeong, E., Jeon, W., Cho, M., Ban, C., 2012a. Analytical and Bioanalytical Chemistry 402 (6), 2153–2161, http://dx.doi.org/10.1007/s00216-011-5662-3.
Song, K.-M., Lee, S., Ban, C., 2012b. Sensors 12 (1), 612–631.
Sotzing, G.A., Reynolds, J.R., Steel, P.J., 1996. Chemistry of Materials 8 (April (4)), 882–889.
Syritski, V., Gyurcsányi, R.E., Öpik, A., Tóth, K., 2005. Synthetic Metals 152 (1–3), 133–136.
Tuerk, C., Gold, L., 1990. Science 249 (4968), 505–510.
Vidal, J.C., Méndez, S., Castillo, J.R., 1999. Analytica Chimica Acta 385 (1–3), 203–211.
Wang, J., Wang, L., Liu, X., Liang, Z., Song, S., Li, W., Li, G., Fan, C., 2007. Advanced Materials 19 (22), 3943–3946.
White, A.R., on behalf of the BSAC Working Party on The Urgent Need: Regenerating Antibacterial Drug Discovery and Development, Blaser, M., Carrs, O., Cassell, G., Fishman, N., Guidos, R., Levy, S., Powers, J., Norrby, R., Tillotson, G., Davies, R., Projan, S., Dawson, M., Monnet, D., Keogh-Brown, M., Hand, K., Garner, S., Findlay, D., Morel, C., Wise, R., Bax, R., Burke, F., Chopra, I., Czaplewski, L., Finch, R., Livermore, D., Piddock, L. J.V., White, T., 2011. Journal of Antimicrobial Chemotherapy 66(9), 1948–1953.
Winkler, W., Nahvi, A., Breaker, R.R., 2002. Nature 419 (October (6910)), 952–956.
Winther-Jensen, B., West, K., 2004. Macromolecules 37 (12), 4538–4543.
Winther-Jensen, B., West, K., 2006. Reactive and Functional Polymers 66 (5), 479–483.
Witte, W., 1998. Science 279 (5353), 996–997.
Wu, S., Duan, N., Wang, Z., Wang, H., 2011. Analyst 136, 2306–2314.
Xie, H., Luo, S.-C., Yu, H.-H., 2009. Small 5 (22), 2611–2617.
Yamato, H., Ohwa, M., Wernet, W., 1995. Journal of Electroanalytical Chemistry 397 (1–2), 163–170.
Yan, X., Cao, Z., Lau, C., Lu, J., 2010. Analyst 135, 2400–2407.
Zuo, X., Xiao, Y., Plaxco, K., 2009. Journal of the American Chemical Society 131 (20), 6944–6945.

Comparative study on aptamers as recognition elements for antibiotics in a label-free all-polymer biosensor

Johannes Daprà[a], Lasse Holm Lauridsen[b], Alex Toftgaard Nielsen[b], Noemi Rozlosnik[a]

[a] *Department of Micro-and Nanotechnology, Technical University of Denmark, Produktionstorvet 423, DK-2800 Kgs. Lyngby, Denmark.*
[b] *The Novo Nordisk Foundation Center for Biosustainability, Scion-DTU, Fremtidsvej 3, DK-2970 Hørsholm, Denmark.*

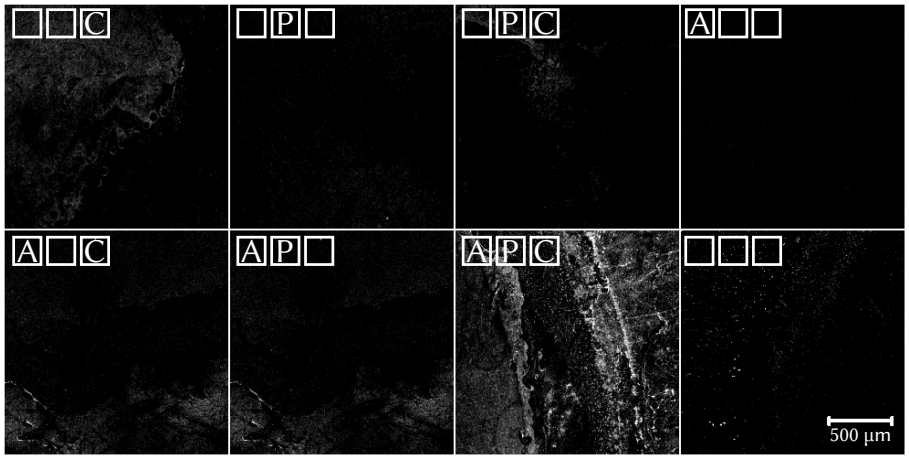

Figure S1: Control experiments for the immobilisation of DNA on a PEDOT-OH film are shown. The boxed letters in the upper left corner of each image list the treatments to which the surfaces were subjected to. The markings read as follows: A activated with EDC and NHS, P immobilised probe strand, and C hybridised with complementary DNA (cDNA). An empty square means that the respective treatment was left out. As can be seen in the figure only the surface with all three treatments, i. e. activation with the coupling agents, immobilisation of the DNA probe and hybridisation with cDNA, showed significant fluorescence, while the others show nothing or traces. The weak signal on some of the surfaces where no fluorescence was expected can probably be attributed to spilled DNA from neighbouring spots on the chip.

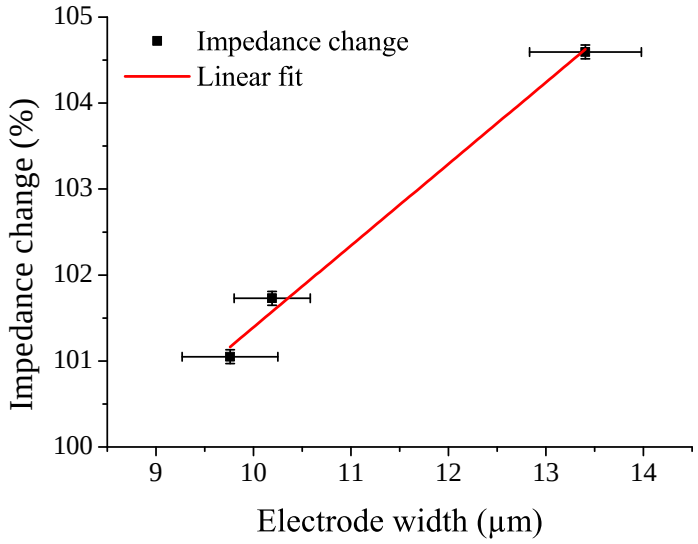

Figure S2: Correlation of impedance response and wire width based on measurements performed on three different chips using 1 µM ampicillin and electrodes functionalized with the anti-ampicillin aptamer.

Title:

All-polymer Chip for electrochemical detection of DNA hybridisation

Authors & affiliations:

J. Daprà*, D. Kwasny, W. E. Svendsen, N. Rozlosnik
DTU Nanotech, Denmark

Abstract: (Your abstract must use **Normal style** and must fit in this box. Your abstract should be no longer than 300 words. The box will 'expand' over 2 pages as you add text/diagrams into it.)

Hybridisation is a powerful tool for fast and uncomplicated oligonucleotide sequencing. Different ssDNA strands of known sequence are immobilised spatially separated onto a surface and incubated with the unknown sample. Successful hybridisation can be detected and thus the sequence of DNA samples can be revealed. For example, in clinical screenings of cervical cancer, the genotype of HP virus is commonly determined by such arrays.

Most hybridisation chips work with optical detection methods using fluorescent dyes. In our project we aim to establish an electrochemical sensing unit, which would save costs for optical systems and thus allow for usage as point-of-care device. Employing conductive polymers, we designed an all-polymer device for the electrochemical detection of DNA hybridisation.

The usage of conductive polymers as electrode material is beneficial because of its outstanding biocompatibility and transparency. In our system, the highly conductive poly(3,4-ethylenedioxythiophene) (PEDOT) based, micropatterned electrodes were used. The low price and ease of handling of this material provide a possibility for fabrication of disposable chips at a large scale.

We succeeded in immobilising oligonucleotides on the surface electrodes via direct covalent bonding.

The hybridisation of complementary oligonucleotide strands employing fluorescent markers with a biotin/streptavidin system was successful and proved to be very specific (see figure 1).

Further development aims a fast and sensitive electrochemical detection of hybridisation via electrochemical measurements of the redox-behaviour of the intercalate methylene blue.

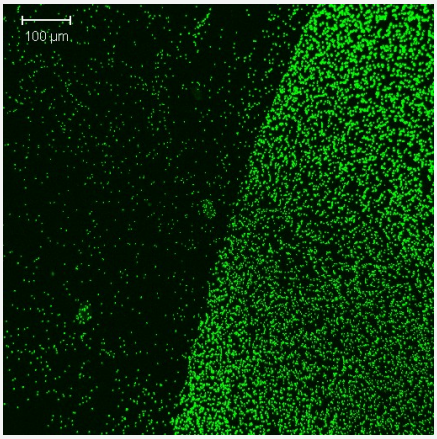

Figure 1: Immobilised DNA probes on PEDOT made visible by fluorescent beads.

OMICS Group Conferences
Accelerating Scientific Discovery

International Conference and Exhibition on
Biosensors & Bioelectronics

May 14-16, 2012 Embassy Suites Las Vegas, USA

Application of aptamers for label-free all-polymer biosensors

Johannes Daprà and Noemi Rozlosnik

Department of Micro-and Nanotechnology, Technical University of Denmark, Denmark

Aptamers, which are artificial oligonucleic acids, having high affinity, specificity and selectivity to specific target molecules, are getting more and more attention in biosensors, as they are more robust molecules with long-term thermal stability compared to antibodies or enzymes. The coupling of electrochemical devices with these nanoscale materials offers a unique capability for label-free transduction realizing the easy-to-stock, easy-to-use applications. However, the technique requires the immobilization of reagents - namely the aptamers - directly to the surface of the electrodes allowing an intimate physical contact between the receptor and the transducer, which ensures an optimum signal transfer. Our research group has successfully developed an all-polymer electrochemical biosensor employing a conductive polymer as electrodes. In this paper we report a new transducer material for impedimetric sensing: aptamers, which are conjugated to a chemically modified conductive polymer (poly (3,4-ethylenedioxythiophene), PEDOT. In this paper the detection of antibiotics will be shown as an example. Antibiotics are heavily used in food industry and in aquaculture, and a selective and sensitive, field based detection system is essential for diagnostics of their harmful effect.

Biography

Johannes Daprà has received his master degree in chemistry at the Technical University of Munich, and now finishing his PhD in nanotechnology at the Technical University of Denmark. He has expertise in polymer chemistry and in conductive polymers. He is co-inventor of the patent “Biosensor for point-of-care diagnostic and on-site measurements”.

Johannes.Dapra@nanotech.dtu.dk

Application of Label-free Aptasensors in Environmental Monitoring*

Johannes Daprà[1] and Noemi Rozlosnik[2]

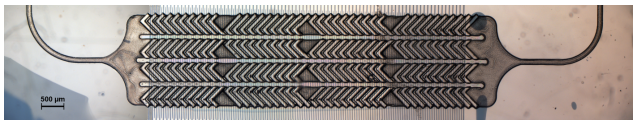

Fig. 1. Channel

***Abstract*— Anthropogenic pollutants are a growing ... I should write about this much of text in this section, so that it makes sense. More would not be necessary.**

I. Introduction

It has long been known that extensive use of antibiotics causes evolutionary selection of resistant bacteria. Since antibiotics are not only used for human and veterinary health treatment but to the greatest extent for prophylaxis and growth promotion in animal husbandry, enormous amounts are constantly released into the environment[1], [2].

While the general belief in the past was that selection towards resistant mutants only occurs at sufficiently high concentrations of the antimicrobial (i.e. between the minimal inhibitory concentrations of the wild type and the resistant mutant)[3], it has recently been shown that the both enrichment of resistant mutants and *de novo* development occurs at concentrations far below those levels[4], [5].

Anthropogenic pollution of soil and aqueous environment

II. Methodology

The chip system is an all-polymer microfluidic device consisting of a channel system with herringbone structures for enhanced mixing and an electronic detection layer. This micro-fabricated electrode system is made of the conductive polymer 3,4-ethylenedioxythiophene (PEDOT) which was patterned with a novel wet-chemical etching method. Aptamer-probes were applied by ink-jet spotting (???) and UV-immobilised. This method allowed the directed coverage of electrodes with probes and at the same time the blocking of the remaining surface to get a defined surface-coverage.

The biosensor is characterised extensively by cyclic volatammetry and impedance spectroscopy. Analyte detection is performed label-free with electrochemical impedance spectroscopy (EIS).

*This work was sponsored by DTU Nanotech

[1]J. Daprà is with DTU Nanotech, Department for Micro- and Nanotechnology, Technical University of Denmark, 2840 Kgs. Lyngby, Denmark jdap@nanotech.dtu.dk

III. Results

I describe our model system which has been used for detection of multiple compounds, first of all the two antibiotics ampicillin and kanamycin. LOD values can be shown and explanations for the signal change will be given.

The only medical diagnostic related results I have are from the morbilli experiments, and they are not really great so far, but on the other hand I could use the aptamer/antibiotics results as some sort of proof-of-concept.

IV. Conclusions

Here I'll summarise the observed outcome of our experiments and tell that this device is a good prototype for proof of concept. Further development into a multi-target array will make sense, and we're at it.

References

[1] W. Witte, "Medical consequences of antibiotic use in agriculture," *Science*, vol. 279, no. 5353, pp. 996–997, 1998. [Online]. Available: http://www.sciencemag.org/content/279/5353/996.short

[2] F. M. Aarestrup, "Veterinary drug usage and antimicrobial resistance in bacteria of animal origin," *Basic & Clinical Pharmacology & Toxicology*, vol. 96, no. 4, pp. 271–281, 2005. [Online]. Available: http://dx.doi.org/10.1111/j.1742-7843.2005.pto960401.x

[3] K. Drlica, "The mutant selection window and antimicrobial resistance," *Journal of Antimicrobial Chemotherapy*, vol. 52, no. 1, pp. 11–17, 2003. [Online]. Available: http://jac.oxfordjournals.org/content/52/1/11.abstract

[4] E. Gullberg, S. Cao, O. G. Berg, C. Ilbäck, L. Sandegren, D. Hughes, and D. I. Andersson, "Selection of resistant bacteria at very low antibiotic concentrations," *PLoS Pathog*, vol. 7, no. 7, p. e1002158, 07 2011.

[5] A. Liu, A. Fong, E. Becket, J. Yuan, C. Tamae, L. Medrano, M. Maiz, C. Wahba, C. Lee, K. Lee, K. P. Tran, H. Yang, R. M. Hoffman, A. Salih, and J. H. Miller, "Selective advantage of resistant strains at trace levels of antibiotics: a simple and ultrasensitive color test for detection of antibiotics and genotoxic agents," *Antimicrobial Agents and Chemotherapy*, vol. 55, no. 3, pp. 1204–1210, March 2011. [Online]. Available: http://aac.asm.org/content/55/3/1204.abstract

(12) INTERNATIONAL APPLICATION PUBLISHED UNDER THE PATENT COOPERATION TREATY (PCT)

(19) World Intellectual Property Organization
International Bureau

(43) International Publication Date
14 March 2013 (14.03.2013)

WIPO | PCT

(10) International Publication Number
WO 2013/034688 A1

(51) International Patent Classification:
G01N 33/543 (2006.01) *G01N 27/327* (2006.01)

(21) International Application Number:
PCT/EP2012/067508

(22) International Filing Date:
7 September 2012 (07.09.2012)

(25) Filing Language: English

(26) Publication Language: English

(30) Priority Data:
11180774.9 9 September 2011 (09.09.2011) EP
61/532,721 9 September 2011 (09.09.2011) US

(71) Applicant *(for all designated States except US)*: **DANMARKS TEKNISKE UNIVERSITET** [DK/DK]; Anker Engelundsvej 1, DK-2800 Kgs. Lyngby (DK).

(72) Inventors; and
(75) Inventors/Applicants *(for US only)*: **ROZLOSNIK, Noemi** [DK/DK]; Bagsværd Hovedgade 14A, DK-2880 Bagsværd (DK). **DAPRÁ, Johannes** [IT/DK]; Skovlyporten 7.1, Holte, DK-2840 (DK).

(74) Agent: **ZACCO DENMARK A/S**; Hans Bekkevolds Allé 7, DK-2900 Hellerup (DK).

(81) Designated States *(unless otherwise indicated, for every kind of national protection available)*: AE, AG, AL, AM, AO, AT, AU, AZ, BA, BB, BG, BH, BN, BR, BW, BY, BZ, CA, CH, CL, CN, CO, CR, CU, CZ, DE, DK, DM, DO, DZ, EC, EE, EG, ES, FI, GB, GD, GE, GH, GM, GT, HN, HR, HU, ID, IL, IN, IS, JP, KE, KG, KM, KN, KP, KR, KZ, LA, LC, LK, LR, LS, LT, LU, LY, MA, MD, ME, MG, MK, MN, MW, MX, MY, MZ, NA, NG, NI, NO, NZ, OM, PA, PE, PG, PH, PL, PT, QA, RO, RS, RU, RW, SC, SD, SE, SG, SK, SL, SM, ST, SV, SY, TH, TJ, TM, TN, TR, TT, TZ, UA, UG, US, UZ, VC, VN, ZA, ZM, ZW.

(84) Designated States *(unless otherwise indicated, for every kind of regional protection available)*: ARIPO (BW, GH, GM, KE, LR, LS, MW, MZ, NA, RW, SD, SL, SZ, TZ, UG, ZM, ZW), Eurasian (AM, AZ, BY, KG, KZ, RU, TJ, TM), European (AL, AT, BE, BG, CH, CY, CZ, DE, DK, EE, ES, FI, FR, GB, GR, HR, HU, IE, IS, IT, LT, LU, LV, MC, MK, MT, NL, NO, PL, PT, RO, RS, SE, SI, SK, SM, TR), OAPI (BF, BJ, CF, CG, CI, CM, GA, GN, GQ, GW, ML, MR, NE, SN, TD, TG).

Published:

— *with international search report (Art. 21(3))*

(54) Title: BIOSENSOR FOR POINT-OF-CARE DIAGNOSTIC AND ON-SITE MEASUREMENTS

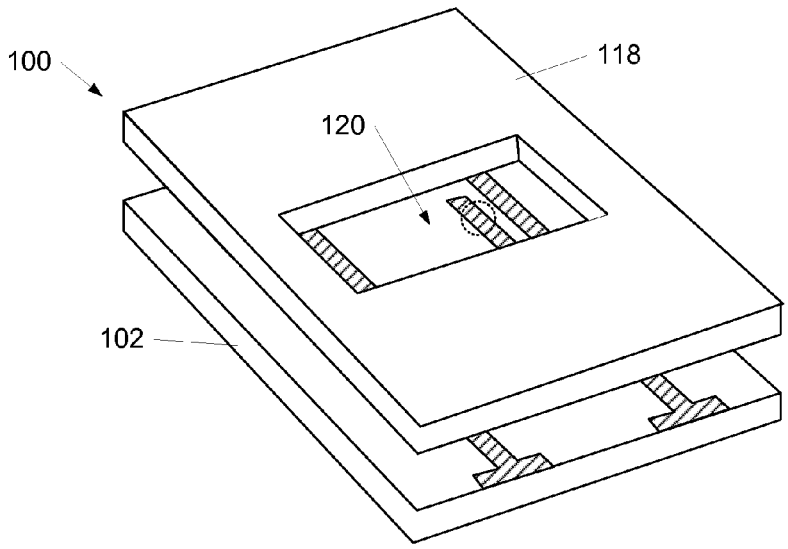

Fig. 1a

(57) Abstract: Disclosed herein is a biosensor for detection of a target substance in a sample with impedance spectroscopy, the biosensor comprising 1) a first non-conducting substrate comprising a primary substrate surface; 2) a conducting polymer electrode layer comprising one or more conducting polymers layers, the conducting polymer electrode layer comprising a primary electrode surface and a secondary electrode surface, wherein the secondary electrode surface covers part of the primary substrate surface; 3) a probe layer bonded to part of the primary electrode surface; and 4) a second non-conducting substrate comprising a secondary substrate surface, wherein the secondary substrate surface of the second substrate and the primary substrate surface of the first substrate are interconnected such that the electrode layer and the probe layer are confined within an area defined by the first substrate and the second substrate; wherein the electrode layer comprises at least a first electrode pair, the first electrode pair comprising a primary electrode and a secondary electrode, where the probe layer is bonded to the primary electrode and the secondary electrode of the at least first electrode pair, the probe layer being adapted for selectively binding of the target substance.

WO 2013/034688 A1

Biosensor for point-of-care diagnostic and on-site measurements

The invention relates to an improved biosensor for fast, easy and reliable point-of-care diagnostics and on-site measurements using impedance spectroscopy.

In a global community, the outbreak of infectious diseases contributes to the fear of severe pandemics, and is a source of worry for the population. In recent years, emerging viruses such as e.g. Dengue virus, West Nile virus, and influenza A virus, have been a focus of massive attention.

Conventional diagnostic methods for detection of acute viral disease count e.g. polymerase chain reactions (PCR) and enzyme linked immunosorbent assays (ELISA). These diagnostic methods give reliable results, but require rather complicated procedures. PCR and ELISA diagnostic methods are time consuming, expensive, labour intensive, and require trained personnel and specialised laboratories.

The demands in modern medical diagnosis thus put forward an enormous need for faster and cheaper detection methods for detecting viral infections, which give a prompt result. If it had been possible to efficiently diagnose humans for Swine-Origin influenza A (H1N1)-virus, back in 2009, treatment could have been applied quickly and the flu might not have been so widespread.

Impedimetric biosensors are a class of biosensors used for detection of e.g. viruses using electrochemical impedance spectroscopy (EIS). When a target substance, such as e.g. a target molecule, binds to an impedance biosensor, it will induce a change in the electrode surface/liquid solution interface. The difference in the impedance measured before and after the target substance binds to the biosensor provides a direct indication of the amount of target substance in the sample. Thus, the presence of a target substance in a

sample can be detected very efficiently with a biosensor using electrochemical impedance spectroscopy (EIS).

EIS measures the electrical impedance by imposing a small sinusoidal voltage at a certain frequency to an electrochemical cell and measuring the resulting current through the cell. The time dependent current-voltage ratio and the phase shift give the impedance. Since the impedance changes when the target analyte is captured on the surface of the electrodes, EIS represents a powerful method for probing the interfacial reactions of modified electrodes, providing a rapid approach for monitoring the dynamics of biomolecular interactions.

The impedance of a system is frequency dependent, and can be expressed as a complex number:

$$Z(f) = Z_0 (\cos(\phi) + i \sin(\phi)) \quad [1]$$

where f is the frequency, Z_0 is the magnitude of the impedance, and ϕ is the phase shift. Thus, the impedance $Z(f)$ consists of a real and an imaginary part. The graph, on which the imaginary part of the impedance is plotted against the real part (so-called “Nyquist Plot”), can be used to determine the most efficient frequency for the detection of the target binding.

Impedance biosensors are very promising for a variety of applications such as point-of-care diagnostics, on-site measurements, consumer test kits, bioprocess monitoring, water quality testing, and biowarfare agent detection, due to among others the advantage of label-free operation.

Especially point-of-care diagnostic applications (diagnostic testing at or near the site of patient care) are promising in connection with impedance

biosensors, as it brings the test conveniently and immediately to the patient, facilitating rapid treatment.

Existing technologies for point-of-care diagnostics, often based on laminar flow assays (LFA), are usually not very specific and have high detection limits.

Today, screening of blood samples for disease markers is expensive both in hours and reagents. Further, screenings are labour intensive and need to be conducted in specialised laboratories by trained personnel. Accordingly it is an object of the invention to provide an improved, user friendly and cheap biosensor for point-of-care testing and onsite diagnostics.

Disclosed herein is a biosensor for detection of a target substance in a sample with impedance spectroscopy. The biosensor comprises 1) a non-conducting substrate comprising a primary substrate surface; 2) a conducting polymer electrode layer comprising one or more conducting polymers layers, the conducting polymer electrode layer comprising a primary electrode surface and a secondary electrode surface, wherein the secondary electrode surface covers part of the primary substrate surface; 3) a probe layer bonded to part of the primary electrode surface; and 4) a second non-conducting substrate comprising a secondary substrate surface, wherein the secondary substrate surface of the second substrate and the primary substrate surface of the first substrate are interconnected such that the electrode layer and the probe layer are confined within an area defined by the first substrate and the second substrate; wherein the electrode layer comprises at least a first electrode pair, the first electrode pair comprising a primary electrode and a secondary electrode, where the probe layer is bonded to the primary electrode and/or the secondary electrode of the at least first electrode pair, the probe layer being adapted for selectively binding of the target substance.

Examples of materials for the first and the second substrate comprise glass, non-conducting polymers and similar. By non-conducting polymer is meant a polymer with a conductivity of less than 10^{-8} S/m and by conducting polymer is meant a polymer with a conductivity of at least 10 S/m

Hereby is obtained a biosensor, which can be used for routine medical check-up, thereby greatly reducing the cost and time per analysis, allowing more people to be screened for different diseases both inside and outside of medical facilities. Thus, by the biosensor is provided an effective point-of-care biosensor to detect, control and confine the spread of virulent diseases in the near future.

Further, the biosensor provides a fast, sensitive, reliable and selective method for analysis of non-human sample types, such as e.g. water samples possibly containing bacteria.

The target substance, which is detectable with the biosensor according to the above-mentioned method, may be a target molecule, nanoparticles, viruses, bacteria, chemicals, antibiotics, fertiliser or medicines in general and is thus not limited to being a biological sample. A large variety of target substances may be selectively detected upon choosing the correct corresponding probes.

The selective binding of the target substance facilitated by the probe ensures that only the target of interest is detected in the sample. This is a clear advantage compared to using a non-specific biosensor, where e.g. a known cell is attached directly to a non-specifically binding surface, and the subsequent influence of the virus infection on the cell is studied as disclosed in *'Polymer based biosensor for rapid electrochemical detection of virus infection of human cells'* by Kiilerich-Pedersen *et al* published in Biosensors and Bioelectronics, vol. 28 (2011), p. 386-392.

By covalently coupling the probe to the electrode surface it is ensured that it does not detach. Electrochemical impedance spectroscopy also requires the binding event to be in close proximity to the surface. A direct link to the conductive polymer thus provides a defined distance of the binding event to the electric transducer.

As impedance spectroscopy is used for the direct detection of target substances binding to the electrodes, thus there is no need for adding any tag or redox mediator for the selective sensing for the detection to work.

The biosensor is an all-in-one device, where the sample is added to the biosensor instead of the biosensor having to be placed in a sample solution. Further as the biosensor includes both a primary electrode acting as the working electrode and a secondary electrode acting as a counter electrode, the need for additional electrodes – as used in conventional three electrode electrochemical cells – is absent. This reduces the amount of material needed for the device at the same time making the device highly adequate for mass production. Thus, production cost is reduced.

The electrodes in the biosensor are not metal based, which provides for a low material cost. The biosensor may consequently be used as a disposable device, which is advantageous when using the biosensor for point-of-care testing in a location, e.g. an airport, a school or a workplace, where multiple people need to be tested for a given virus and adequate cleaning of the biosensor between testing different people is impossible. Since it is a non-metal device, the used biosensor can be burned along with other types of biochemical waste, as there is no need for metal recovery.

Further, the biosensor only needs to be filled with the sample solution and connected electrically to a docking station. The detection results obtained by

using the biosensor can thus be obtained in significantly shorter time with much less subsequent lab work as compared to standard testing methods such as e.g. ELISA and PCR. This makes the biosensor highly applicable in point-of-care methods and on-site measurements.

Thus, the biosensor according to the invention makes the process of detecting a specific target substance/object effortless due to the fact that the measurements now can take place on a localized electrode surface in contrast to targeting the point of interest in a solution e.g. using a standard three electrode electrochemical cell. This is especially advantageous when detecting target substances in small amounts of samples.

In one or more embodiments the primary electrode comprises a plurality of primary legs and the secondary electrode comprises a plurality of secondary legs, the primary legs and the secondary legs forms an interwoven pattern. The two electrodes are thereby in the same plane making calibration of the two in relation to each other unnecessary.

In one or more embodiments the second non-conducting substrate is provided with ports for inlet/outlet of the sample and/or for facilitating an electrical connection. The sample can thereby be added to the biosensor in a very easy manner, and likewise electrical connection to the electrodes in the biosensor is easily obtained by the ports.

In one or more embodiments the first substrate and/or the second substrate is a non-conducting polymer substrate. Alternatively, the first substrate and/or the second substrate can be a glass substrate or similar. The first and the second substrate can be in the same material, which can be beneficial production wise, but it is not a requirement.

In one or more embodiments the non-conducting polymer substrate is selected from the group of polystyrenes, polyolefins and cyclic olefin copolymers such as e.g. TOPAS 5013L (TOPAS Advanced Polymers, Germany).

In one or more embodiments the one or more conducting polymer layers of the conducting polymer electrode layer is selected from the group of poly(3,4-ethylenedioxythiophene) (PEDOT), polypyrrole (PPy), poly(3,4-propylenedioxythiophene), triacetonamine (TAA), polyaniline (PANI), derivatives thereof and/or co-polymers thereof.

In one or more embodiments the one or more conducting polymer layers of the conducting polymer electrode layer is selected from the group of PEDOT and PEDOT derivatives, which have shown to be highly stable with a high conductivity.

In one or more embodiments the PEDOT derivatives contain one or more functional groups selected from the group of alcohols (OH), carboxylic acids (COOH), azides (N_3) and alkynes. These functional groups facilitate binding with the probe layer.

In one or more embodiments the conducting polymer electrode layer comprises a first conductive polymer layer and a second conducting polymer layer, wherein the probe layer is bonded to the second conducting polymer layer. The first conductive polymer layer may be PEDOT and the second conducting polymer layer may be a PEDOT-derivative for facilitating improved binding with the probe layer.

In one or more embodiments the probe layer is covalently bonded to part of the primary electrode surface, thereby creating a strong bond between the probe layer and the electrode layer.

In one or more embodiments the probe layer comprises an entity selected from the group of aptamers, oligonucleotides and/or peptides. Probes of aptamers, oligonucleotides and/or peptides are a superior substitute to probes comprising antibodies in immunoassays, since aptamers, oligonucleotides and peptides have a higher stability, affinity, and specificity compared to antibodies in immunoassay. As aptamers, oligonucleotides and peptides are significantly smaller in size than their antibody counter parts, the target substances captured by an aptamer, oligonucleotide and/or peptide probe will be much closer to the polymer layer than if using antibodies as probes. As a consequence, the change in the impedance signal due to the capture of the target substance by an aptamer, oligonucleotide and/or peptide probe will be much stronger, enabling a more precise detection result, and higher sensitivity.

In one or more embodiments the electrode layer comprises a second electrode pair comprising a second primary electrode and a second secondary electrode. The probe layer is normally not bonded to the secondary electrode pair, thereby serving as a reference electrode.

Disclosed herein is further the use of a biosensor for point-of-care measurement and/or on-site detecting of a target substance in a liquid sample such as e.g. water, blood, urine and saliva.

Also disclosed herein is a system for detection of a target substance in a sample, the system comprising a biosensor, a docking station, and connectors for operational connection between the docking station and the biosensor, wherein the docking station measures changes in the impedance over the first and/or second electrode pair before and after applying sample to the biosensor. By docking station is meant an apparatus for measuring the current over and/or imposing a current through the system, e.g. an apparatus

which imposes a small sinusoidal voltage at a certain frequency to the biosensor and measures the resulting current through the biosensor. Hereby is obtained a fast, sensitive, reliable and selective impedance biosensor-based system for fast, cheap, and reliable point-of-care diagnostics and on-site measurements.

Brief description of the drawings

Figures 1a-b are schematic illustrations of a biosensor with a non-limiting electrode design according to the invention displayed in a perspective view with (1a) and without (1b) the second substrate layer.

Figure 2 shows an enlargement of the electrode of the biosensor in figures 1a-b displayed in a perspective view.

Figure 3 shows the structure of four different monomer building blocks; A) EDOT, B) EDOT-OH, C) EDOT-COOH, and D) EDOT-N_3.

Figure 4 illustrates the synthesis of PEDOT.

Figure 5 shows the steps involved in producing a biosensor according to the invention using one possible production method. The biosensor is illustrated in a side view.

Figure 6a shows an embodiment of the biosensor viewed from the top and figure 6b shows the second substrate layer in a perspective view.

Figures 7a-b illustrate different working/counter electrode design options.

Detailed description

Figure 1a-b illustrate the basic layout of a biosensor 100 according to the invention as seen in a perspective view with (figure 1a) and without (figure 1b) the second substrate layer.

The biosensor 100 for detection of a target substance in a sample comprises a first non-conducting substrate 102 comprising a primary substrate surface 101. The biosensor 100 further comprises a conducting polymer electrode layer 108 comprising one or more conducting polymer layers, the conducting polymer electrode layer comprising a primary electrode surface and a secondary electrode surface, wherein the secondary electrode surface covers part of the primary substrate surface 101.

The biosensor further comprises a probe layer 110 bonded to part of the primary electrode surface and a second non-conducting substrate 118 comprising a secondary substrate surface, wherein the secondary substrate surface of the second substrate and the primary substrate surface of the first substrate are interconnected such that the electrode layer and the probe layer are confined within an area defined by the first substrate and the second substrate.

The electrode layer 108 comprises at least a first electrode pair 103, the first electrode pair comprising a primary electrode 104 and a secondary electrode 106, where the probe layer 110 is bonded to the primary electrode 104 and/or the secondary electrode 106 of the at least first electrode pair 103.

On top of the first substrate layer 102 and the electrodes 104, 106 is a second substrate layer 118. The two substrate layers 102, 118 are of a non-conducting material such as a non-conducting polymer, glass or similar. Some examples of non-conducting polymers are polystyrenes, polyolefins and cyclic olefin copolymers such as e.g. TOPAS 5013L (TOPAS Advanced Polymers, Germany).

The second substrate layer 118 has an opening 120 forming a channel allowing samples to come in contact with the electrodes 104, 106. The electrodes 104, 106 are made from conducting polymers and are thus not metal based. Non-limiting examples of suitable conducting polymers with high conductivity and high stability are polypyrrole (PPy), poly(3,4-ethylenedioxythiophene) (PEDOT), poly(3,4-propylenedioxythiophene), triacetonamine (TAA), polyaniline (PANI), derivatives thereof and/or co-polymers formed by two or more of the monomeric units in the mentioned polymer examples.

Non-limiting examples of functional groups in the derivatives, e.g. the PEDOT derivatives, are alcohols (OH), carboxylic acids (COOH), azides (N_3) and alkynes.

Figure 3 shows 3,4-ethylenedioxythiophene (EDOT) (figure 3A) and the OH, COOH, and N_3 based EDOT-derivatives; EDOT-OH (figure 3B) EDOT-COOH (figure 3C) and EDOT-N_3 (figure 3D) used as the monomeric building block for PEDOT, PEDOT-OH, PEDOT-COOH, and PEDOT-N_3, respectively.

The synthesis of PEDOT (and similarly for derivatives thereof) can be done using different polymerization schemes starting from EDOT monomer. Figure 4 shows one possible synthesis way, wherein Fe(III) *p*-toluene sulfonate (iron tosylate) is used for the oxidative chemical polymerization of the EDOT monomer. To inhibit the spontaneous oxidation of the monomer by iron tosylate, pyridine can be added to the solution. The substrate can then be spin coated on the support wafers. By heating, the inhibitor evaporates and the oxidative polymerisation of EDOT starts, whereby PEDOT is formed. Fe(II)-salts formed under polymerization are washed away afterwards by rinsing with water, leaving the doped conducting form of PEDOT, which is insoluble in any common solvent, transparent and mechanically durable.

The electrodes 104, 106 shown in figure 1 may comprise one layer of a conducting polymer or multiple layers of the same or different conducting polymers. Figure 2 shows an enlargement view 105 of part of the primary electrode 104 functioning as the working electrode, wherein the polymer layer 108 coated onto the first substrate layer 102 comprises two layers of polymers; a first polymer layer 108a of e.g. PEDOT and a second polymer layer 108b of e.g. the PEDOT-derivative hydroxymethyl-PEDOT (PEDOT-OH). The secondary electrode 106 is constructed in a similar manner and functions as a counter electrode.

Covalently bound to the polymer layer 108 is a probe layer 110 comprising an entity such as an aptamer, an oligonucleotide and/or a peptide. The entity in the probe layer 110 binds selectively to a specific target substance 112. The target substance could be a virus, a protein, a cell, a peptide, a molecule (both organic and inorganic), a structured nano-particle, an antibiotic, a fertiliser or similar. Thereby, when a sample, such as e.g. a blood sample, urine and saliva, or water, containing target substances 112 come in contact with the biosensor 100 (by adding the sample to the opening(s) 120 in the biosensor), the target substances 112 will form bonds, e.g. ionic bonds, hydrogen bonds or other electrostatic interaction bonds, with the probe 110.

For specific detection of target objects such as DNA strands and proteins, an aptamer, oligonucleotide and/or peptide probe 110 is a superior substitute compared to probes comprising antibodies, since aptamers, oligonucleotides and peptides have a higher stability, affinity, and specificity compared to antibodies. As aptamers, oligonucleotides and peptides are significantly smaller in size than their antibody counter parts, the target substances captured by an aptamer/oligonucleotide/peptide probe will be much closer to the polymer layer 108 than when using antibody in immunoassay as probe. As a consequence, the change in the impedance signal due to the capture of

the target substance 112 by an aptamer/oligonucleotide/peptide probe will be much stronger, enabling a more precise detection result.

In contrast to enzymes or antibodies, aptamers e.g. have a capability to bind a wide range of targets: nucleic acids, proteins, ions, toxic substances, viruses, cells and other compounds with high affinity and sensitivity.

Aptamers are peptides or oligonucleotides (RNA or single stranded DNA) which typically fold into a three-dimensional structure, and whose conformation is changing upon ligand binding. Novel aptamers can be developed using a process called SELEX (Systematic Evolution of Ligands by Exponential enrichment). It enables the selection of high-affinity nucleic acid sequences from a random pool of candidates. The oligonucleotide aptamers can easily be modified with signal moieties and can be produced at low cost. Thus, the probe 110 may be a biological entity or a synthetically produced replica and/or modification of such.

The second polymer layer 108b, which binds covalently to the probe 110 is normally chosen such that it facilitates an improved binding capacity for forming covalent bonds between the second polymer layer 108b and the probe 110. Depending on production cost and productions lines, a single polymer layer of e.g. PEDOT-OH may be preferable over the double layering design shown in figure 2.

Figure 5 illustrates the steps involved in one possible method for the production of the all polymer biosensor according to the invention. The first substrate layer 102 in the wafer 200 is a non-conductive substrate layer 102 fabricated from e.g. the cyclic olefin copolymer TOPAS 5013L (TOPAS Advanced Polymers, Germany) by injection moulding.

After rinsing the substrate layer 102 with isopropanol, ethanol and demineralised water, a polymer layer 108 of e.g. PEDOT and/or PEDOT derivatives is spun upon the substrate 102 at 1000 rpm for 20 seconds to achieve a height of approximately 100-400 nm. Higher or lower heights of the polymer layer 108 could also be obtained. The substrate 102 with the polymer layer 108 is subsequently placed in a nitrogen oven for approximately 2-10 minutes at 70 °C and next rinsed thoroughly with demineralised water.

PEDOT and derivatives thereof are examples of homopolymers, where the polymer comprises one type of monomer unit. As an alternative to homopolymers, the polymer layer 108 could also be a co-polymer comprising two or more different monomer units. Non-limiting examples of other suitable conducting polymers with high conductivity and high stability are polypyrrole (PPy), poly(3,4-propylenedioxythiophene), triacetonamine (TAA), polyaniline (PANI) derivatives thereof and/or co-polymers formed by two or more of the monomeric units in the mentioned polymers possibly in combination with PEDOT and/or PEDOT derivatives.

A positive photoresist 114, such as e.g. S1813 (Shipley Company, USA), is spun on the polymer layer 108 at 3000 rpm for 30 seconds, thereby creating a protective layer with the height of approximately 1500 nm. The photoresist 114 is formed in a predetermined pattern for creating a preselected primary/secondary electrode design in the electrode pair(s) 103 for obtaining a working/counter electrode pair. To harden the photoresist, the wafer 200 is placed in a nitrogen oven for 10 minutes at 70 °C. This insures that excess solvent evaporates from the photoresist 114.

By exposing the wafer 200 to UV light for 35 seconds (at 275 W and 5:98 mJ/cm^2) the preselected pattern in the wafer is produced yielding the wafer 202. Reactive ion etching creates the preselected pattern in the polymer electrode

layer 108 as shown in the wafer 204. The photoresist 114 is subsequently removed by flood exposing the wafer 204 with UV light and then removing the photoresist 114 with a four minute ethanol bath thereby obtaining the wafer 206.

Alternatively to the above, the electrode pattern can be formed by other standard methods of photolithography.

A probe is covalently bound to the polymer layer 108 normally by flushing a liquid containing the probe through the wafer thereby leaving the probes 110 on the polymer layer 108. The probe is selectively chosen for binding with the target substance, e.g. a virus, to be detected in a given sample. Examples of suitable probes include peptides, aptamers and/or oligonucleotides.

As an alternative to flushing the probe solution through the water, the polymer layer 108 can first be modified with succinic anhydride to have an acid group rather than a hydroxyl group, and then afterwards further activate the acid group using the standard EDC/NHS (1-ethyl-3-(3-dimethylaminopropyl)carbodiimide/*N*-hydroxysuccinimide) method. The further activated acid group can then react with the amino-terminated probe.

A second substrate layer 118 may be secured to the wafer 208 by use of e.g. a transfer adhesive 116 thereby yielding the biosensor 210. Alternatively, the transfer adhesive 116 layer can be abandoned if there are sample channels in the second substrate layer 118 allowing the second substrate layer 118 and the first substrate layer 102 to be connected directly.

The second substrate layer 118 contains access ports 120, e.g. in standard Luer lock size, for fluid inlets, outlets and/or electrical connections. The second substrate layer 118 is a non-conductive substrate layer (similarly to the first substrate layer 102) fabricated from e.g. the cyclic olefin copolymer

TOPAS 5013L (TOPAS Advanced Polymers, Germany) by injection moulding.

The second substrate layer 118 and the first substrate layer 102 are preferably in the same material for reduced production costs. The second substrate layer 118 may also be patterned in a channel area situated opposite the patterned area 302 in the first substrate layer 102 when the two parts are assembled. This is beneficial production wise, as the second substrate layer 118 and the first substrate layer 102 can be produced in the same production line. Also, the patterned design forces the sample substances to distribute more evenly and thereby bind more efficiently to the probe 110 attached to the polymer 108.

Alternatives to the lithography biosensor production method producing the patterned electrode design as described in connection with figure 5 are methods such as stamping, ink-jet printing, screen printing or similar.

The probe 110 can be applied before or after assembling the second substrate layer 118 and the first substrate layer 102. This is highly advantageous in mass production, because the target substance specificity of the biosensor can be selected after the production process. This can provide for an extremely fast production of biosensors with probe selectivity for a specific virus for example in case of an epidemic situation.

Figure 6a shows an embodiment of the biosensor 300 according to the invention seen in a top down view where the second substrate is shown as a see-through object. Figure 6b shows the second substrate 118 in a perspective view clearly showing the access ports 120 in the second substrate 118 for sample inlet/outlet and for providing electrical connections.

The biosensor 300 comprises a first substrate layer 102 and a second substrate layer 118, the latter comprising access ports 120 in standard Luer lock size. Two of the ports 122a, 122b provide inlet/outlet openings for the sample possibly containing target substances. Connection between the two inlet/outlet ports 122a, 122b is facilitated by a channel 128 formed in the second substrate layer 118 and/or the first substrate layer 102.

Electrical connection between the primary electrode 104 (acting as the working electrode) and the secondary electrode 106 (acting as the counter electrode) is provided through the electrode ports 124a and 124b, respectively, using connectors. The connectors further provide for operational connection between a docking station and the biosensor. By docking station is meant an apparatus for measuring the current over and/or imposing a current through the system, e.g. an apparatus which imposes a small sinusoidal voltage at a certain frequency to the biosensor and measures the resulting current through the biosensor.

A patterned electrode design, e.g. created by the method described in figure 5, is present in the sensing area 302 of the biosensor 300 where the primary electrode 104, the secondary electrode 106 and the sample channel 128 overlap, thereby creating an interwoven electrode pattern.

Figure 7a and 7b are enlargement top-down views of the interwoven electrode array design (found in the sensing area 302 marked in figure 6a) showing different examples of possible primary electrode 104 and secondary electrode 106 designs. In figure 7a the primary electrode legs 134 and the secondary electrode legs 136 form a woven leg pattern. In figure 7b a different design is shown and many other design options could also be possible.

The ports 126 seen as an upper line in figure 6a are in the shown embodiment not used for detection of target substances. Instead the ports 126 represent the option that multiple electrode pairs 103 and sample channels 128 can be present. This will allow for simultaneous detection of more than one target substance by using different probes 110 attached to the polymer layer 108 in different electrode pairs 103.

Detecting several targets with one device is favourable for reducing cost, time and number of samples necessary for the test. In order to ensure that only one type of probe is attached to one set of electrode pairs 103, different polymers selectively forming covalent bonds with specific probes could be used for the different electrode pairs 103. Alternatively, physically blocking access to all but one set of electrode pairs 103 could also ensure that the probe only binds to the polymer in this set of electrode pairs 103. The latter method is preferable if different probes are capable of forming covalent bonds with the same polymer.

Physically blocking access to all but one set of electrode pairs also allows for the use of the same polymer in all the electrodes pairs, thereby reducing production costs and complications regarding different conductivities. The multiple port design shown in figure 6a and 4b makes it possible to covalently bind different probes to different electrode pairs by using different ports connected two and two each by an individual sample channel 128.

The biosensor 300 shown in figure 6a has two symmetric sides; the measurement side 304 and the reference measurement side 306. The only difference between the electrodes 104, 106 and the sample channel 128 on the measurement side 304 and the electrodes 104', 106' and channel 128' on the reference side 306 is that the measurement side electrodes 104, 106 has a probe 110 covalently bound to the polymer layer 108, whereas the reference side electrodes 104', 106' lack the probe.

When a sample containing a target substance is added to the channels 128, 128' on both the measurement side 304 and the reference side 306, the target substances 112 will bind to the probe 110 on the electrodes 104, 106 on the measurement side 304, but not to the electrodes 104', 106' on the reference side 306. This will introduce a change in the impedance on the measurement side 304 but not on the reference side 306. The difference in the impedance measured on the measurement side 304 and the reference side 306 thereby provides a direct indication of the amount of target substance in the sample. Thus, the presence of a target substance 112 in a sample can be detected very efficiently with a biosensor according to the invention by using EIS.

Contributions to the impedance from target substances 112 binding directly to the polymer layer 108 are also eliminated by measuring the impedance both on the reference side 306 and the measurement side 304 of the biosensor 300.

The impedance biosensor incorporates both the primary electrode 104 and the secondary electrode 106 and does not necessitate an extra reference electrode. This makes the process of detecting a specific substance extremely simple due to the fact that the measurements can take place using only one electrode pair instead of the standard three-electrode electrochemical cell. This is especially advantageous when detecting target substances in small amounts of samples, as using a standard three-electrode electrochemical cell requires a relatively large sample volume in order to a reliable result.

The all-polymer biosensor is further easily mass-produced and holds several other advantages such as high integration, low sample- and reagent volume, short analysis time, low sample waste and low material cost.

Low material cost, obtained among others by using non-metal based electrodes, further allows the biosensor to be used as a disposable device. This is advantageous, if the biosensor is used for point-of-care testing in a location, e.g. an airport, a school or a workplace, where multiple people need to be tested for a given virus and adequate cleaning of the biosensor in between testing different people is impossible.

Alternatively, the probe can be heated or treated with a high concentrated salt solution in order to release the target substance, whereby the biosensor can be used multiple times.

The biosensor shown in figure 6a is typically 3-10 cm in diameter and 0,5-2 cm thick. The sample volume required for obtaining a reliable result is approximately 10-200 µl.

The detection of target substances in a sample using the biosensor and EIS is an advantageous method as it eliminates the need for labelling the target substance due to the fact that the binding event is detected directly by a change in the surface properties of the electrode. Thus, impedance biosensors are favourable due to their high sensitivity and ability to perform label free detection. Labelling a bio-substance can drastically change its binding properties, thereby giving a highly variable detection results.

Figures 8-10 show measurements conducted on an all-polymer biosensor using Topas as the non-conducting polymer substrate and tosylate doped poly(3,4-ethylenedioxythiophene) (PEDOT:TsO) as the electrode material. The electrode material is covalently functionalized with two different aptamers as probes for studying the selective capture of correspondingly two different target substances; the antibiotics ampicillin and kanamycin.

The measurements of the impedance changes were performed by connecting an impedance spectrometer (VersaSTAT 3, Princeton Applied Research, USA) to the electrodes by spring-loaded (Pogo Pin) contacts. The impedance of the system was measured with two methods: single frequency time scans at 501 mHz as shown in figure 8 and wide spectrum sweeps with a frequency range from 1 MHz to 251 mHz (logarithmic scale with 10 points per decade) as shown in figure 10. After the baseline was recorded the target was added and the change of the impedance signal monitored.

Figure 8 shows the impedance changes measured at 501 mHz of the biosensor without having an antibiotic immobilized on patterned surfaces 402, after binding of 1 μM kanamycin 404 to its corresponding aptamer, and after binding of 1 μM ampicillin 406 to its corresponding aptamer.

Measuring the impedance as shown in figure 8 can not only give us information about the fact that a binding event has taken place, but it can also give us an insight in the change caused by the binding event. The immobilization of the aptamers alone provoked an increase in the impedance, as expected. Furthermore, we observed two distinct and reproducible responses from our sensor with the two different aptamer-target binding events: The kanamycin binding to the corresponding aptamer caused an increase in the impedance measured at a single frequency (501 mHz) relative to the pristine state (only the aptamer is immobilized on the surface), while adding ampicillin to a sensor equipped with the corresponding aptamer lead to a decrease of impedance.

Control experiments, where the antibiotics were reacted with the mismatching aptamers, gave no changes in the impedance signal. After that, injecting the matching antibiotics into the biosensor resulted in the expected increase or decrease of impedance. This fact shows that the immobilization

of the aptamers on the electrodes didn't affect the ability of specific binding to their target.

The total impedance change at 1 μM concentration was in average +0.6% for kanamycin 404 and -2.4% for ampicillin 406. The sensitivity is strongly dependent on the effective wire size.

Figure 9 shows the measurement 500 made in an analyte concentration range between 10 nM – 1 μM of ampicillin. For ampicillin in concentrations above 200 nM no further decrease of impedance is detectable, which means that the sensor is saturated at that point. For kanamycin, the lower detection limit is around 500 pM target concentration (not shown in the figure).

The curve 500 shows that there is a logarithmic relation between the analyte concentration and the change of impedance. Because of the strong binding of the target to the aptamers the sensor is not suited for continuous detection in a passing fluid. The analyte would accumulate and saturate the available probes after a certain time.

The range represented in figure 9 reaches from 10 nM to 1 μM, but detection of ampicillin in a concentration as low as 500 pM is also possible. Thus, the biosensor presented here also has the capability of quantitative analyte detection.

The wide spectrum swept with a frequency range from 1 MHz to 251 mHz (logarithmic scale with 10 points per decade) is shown as a Nyquist plot in figure 10 for the biosensor with the aptamer and no target molecule bound thereto 602, the biosensor with kanamycin bound to its specific aptamer 604, the biosensor with ampicillin bound to its corresponding aptamer 606.

List of references

100	biosensor
101	primary surface of the first substrate layer
102	first substrate layer
103	electrode pair
104, 104'	primary electrode, acting as working electrode
105	part of the primary electrode
106, 106'	secondary electrode, acting as counter electrode
108	polymer layer
108a	first polymer layer
108b	second polymer layer
110	probe
112	target substance
114	photoresist
116	adhesive
118	second substrate layer
120	opening, port
122a, 122b	port for the sample
124a, 124b	port for providing electrical connection
126	port not in use
128, 128'	channel connecting sample ports
130	sample
134	primary electrode legs
136	secondary electrode legs
300	biosensor
302	sensing area of the biosensor
304	measurement side of the biosensor 300
306	reference side of the biosensor 300
402	impedance changes without an immobilized target
404	impedance changes after binding of 1 μM kanamycin
406	impedance changes after binding of 1 μM ampicillin

500	concentration dependency in the impedance changes
600	Nyquist plot
602	the aptamer and no target molecule
604	kanamycin bound to its specific aptamer
606	ampicillin bound to its corresponding aptamer

Claims

1. A biosensor for detection of a target substance in a sample with impedance spectroscopy, the biosensor comprising:
   - a first non-conducting substrate comprising a primary substrate surface;
   - a conducting polymer electrode layer comprising one or more conducting polymers layers, the conducting polymer electrode layer comprising a primary electrode surface and a secondary electrode surface, wherein the secondary electrode surface covers part of the primary substrate surface;
   - a probe layer bonded to part of the primary electrode surface; and
   - a second non-conducting substrate comprising a secondary substrate surface, wherein the secondary substrate surface of the second substrate and the primary substrate surface of the first substrate are interconnected such that the electrode layer and the probe layer are confined within an area defined by the first substrate and the second substrate;

   wherein the electrode layer comprises at least a first electrode pair, the first electrode pair comprising a primary electrode and a secondary electrode, and wherein the probe layer is bonded to the primary electrode and/or the secondary electrode of the at least first electrode pair, the probe layer being adapted for selectively binding of the target substance.

2. A biosensor according to claim 1, wherein the primary electrode comprises a plurality of primary legs and the secondary electrode comprises a plurality of secondary legs, the primary legs and the secondary legs forms an interwoven pattern.

3. A biosensor according to claim 1 or 2, wherein the second non-conducting substrate is provided with ports for inlet/outlet of the sample and/or for facilitating an electrical connection.

4. A biosensor according to any of the preceding claims, wherein the first substrate and/or the second substrate is a non-conducting polymer substrate.

5. A biosensor according to claim 4, wherein the non-conducting polymer substrate is selected from the group of polystyrenes, polyolefins and cyclic olefin copolymers such as e.g. TOPAS 5013L (TOPAS Advanced Polymers, Germany).

6. A biosensor according to any of the preceding claims, wherein the one or more conducting polymer layers of the conducting polymer electrode layer is selected from the group of poly(3,4-ethylenedioxythiophene) (PEDOT), polypyrrole (PPy), poly(3,4-propylenedioxythiophene), triacetonamine (TAA), polyaniline (PANI), derivatives thereof and/or co-polymers thereof.

7. A biosensor according to any of the preceding claims, wherein the one or more conducting polymer layers of the conducting polymer electrode layer is selected from the group of PEDOT and PEDOT derivatives.

8. A biosensor according to claim 7, wherein the PEDOT derivatives contain one or more functional groups selected from the group of alcohols (OH), carboxylic acids (COOH), azides (N_3) and alkynes.

9. A biosensor according to any of the preceding claims, wherein the conducting polymer electrode layer comprises a first conductive

polymer layer and a second conducting polymer layer, wherein the probe layer is bonded to the second conducting polymer layer.

10. A biosensor according to any of the preceding claims, wherein the first conductive polymer layer is PEDOT and the second conducting polymer layer is a PEDOT-derivative.

11. A biosensor according to any of the preceding claims, wherein the probe layer is covalently bonded to part of the primary electrode surface.

12. A biosensor according to any of the preceding claims, wherein the probe layer comprises an entity selected from the group of aptamers, oligonucleotides and/or peptides.

13. A biosensor according to any of the preceding claims, wherein the electrode layer comprises a second electrode pair comprising a second primary electrode and a second secondary electrode.

14. The use of a biosensor according to any of claims 1-13 for point-of-care measurement and/or on-site detecting of a target substance in a liquid sample such as e.g. water, blood, urine, saliva.

15. A system for detection of a target substance in a sample, the system comprising a biosensor according to any of claims 1-13, a docking station, and connectors for operational connection between the docking station and the biosensor, wherein the docking station measures changes in the impedance over the first and/or second electrode pair before and after applying sample to the biosensor.

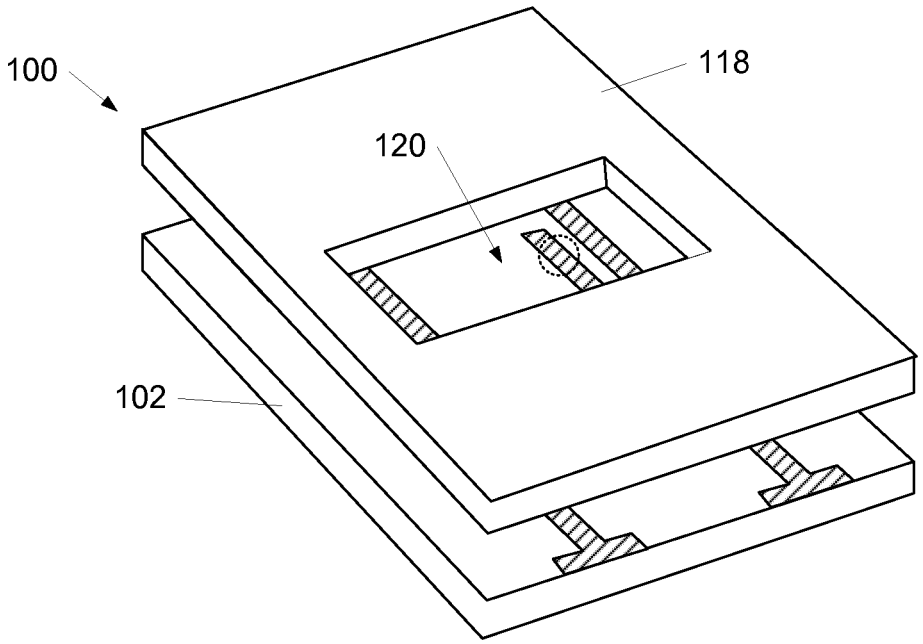

Fig. 1a

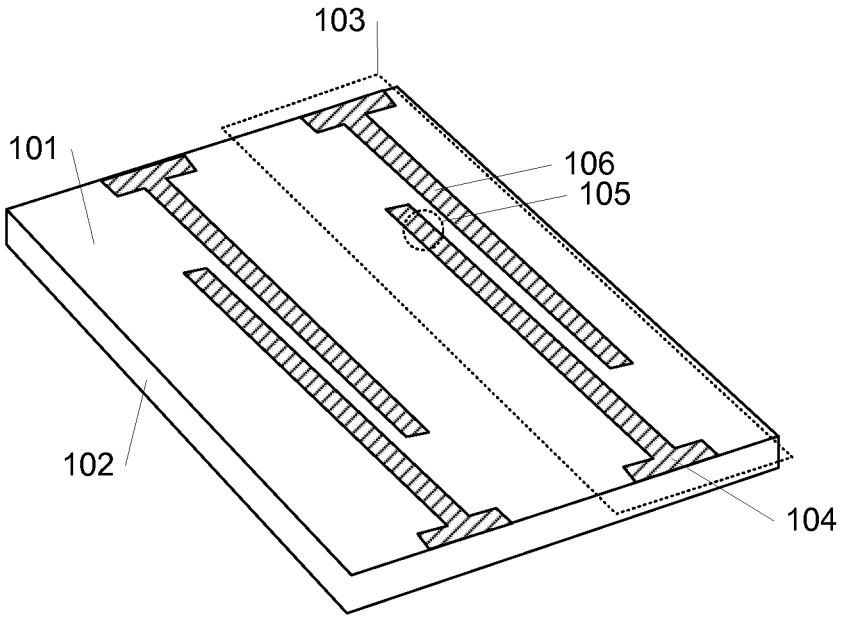

Fig. 1b

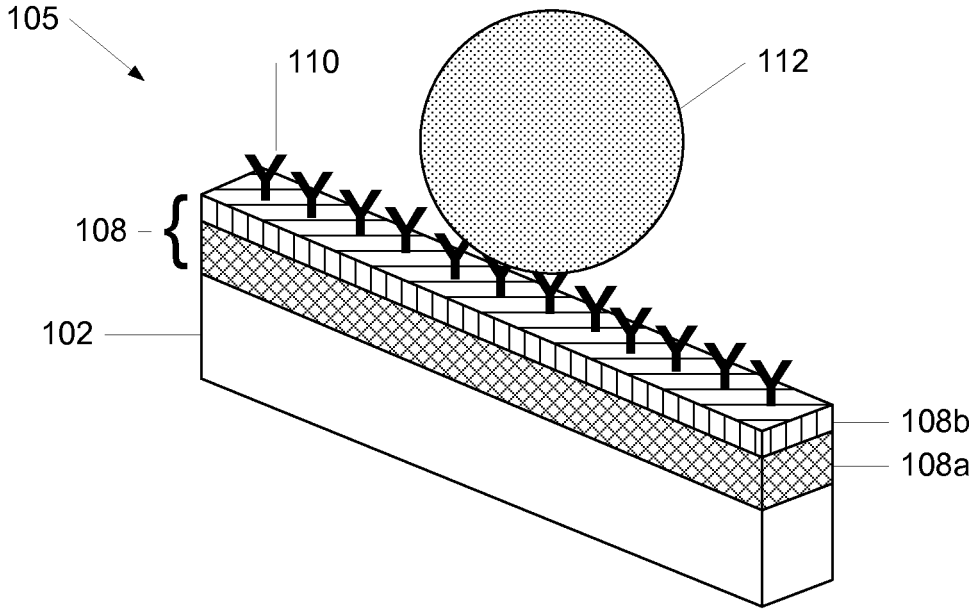

Fig. 2

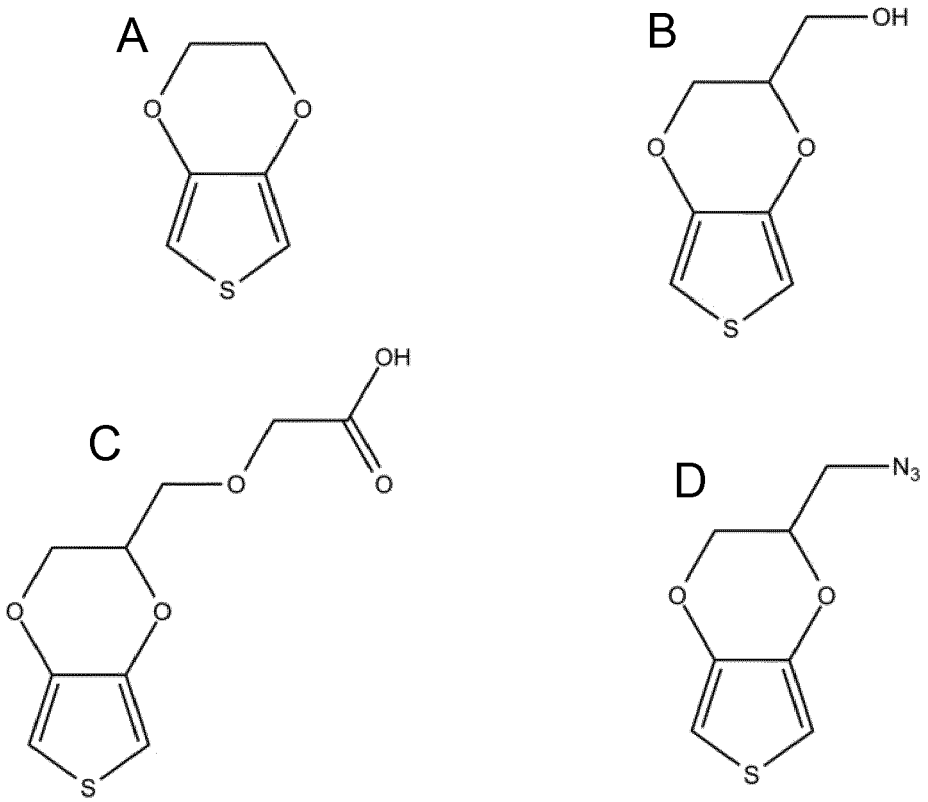

Fig. 3

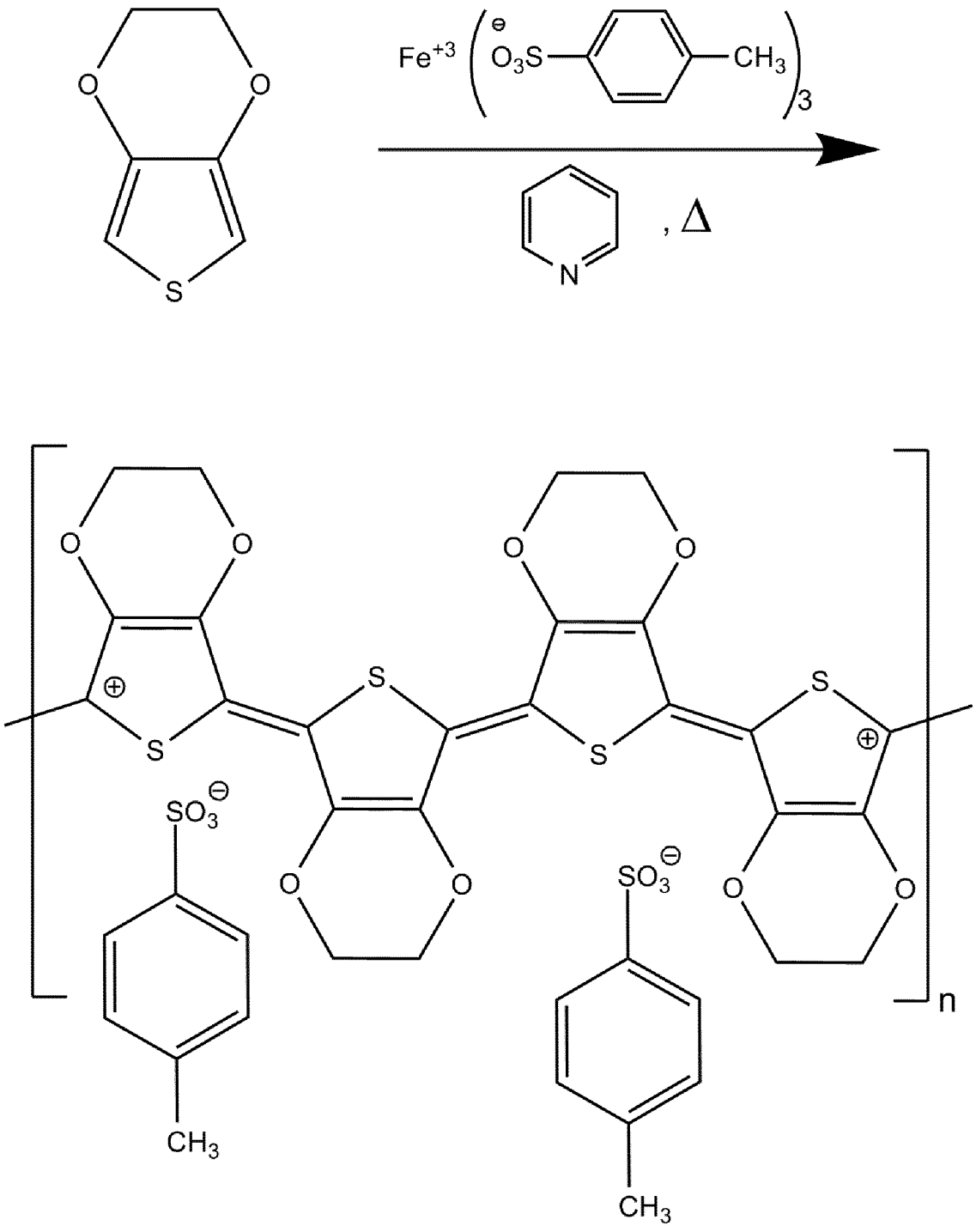

Fig. 4

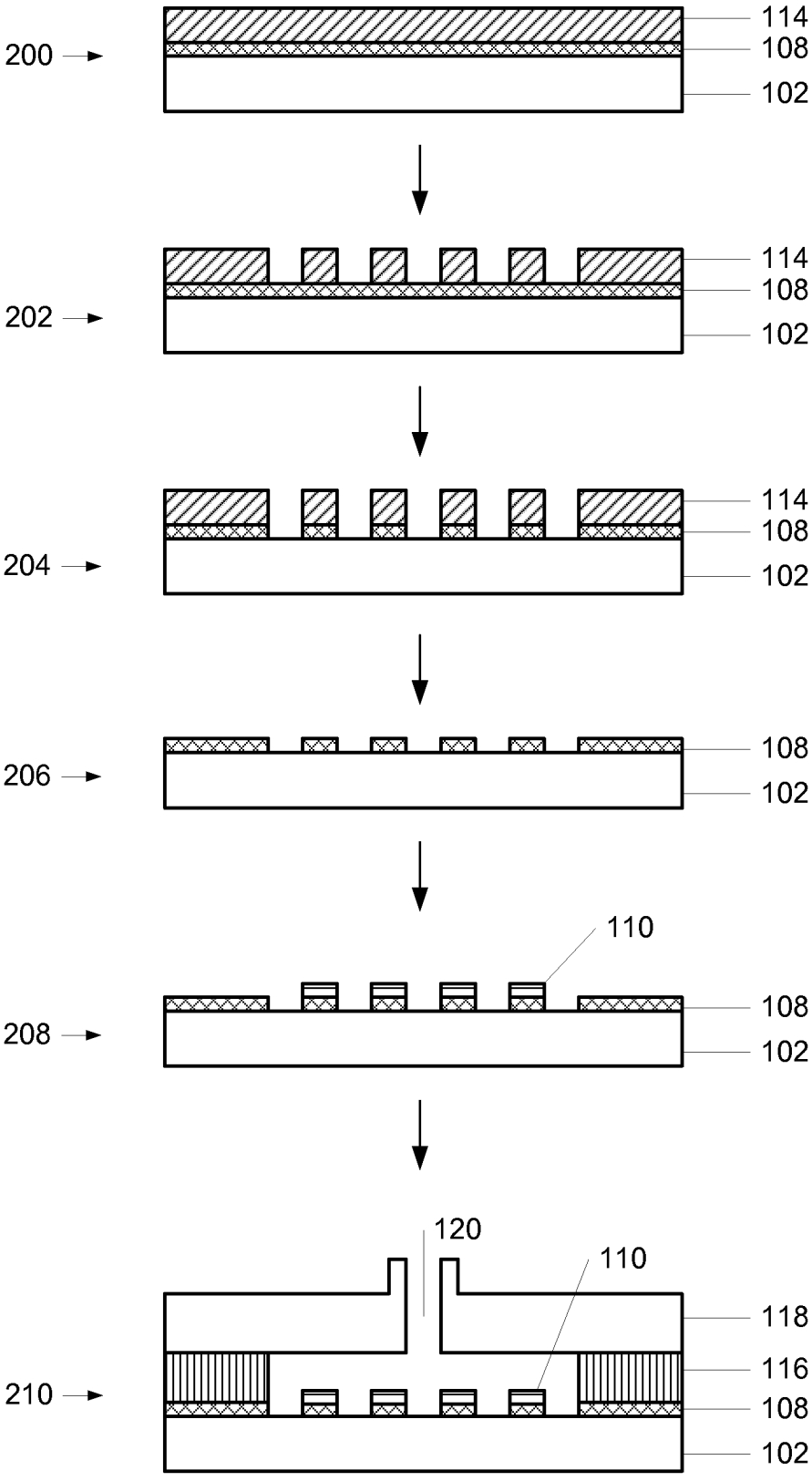
200
114
108
102
202
114
108
102
204
114
108
102
206
108
102
208
110
108
102
210
120
110
118
116
108
102

Fig. 5

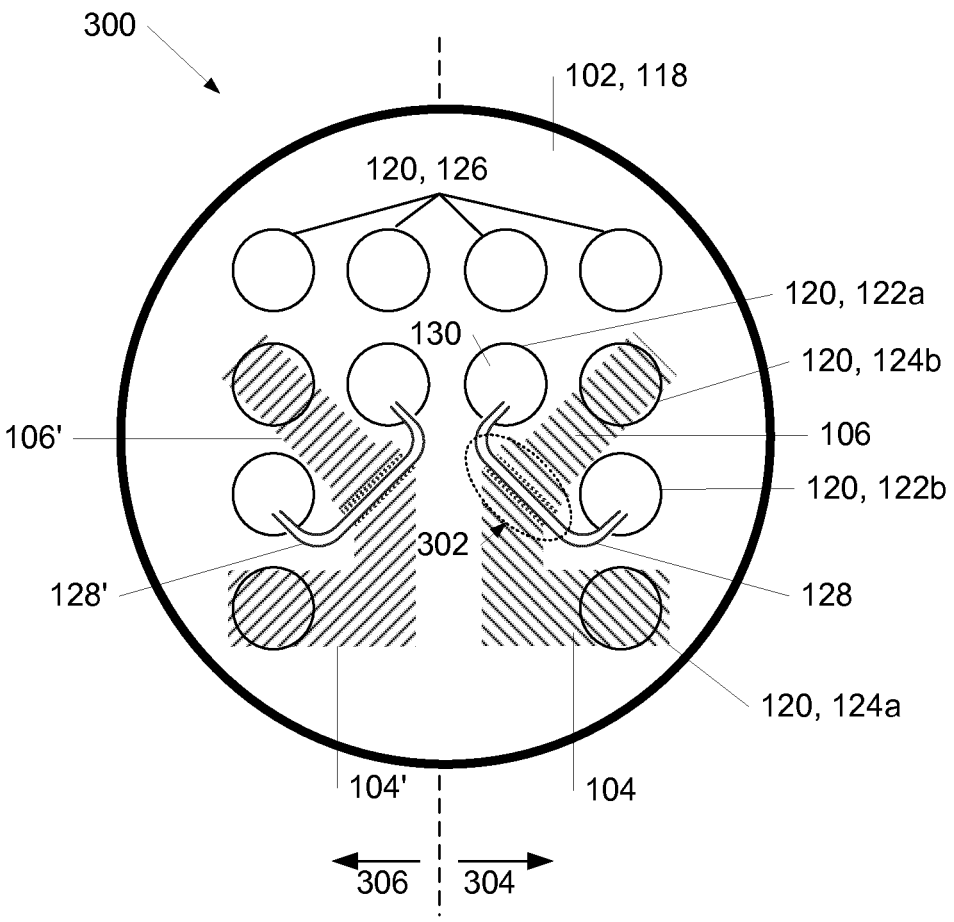
300
102, 118
120, 126
120, 122a
130
120, 124b
106'
106
120, 122b
302
128'
128
120, 124a
104'
104
306
304

Fig. 6a

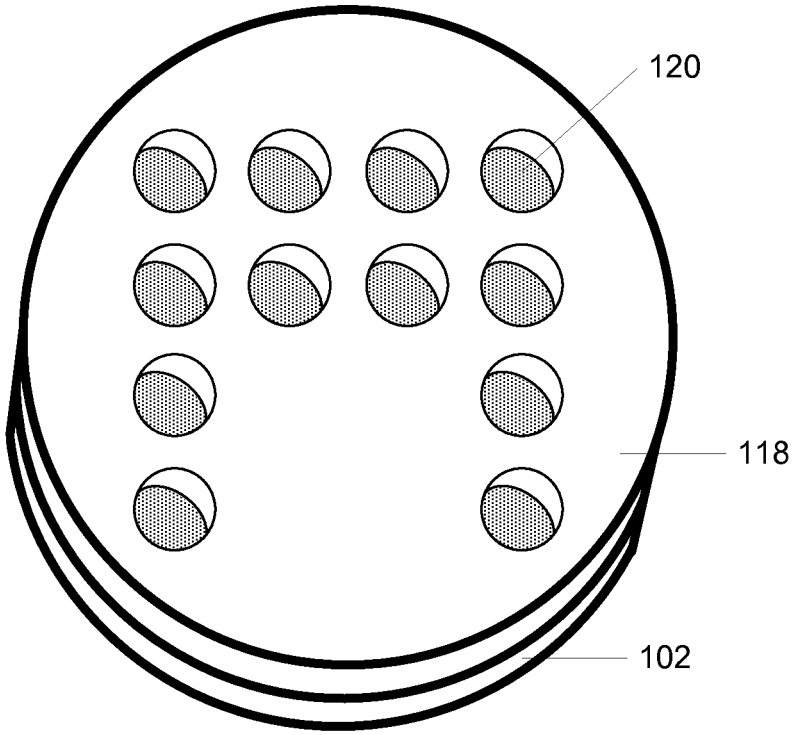
120
118
102

Fig. 6b

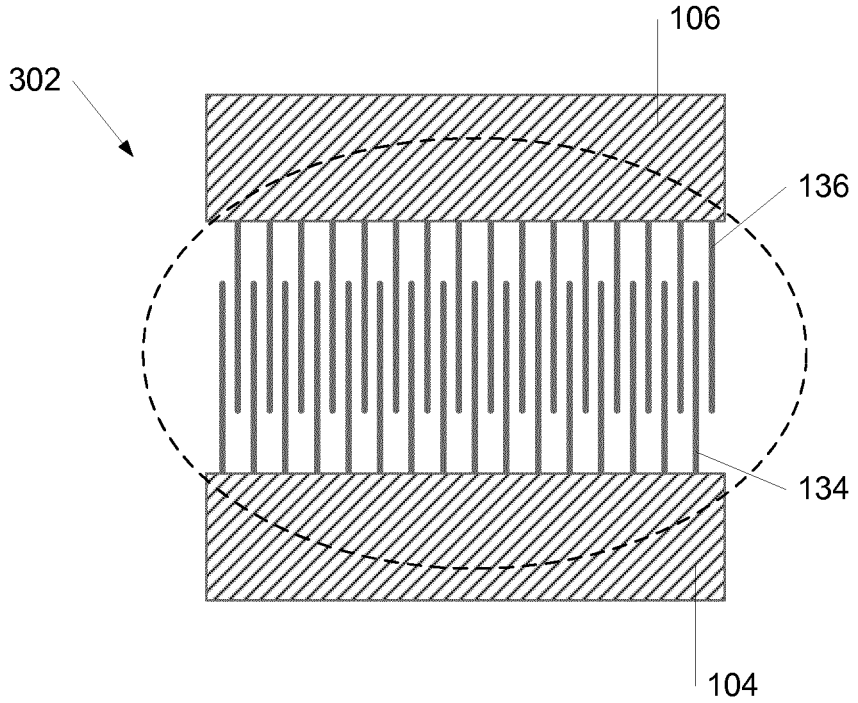

Fig. 7a

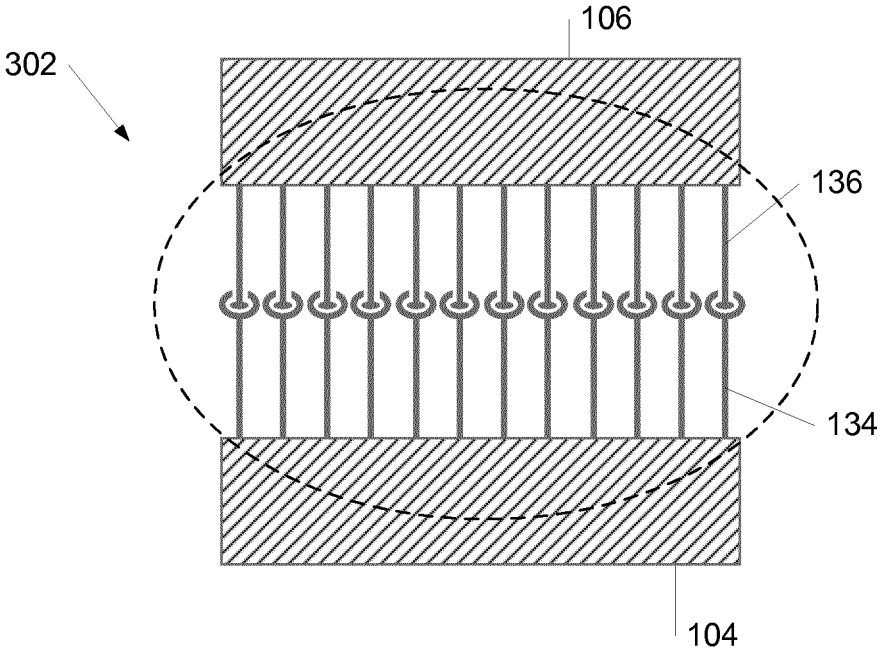

Fig. 7b

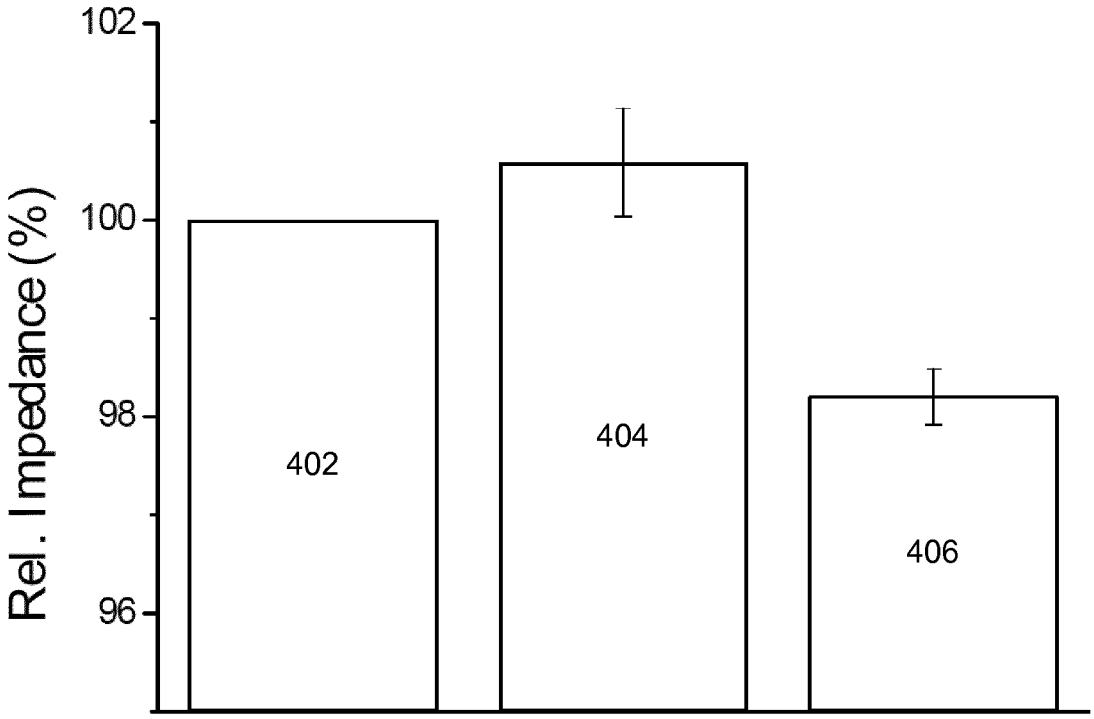
102
100
98
96
Rel. Impedance (%)
402
404
406

Fig. 8

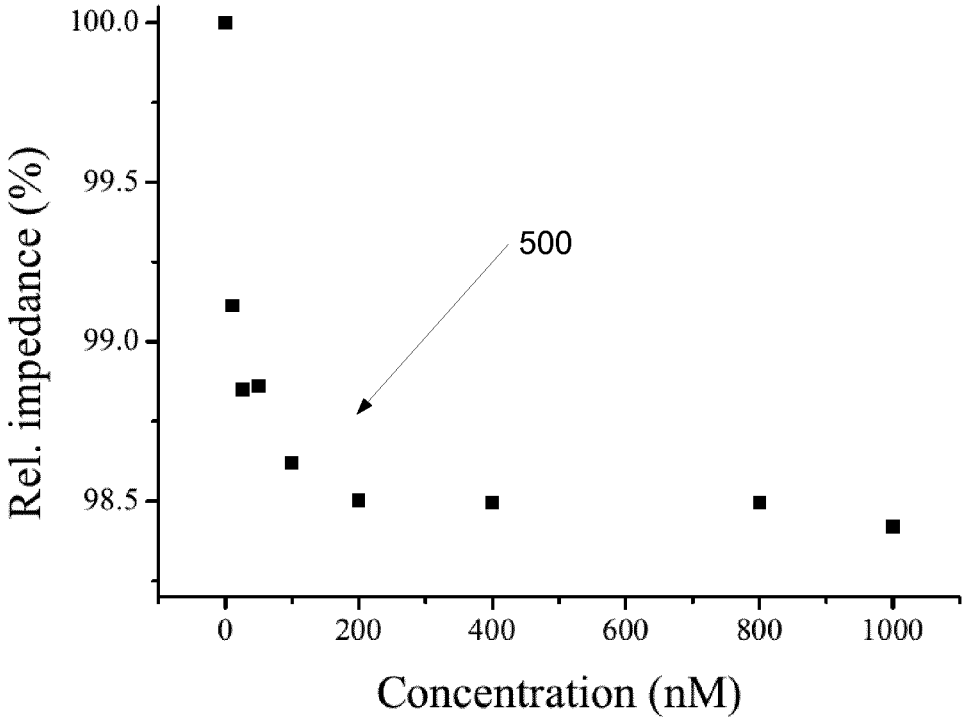
100.0
99.5
99.0
98.5
Rel. impedance (%)
500
0
200
400
600
800
1000
Concentration (nM)

Fig. 9

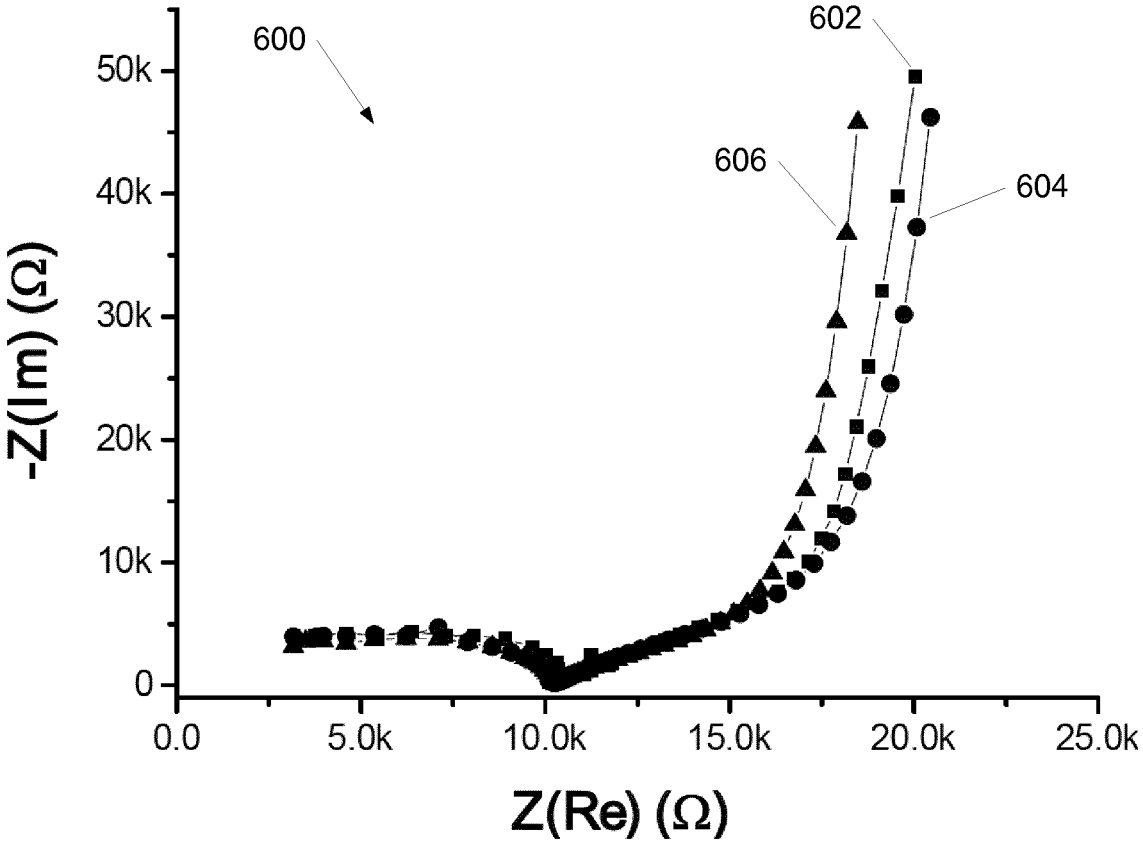
600
602
606
604
50k
40k
30k
20k
10k
0
-Z(Im) (Ω)
0.0
5.0k
10.0k
15.0k
20.0k
25.0k
Z(Re) (Ω)

Fig. 10

INTERNATIONAL SEARCH REPORT

International application No
PCT/EP2012/067508

A. CLASSIFICATION OF SUBJECT MATTER
INV. G01N33/543 G01N27/327
ADD.

According to International Patent Classification (IPC) or to both national classification and IPC

B. FIELDS SEARCHED

Minimum documentation searched (classification system followed by classification symbols)
G01N

Documentation searched other than minimum documentation to the extent that such documents are included in the fields searched

Electronic data base consulted during the international search (name of data base and, where practicable, search terms used)
EPO-Internal, WPI Data, INSPEC, BIOSIS, EMBASE

C. DOCUMENTS CONSIDERED TO BE RELEVANT

Category*	Citation of document, with indication, where appropriate, of the relevant passages	Relevant to claim No.
Y	KATRINE KIILERICH-PEDERSEN ET AL: "Polymer based biosensor for rapid electrochemical detection of virus infection of human cells", BIOSENSORS AND BIOELECTRONICS, vol. 28, no. 1, 28 July 2011 (2011-07-28), pages 386-392, XP055016878, ISSN: 0956-5663, DOI: 10.1016/j.bios.2011.07.053 the whole document ----- -/--	1-15

[X] Further documents are listed in the continuation of Box C. [ ] See patent family annex.

* Special categories of cited documents :

"A" document defining the general state of the art which is not considered to be of particular relevance

"E" earlier application or patent but published on or after the international filing date

"L" document which may throw doubts on priority claim(s) or which is cited to establish the publication date of another citation or other special reason (as specified)

"O" document referring to an oral disclosure, use, exhibition or other means

"P" document published prior to the international filing date but later than the priority date claimed

"T" later document published after the international filing date or priority date and not in conflict with the application but cited to understand the principle or theory underlying the invention

"X" document of particular relevance; the claimed invention cannot be considered novel or cannot be considered to involve an inventive step when the document is taken alone

"Y" document of particular relevance; the claimed invention cannot be considered to involve an inventive step when the document is combined with one or more other such documents, such combination being obvious to a person skilled in the art

"&" document member of the same patent family

Date of the actual completion of the international search	Date of mailing of the international search report
16 November 2012	22/11/2012

Name and mailing address of the ISA/	Authorized officer
European Patent Office, P.B. 5818 Patentlaan 2 NL - 2280 HV Rijswijk Tel. (+31-70) 340-2040, Fax: (+31-70) 340-3016	Komenda, Peter

C(Continuation). DOCUMENTS CONSIDERED TO BE RELEVANT

Category*	Citation of document, with indication, where appropriate, of the relevant passages	Relevant to claim No.
Y	Katrine Kiilerich-Pedersen: "Polymer Based Biosensors for Pathogen Diagnostics" In: "Environmental Biosensors", July 2011 (2011-07), InTech, XP055016998, ISBN: 978-9-53-307486-3 pages 193-212, cited in the application Paragraphs 3.3 and 4.	1-15
Y	KUN HAN ET AL: "Design Strategies for Aptamer-Based Biosensors", SENSORS, vol. 10, no. 5, 1 January 2010 (2010-01-01), pages 4541-4557, XP055044381, ISSN: 1424-8220, DOI: 10.3390/s100504541 Abstract and "I. Introduction"	1-15
Y	SONG ET AL: "Aptamer-based biosensors", TRAC, TRENDS IN ANALYTICAL CHEMISTRY, ELSEVIER, AMSTERDAM, NL, vol. 27, no. 2, 23 December 2007 (2007-12-23), pages 108-117, XP022520321, ISSN: 0165-9936, DOI: 10.1016/J.TRAC.2007.12.004 Abstract and sections 1.-2.	1-15
A	NOEMI ROZLOSNIK: "New directions in medical biosensors employing poly(3,4-ethylenedioxy thiophene) derivative-based electrodes", ANALYTICAL AND BIOANALYTICAL CHEMISTRY, SPRINGER, BERLIN, DE, vol. 395, no. 3, 31 July 2009 (2009-07-31) , pages 637-645, XP019736666, ISSN: 1618-2650, DOI: 10.1007/S00216-009-2981-8 abstract	1-15